AEROSPACE INFORMATION REPORT

AIR6908™	REV. A
Issued 2018-09 Revised 2024-06 Superseding AIR6908	

Impact Characteristics of Seat Back Mounted IFE Monitors - Basis for ARP6330

RATIONALE

Document being updated to add rationale and project data on development of component impact test for seat back monitors.

FOREWORD

To meet the head injury criterion (HIC) of AS8049, seat manufacturers may be required to perform row-to-row seat dynamic testing to assess the seat design's ability to attenuate the severity of blunt trauma to the head, as measured by the HIC. As part of the test, seat back mounted in-flight entertainment (IFE) monitors are included in the tested configuration of the seat. While the primary purpose of the HIC test is to measure the HIC value, the seat is also evaluated in its post-test state for unacceptable sharp edges, loose pieces, and potential occupant egress impediments. Numerous difficulties for seat manufacturers, IFE manufacturers, and the seat installer occur when demonstrating and maintaining compliance.

- Obsolescence of parts within the IFE monitor is driven by the pace of change in the consumer electronics industry. Therefore, evaluation of IFE monitor changes for effects on HIC and post-impact sharp edges (refer to ARP6448 Item 3) is frequently performed by the IFE manufacturer, seat manufacturers, and the seat installers. As an IFE monitor can be integrated within various seat designs manufactured by multiple seat manufacturers, a single change to an IFE monitor design could affect a large number of different seat installations.

- Seat manufacturers are knowledgeable in seat system behavior, while IFE manufacturers are knowledgeable about the construction of their IFE monitors. Test failures that include both the seat and the IFE monitor (especially unacceptable post-impact sharp edges of the IFE monitor) are problematic due to shared involvement in the integrated seat design. Therefore, it can be difficult to identify the design change needed to meet requirements.

To address these difficulties, the SAE SEAT Committee initiated a working group in February 2014 to develop recommended practices that could characterize IFE monitor impact performance separate from the seat installation, for both initial seat HIC testing and subsequent IFE monitor changes. The SAE working group consisted primarily of seat, IFE, and airframe manufacturers. Characterizations would be for blunt trauma to the head, sharp edges formed after impact, and potential for egress impediment. By evaluating the IFE monitor performance separate from its installation, a simpler, less expensive, standardized, and more accurate assessment of monitor design characteristics can be performed compared to seat dynamic testing. This type of component data could supplement the head impact data generated during the initial certification of the seat design, as well as evaluate the significance of a monitor design change on blunt trauma and post-impact sharp edge performance.

TO PLACE A DOCUMENT ORDER: **Tel: 877-606-7323 (inside USA and Canada)**
Tel: +1 724-776-4970 (outside USA)
Fax: 724-776-0790
Email: CustomerService@sae.org
SAE WEB ADDRESS: **http://www.sae.org**

For more information on this standard, visit
https://www.sae.org/standards/content/AIR6908A

Initial objectives of the working group are as follows:

Evaluation of seat back monitor design changes

a. Seat back IFE monitor revisions can be evaluated at the monitor component level for similarity in regard to blunt trauma to the head and post-impact sharp edge generation, in lieu of testing the integrated seat design.

Initial design and certification of integrated seat

a. Design and validation of a surrogate target that emulates the IFE monitor impact energy attenuation characteristics when being struck by the anthropomorphic test device (ATD) head.

b. Evaluate the propensity of an IFE monitor design to generating sharp and injurious edges without the need for performing a head impact test on the integrated seat.

c. Generate IFE monitor data that could be used in refining analytical models of the integrated seat design.

The initial focus of the working team was to assess whether changes to internal components of seat back mounted IFE monitors (touch screen, display panel, electronics) would appreciably affect how the integrated seat attenuates a head impact. Various test methods were investigated, including row-to-row seat dynamic test methods, head impact devices, and static bend testing. The simplest and most consistent test methods are static bend tests. Parametric studies using computer simulation of various seat designs were undertaken to assess how much variance in seat back IFE monitor static bend test performance would still result in a similar level of performance. These parametric studies were focused on changes to the touch screen and display panel of the IFE monitor, as those subcomponents change most frequently. **The result is static bend test methods and criteria that can be used to evaluate whether two configurations of the same monitor model can be considered similar for HIC when installed on the seat back of a passenger seat.** Another product of this activity is general guidelines for developing IFE monitor analytical models.

Development of a component test to evaluate the monitor for post-impact sharp edges and a recommended practice to validate surrogate targets were in work at the time of publishing ARP6330. Subsequent efforts focused on a monitor component test for assessing the monitor resistance to generating sharp edges due to head impact, which will be incorporated into Revision A of ARP6330.

TABLE OF CONTENTS

1. SCOPE

This document provides background information, rationale, and data (both physical testing and computer simulations) used in defining the component test methods and similarity criteria described in SAE Aerospace Recommended Practice (ARP) 6330. ARP6330 defines multiple test methods used to assess the effect of seat back mounted IFE monitor changes on blunt trauma to the head and post-impact sharp edge generation. The data generated is based on seat and IFE components installed on type A-T (transport airplane) certified aircraft. While not within the scope of ARP6330, generated test data for the possible future development of surrogate target evaluation methods is also included.

2. REFERENCES

2.1 Applicable Documents

The following publications form a part of this document to the extent specified herein. The latest issue of SAE publications shall apply. The applicable issue of other publications shall be the issue in effect on the date of the purchase order. In the event of conflict between the text of this document and references cited herein, the text of this document takes precedence. Nothing in this document, however, supersedes applicable laws and regulations unless a specific exemption has been obtained.

2.1.1 SAE Publications

Available from SAE International, 400 Commonwealth Drive, Warrendale, PA 15096-0001, Tel: 877-606-7323 (inside USA and Canada) or +1 724-776-4970 (outside USA), www.sae.org.

ARP5765 Analytical Methods for Aircraft Seat Design and Evaluation

ARP6330 Methods to Evaluate Impact Characteristics of Seat Back Mounted IFE Monitors

ARP6448 Gaining Approval for Seats with Integrated Electronics in Accordance with AC 21-49 Section 7.b

AS8049 Performance Standard for Seats in Civil Rotorcraft, Transport Aircraft, and General Aviation Aircraft

2.1.2 ASTM Publications

Available from ASTM International, 100 Barr Harbor Drive, P.O. Box C700, West Conshohocken, PA 19428-2959, Tel: 610-832-9585, www.astm.org.

ASTM D6272-17 Standard Test Method for Flexural Properties of Unreinforced and Reinforced Plastics and Electrical Insulating Materials by Four-Point Bending

2.1.3 Code of Federal Regulations (CFR) Publications

Available from United States Government Printing Office, 732 North Capitol Street, NW, Washington, DC 20401, Tel: 202-512-1800, www.gpo.gov.

Title 14 Part 25 Airworthiness Standards: Transport Category Airplanes

Title 49 Part 571.201 Standard No. 201; Occupant protection in interior impact

2.1.4 FAA Publications

Available from Federal Aviation Administration, 800 Independence Avenue, SW, Washington, DC 20591, Tel: 866-835-5322, www.faa.gov.

ANM-03-115-28 Policy Statement on Use of Surrogate Parts When Evaluating Seat backs and Seat back Mounted Accessories for Compliance with §§ 25.562(c)(5) and 25.785(b) and (d) (October 2, 2003)

ANM-03-115-31 Policy Statement on Conducting Component Level Tests to Demonstrate Compliance with §§ 25.785(b) and (d) (May 9, 2005)

AC 21-49 Gaining Approval of Seats with Integrated Electronic Components (February 9, 2011)

AC 25-17A Change 1 Transport Airplane Cabin Interiors Crashworthiness Handbook (May 24, 2016)

AC 25.562-1B Change 1 Dynamic Evaluation of Seat Restraint Systems and Occupant Protection on Transport Airplanes (September 30, 2015)

2.1.5 Other Publications

Mainstone, R.J. (1975). Properties of materials at high rates of straining or loading. *Materials and Structures*, *8*(2), 102-116. https://doi.org/10.1007/BF02476328.

Limbach, R., Rodriguez, B.P., and Wodraczek. L. (2014). Strain-rate sensitivity of glasses. *Journal of Non-Crystalline Solids*, *404*, 124-134. https://doi.org/10.1016/j.jnoncrysol.2014.08.023.

2.2 Definitions

BASELINE IFE MONITOR: The IFE monitor configuration in which the integrated seat was validated for acceptable head impact performance.

HEAD INJURY CRITERION (HIC): A measure of head impact blunt trauma severity as defined in 14 CFR §§ 25.562(c)(5).

INTEGRATED SEAT: An airplane seat approved under a seat TSOA/LODA that includes electronic components. The electronic components may include IFE, in-seat power systems, inflatable restraints, and electrically actuated seat features.

REVISED IFE MONITOR: The IFE monitor configuration proposed to be substituted for the baseline monitor in an integrated seat design.

SURROGATE TARGET: An acceptable substitute for a production part per FAA memorandum ANM-03-115-28.

2.3 Acronyms

AC Advisory Circular

AIR Aerospace Information Report

ARP Aerospace Recommended Practice

AS Aerospace Standard

ASTM American Society of Testing and Materials

ATD Anthropomorphic Test Device

B/C	Business Class
CFR	Code of Federal Regulations
E/C	Economy Class
FAA	Federal Aviation Administration
FEM	Finite Element Model
FMH	Free Motion Headform
FMVSS	Federal Motor Vehicle Safety Standards
HCTD	Head Component Test Device
HIC	Head Injury Criterion
IFE	In-Flight Entertainment
LCD	Liquid Crystal Display
LED	Light Emitting Diode
MMPDS	Metallic Materials Properties Development and Standardization
N/A	Not Applicable
PED	Personal Electronic Device
PCB	Printed Circuit Board
SRP	Seat Reference Point
TSO	Technical Standard Order

3. PROPOSED TEST METHODS INVESTIGATED

In addition to full scale row-to-row HIC dynamic testing commonly employed, three test methods were proposed by working group members during initial development of ARP6330.

a. Row-to-row HIC dynamic testing (baseline).

b. Head component testing of the integrated seat back.

c. Head component testing with a simple seat back fixture.

d. Static compression bend testing.

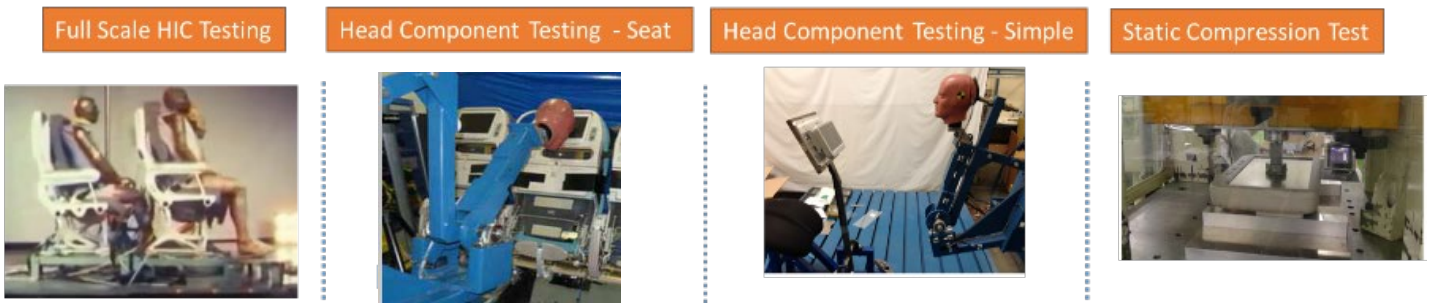

Figure 1 - Testing methods investigated

After the publication of ARP6330, efforts focused on the development of component impact testing to evaluate a monitor design's ability to not generate unacceptable sharp edges or loose pieces when impacted by an ATD head.

3.1 Row-to-Row Dynamic HIC Testing

Row-to-row dynamic HIC testing is described in AS8049. Additional guidance for this testing can be found in FAA Advisory Circular 25.562-1B Change 1.

Initial validation and certification of the integrated seat to AS8049 HIC requirements are done using row-to-row dynamic HIC testing. Test results can be used to substantiate the integrated seat back (seat and IFE monitor) for both blunt trauma (HIC ≤ 1000) and post-impact sharp edges. Data collected using this method can sometimes be used to show compliance to §25.785(d)(2). As stated earlier in this document, there is a need to have test methods that evaluate the IFE monitor modifications separate from its installation within the seat back.

3.2 Head Component Test of Integrated Seat

Impact testing of seat backs has been performed for decades, starting with a bowling ball impactor (refer to FAA Advisory Circular 25-17A Change 1), with additional options of the free motion headform (FMH) and the inverted pendulum head component test device (HCTD) developed later (refer to FAA policy ANM-03-115-31). These test methods have been used to assess §§25.785(b),(d)(2) criteria for blunt trauma to the head and post-impact sharp edges but have not been used in measuring HIC.

Goal: Determine whether the HCTD can evaluate the significance of seat back IFE monitor design changes on seat HIC performance.

Use of the HCTD was pursued instead of the other head impact devices, as the rotational motion of the head and the inclusion of a neck more closely represents the ATD head interaction with the seat back. The bowling ball and FMH test devices have a linear motion and do not include a neck.

3.3 Head Component Test Using Seat Back Test Fixture

This method is similar to the test method described in 3.2, except the impacted structure is a pivoting steel test fixture instead of the integrated seat back. The seat back test fixture is an inverted pendulum with a mounting frame on the top to attach the monitor and associated mounting hardware. A cable tie is used to prevent the test fixture from shifting from its initial position before head impact. See Figure 2 for pictures of the proposed pivoting test fixture.

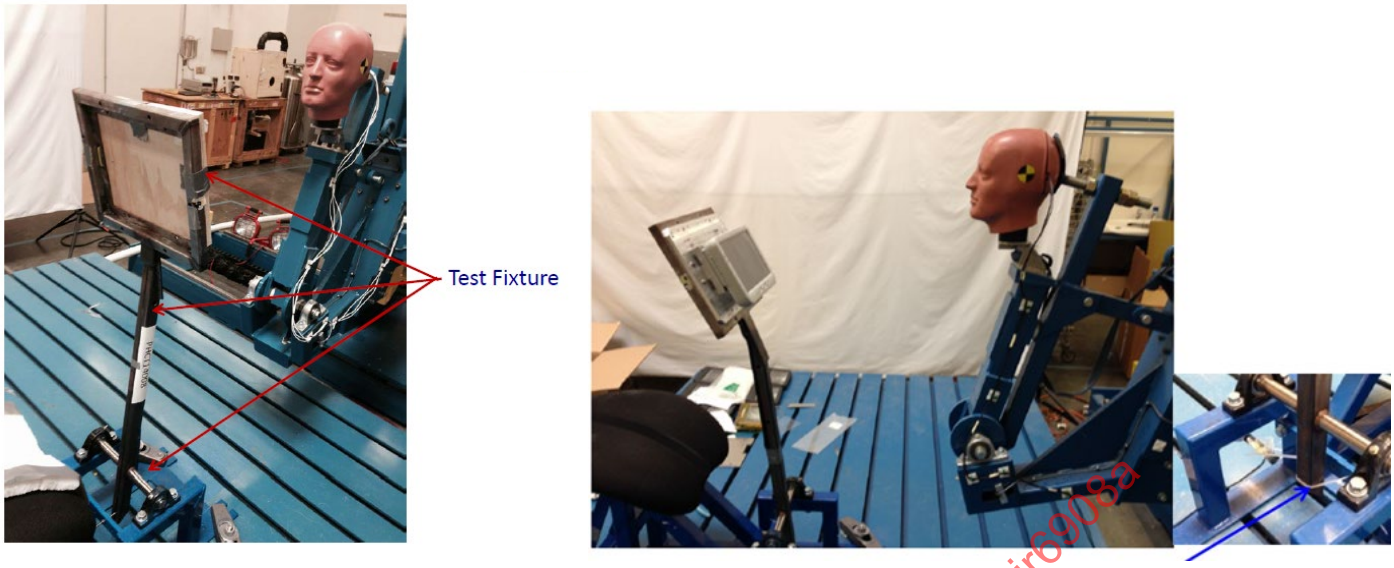

Figure 2 - Seat back test fixture

While not a substitute for row-to-row HIC dynamic testing, the test data might be used to evaluate changes to the seat back monitor (both blunt trauma and post-impact sharp edges), as well as a method to compare a proposed surrogate target to the production article it is designed to substitute for in seat testing. Test data would not be specific to an integrated seat back design and, therefore, could be applicable to a variety of different seat back installations.

Goal: Develop a seat back test fixture/HCTD test method that can evaluate the significance of IFE monitor design changes on blunt trauma to the head and post-impact sharp edges, as well as similarity between a surrogate target and the production IFE monitor.

3.4 Static Compression Bend Tests

The least complex test methods investigated were static compression tests, specifically three- and four-point static bend tests. As this type of test method is not an impact test, static tests are to evaluate changes in monitor stiffness and thereby changes in the performance of the integrated seat back to attenuate head impacts. Evaluation of post-impact sharp edge generation would need to be done with another test method.

Two different static bend tests were evaluated.

a. Three-point bending test to assess the IFE monitor stiffness.

b. Four-point bending test to assess glass material stiffness.

The goal was to use published industry standards to define the static bend tests. ASTM D6272-17 was evaluated and determined to be suitable for performing four-point bend tests on panel materials. Published three-point bend test standards did not define the necessary test definition for this application (test article support locations, load applicator, etc.). Therefore, the three-point test method had to be defined in ARP6330.

The three-point bend test configuration is with the IFE monitor placed on two simple supports and the load applied at the center of the viewing screen. Location of the simple supports is directly under the monitor attachment points, running parallel with the short edges of the monitor. The load is applied until the applicator has pressed into the monitor at least three quarters the component thickness. See Figure 3 for an example of a seat back monitor three-point bend test.

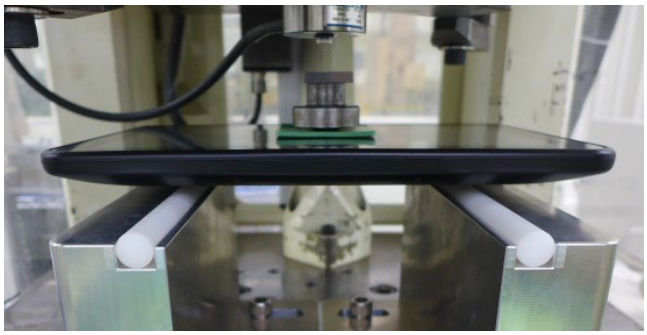

Figure 3 - Three-point bend test

A four-point bend test is similar to the three-point bend test; however, the load is applied using two simple supports to load the test sample more evenly. See Figure 4.

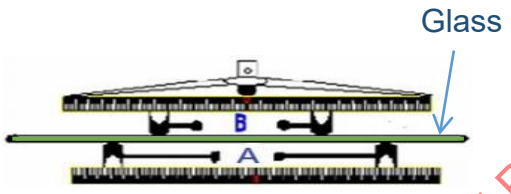

Figure 4 - Four-point bend test

A three-point bend test with the load applied at the center of the viewing screen was determined to be better than a four-point bend test for evaluating the monitor, as this central location typically will cause the maximum amount of deflection in the internal layers of the monitor (touch screen, display panel, printed circuit boards) and would better represent the biaxial stresses induced by a head impact. The load applicator shape was chosen to be circular to reduce stress concentrations between the load applicator and monitor surface. The load applicator diameter range of 1.5 to 2 inches (38.1 to 50.8 mm) is large enough to not become a point load while allowing enough distance between the applicator and test sample supports to cause bending in smaller monitors. The allowance of a hard rubber pad was included to help distribute the load evenly and to avoid stress concentrations at the edge of the load applicator. The monitor test supports are cylindrical to allow the monitor to bend more easily under load and to reduce stress concentrations on the back surface of the monitor. The diameter of the test article supports and loading rate were not critical to the performance of the test; however, parameters were defined in ARP6330 to improve test setup consistency between labs. The specific material of the load applicator and supports is also not critical as long as the material is sufficiently rigid to not deform during testing.

The supports are positioned under the monitor attachment locations, as those areas are where the monitor transmits load to the rest of the seat structure when installed into the seat back. A minimum load applicator test displacement of three quarters the monitor thickness was chosen, as the front face of the monitor typically does not reach that level of displacement during HIC testing. A minimum of three tests was determined to be enough to derive a suitably accurate force-displacement curve of the monitor.

Bend testing of the internal subcomponent only (touch screen, display panel, printed circuit board) was considered, but typically, the internal subcomponent change is accompanied by other internal monitor changes to accommodate the revised subcomponent (subcomponent attachment points, connector locations, etc.). Therefore, the cumulative effect may be more than just the modified subcomponent itself. To address an internal subcomponent change in its entirety, efforts were focused on developing testing methods using the entire monitor.

For evaluation of glass material changes, material science experts consulted concurred that a four-point test of the glass material is preferred, as it more evenly loads the glass pane. Flaws present in the glass material are a significant factor in how the glass panel will perform under load, as flaw locations are where fractures will initiate. Test methods that use more localized loading may have more variation in results due to the location of loading relative to the material flaws in the glass panel. Testing 11 glass samples provides a sufficient sample count to assess changes to the glass stiffness and brittle fracture mechanics, based on a Weibull distribution of the data.

Goal: Develop a static bend test method that can evaluate the significance of seat back IFE monitor design changes on blunt trauma to the head, as well as evaluate proposed surrogate targets.

3.5 Component Testing for Sharp Edges

After the development of static bend test methods, there remained a need for a component test method to assess whether a seat back monitor modification has degraded the monitor's ability to withstand head impacts without generating unacceptable sharp edges or loose pieces (frangibility). Previous efforts had an impactor strike a monitor mounted to a rigid surface so that there was no impact energy attenuation other than the monitor. However, this approach, while potentially valid for older and thicker monitor designs that would fail under a compressive load, would not be valid for newer monitor constructions that are more flexible and bend under impact loads.

Goal: Develop a test method that evaluates the significance of seat back IFE monitor design changes on the monitor's ability to not generate unacceptable sharp edges or loose pieces when undergoing a head impact.

4. EVALUATION OF TEST METHODS FOR HEAD BLUNT TRAUMA

Existing HIC test data was compiled to determine which seat and IFE monitor combinations would be suitable test cases for the different test methods proposed. Five seat/IFE combinations were chosen, based on the following criteria.

a. Typical economy class seat designs.

b. Typical seat back IFE monitor designs.

c. HIC data for the seat/IFE combination, both for the "baseline" monitor configuration and modified IFE monitor.

d. Variation in seat design philosophy (data from Safran, Collins Aerospace, and Recaro).

e. Variation in IFE monitor sizes (8.9, 10.6, and 11.1 inches) and manufacturers (Panasonic and Thales).

Initially, the plan was to have data for all four proposed test methods for all five integrated seat configurations in order to determine any trends between different test methods using the same integrated seat design. During impact testing of integrated seats using the HCTD, it became apparent that the head acceleration data generated would not be able to discern performance differences due to changing IFE monitor internal components. At that point, further testing using head component testing methods was discontinued, and the focus shifted to evaluating static bend testing methods and relating variations in monitor stiffness to HIC. See 4.2 for more details.

The seat /IFE monitor configurations and the associated IFE monitor change being investigated are listed in Appendix A (Configurations #1 through #5). More details on the evaluation of each test method are detailed in the rest of this section.

4.1 Row-to-Row Dynamic HIC Testing

Seating manufacturers typically do not repeat row-to-row HIC tests; therefore, sensitivity of HIC results to testing or design variations has not been previously quantified. However, there are a few references available that indicated that the variance in row-to-row dynamic HIC testing results will be much greater than the effect of a typical subcomponent change within an IFE monitor.

a. Effect of ATD variation on HIC test results (see 4.1.1).

b. ARP5765 development (see 4.1.2).

The HIC results for the seat/IFE configurations evaluated in this study are provided in Appendix B. In general, the HIC result between two variations of the seat back monitor design were within 100; however, two data sets show a difference in HIC results over 100, with one comparison differing by 299. Test data is inconclusive whether the differing test results are due to the IFE monitor change, variations in test parameters, the inherent variance in the glass material used in the touch screen, or a combination of factors.

Conclusion: The variance in row-to-row HIC dynamic testing (possibly up to ±200 HIC) will obscure the effect of a typical IFE monitor change, and, therefore, simpler methods are needed.

4.1.1 Effect of ATD Variation on HIC Test Results

In 2011, Recaro Germany conducted a series of HIC tests to determine the variation in HIC results due to factors other than the seat design. A fully adjustable custom “iron seat” (full rigid seat) was built and used to seat two ATDs next to each other. The seat adjustment features were used to match ATD position and seat reference point (SRP) to a production aircraft passenger seat. The same settings were used throughout the testing. See Figure 5 for a picture of the iron seat and location of ATD positioning targets (leg, arm, hip, and head).

Five calibrated Hybrid II ATDs were used in total. Each test was executed with two out of the five ATDs, with varying combinations of ATDs used. All tests used the same type of nylon lap belt and, where applicable, the same generic prismatic type of bottom cushion.

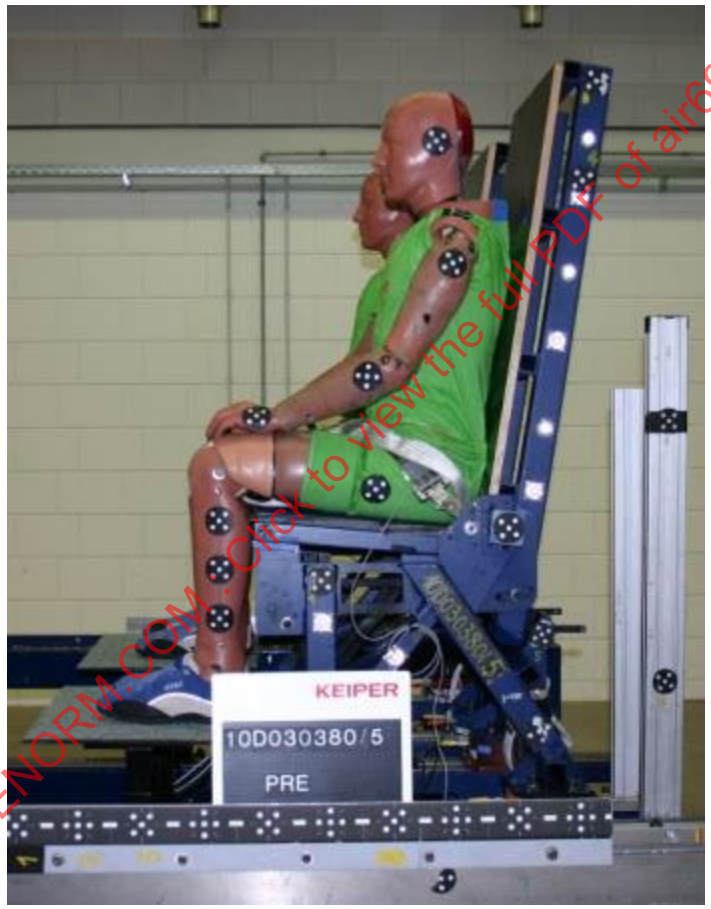

Figure 5 - ATD seated in iron seat

The head impact target was a rigidly supported 2-mm thick Boltaron wall. A wall was used instead of a pivoting seat back in order to generate a more consistent head impact. See Figure 6 for pictures of the impact target.

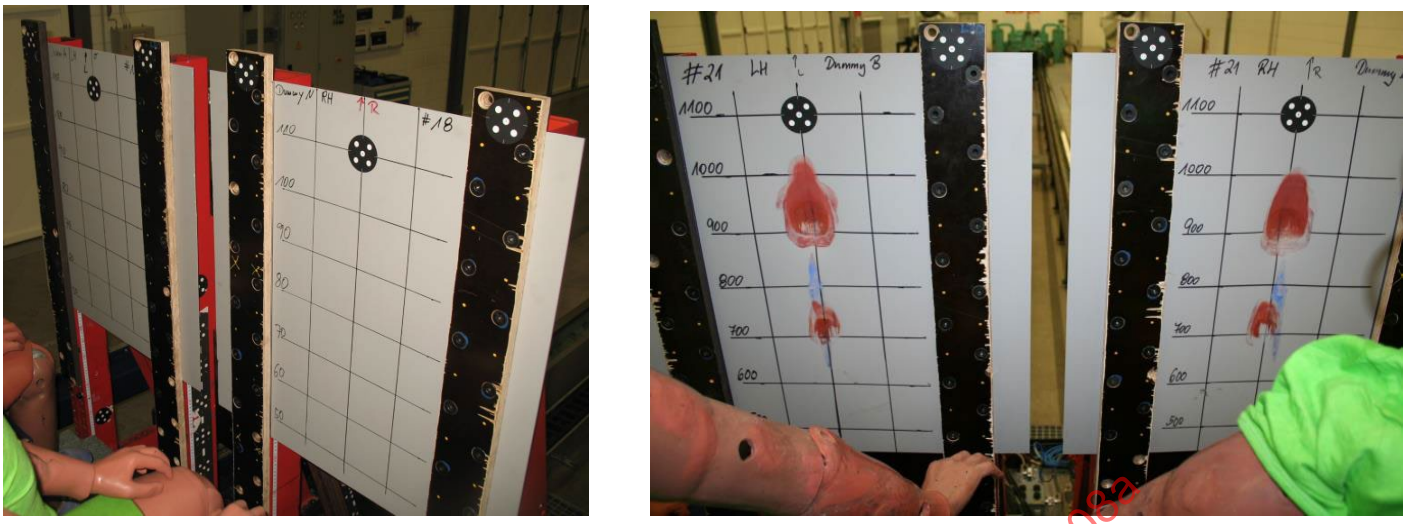

Figure 6 - Head impact test wall

Six tests were performed. Head acceleration results are shown in Table 1. The data was normalized so that the average HIC equaled 100. The HIC range was 1605 to 2177. Tests results show a HIC variance of +12 to -18%, indicating that this one source of variation in HIC testing (the calibrated ATDs) can have a noticeable effect on the HIC measurement.

Table 1 - Head acceleration results from Recaro HIC variation study due to ATD

Test #	ATD #	HIC, avg. = 100	a_max (g)	a_3ms (g)
1	1	104	167	150
2	1	101	160	144
3	1	99	155	142
1	2	98	144	130
2	2	107	160	137
3	2	82	141	125
4	3	96	147	137
5	3	102	150	137
6	3	112	152	144
4	4	89	135	125
5	4	102	142	137
6	4	108	151	139
Average		100	150	137
Min		82	135	125
Max		112	167	150
Variation, total		29	32	25
Variation, from avg.		-18%	-10%	-9%
		12%	11%	9%
Median		101	151	137

Variation within ATD #2 alone: -14% / +12%

Including other test variations (sled deceleration, seat build, lap belt tightness, positioning of ATD in seat, etc.) will increase HIC variation beyond the +12 to -18% variance measured in these tests.

4.1.2 ARP5765 Development

The SAE team working on ARP5765 uses an estimated HIC variance of ±200 for row-to-row dynamic testing criteria, based on industry experience with dynamic testing. While anecdotal, it provides a notional estimate of the variation expected during a typical row-to-row HIC test.

4.2 Head Component Testing of Integrated Seat

Three seat/IFE configurations (#2, #3, and #5) were tested in this investigation. Test results are provided in Appendix C. Testing was performed per FAA policy memorandum ANM-03-115-31, which specifies an initial head strike velocity of 34 ft/s. This specified velocity was verified to be representative of ATD head contact with the seat back during a row-to-row dynamic test. See Appendix D for more details of the seat back head strike velocity study.

The only seat/IFE configuration with head component testing data for two variations of the same monitor design is Configuration #5 (Recaro seat/Panasonic 11.1-inch monitor). The head acceleration plots are consistent, with no indication that the change to the IFE monitor (in this case, the touch screen) made a difference in head impact severity (see Figure C13). However, one test had a head acceleration plot that had a “double peak,” while the other tests only had one peak. As this double peak test was the only one where the touch screen glass fractured, it is reasonable to conclude that the change in head acceleration plot shape can be attributed to the touch screen glass fracturing. Why the glass fractured for this particular test is unknown, as the monitor and seat were built per drawing. However, glass panel failure is sensitive to the flaws in the glass and the location of the applied load relative to flaws, so it could be that there was a flaw in the touch screen glass near the center of the panel.

Configurations #2 and #3 showed considerably more variation in the head acceleration plots. The tested seat and IFE monitor were inspected and were built per the drawing. Due to the variation in test results seen in the integrated seat with the baseline monitor, testing with the modified IFE monitor was suspended. Therefore, all the data presented in Appendix C for Configurations #2 and #3 is of the baseline seat/IFE configuration only.

Unlike the Configuration #5 head component tests where the monitor touch screen did not usually fracture, the touch screen in Configurations #2 and #3 consistently fractured during head impact. The variance in head acceleration between tests is presumed to be due to the variance in flaws within the touch screen glass panel. As this variance is inherent in glass material, it was determined that this test method would likely not provide the consistent test results that could be used to evaluate the effect of a monitor change on HIC.

Conclusion: Head component testing of the integrated seat is acceptable for the defined scope of ANM-03-115-31 (evaluating post-impact sharp edges and non-HIC blunt trauma concerns); however, evaluating the effect of IFE monitor changes on seat HIC performance is doubtful.

In the investigation into the use of head component testing devices, the working team determined that the following additional definition and improvements to the baseline guidance of ANM-03-115-31 could be helpful to those planning on performing head impacts using component test methods. These additions are documented in ARP6330 Section 5.2.

a. Test article configuration definition (both seat and IFE monitor) derived from dynamic test and head component testing experience.

b. An additional head impact when using the FMH. Since the FMH travels in a linear motion, it does not drag down the monitor face similar to an ATD head impact from a seat dynamic test or HCTD. For example, when the FHM impacts the center of the viewing screen, the bottom part of the monitor sustains minimal impact loading. While not a concern for blunt trauma, this lack of direct head contact on the bottom part of the monitor has been an issue for monitor designs where the monitor lower portion has a propensity to break away from the rest of the monitor. Therefore, an additional test in ARP6330 was added to impact the monitor lower edge to evaluate post-impact sharp edges. A 45-degree head impact angle was chosen, as vertical and horizontal vector components are equivalent.

4.3 Head Component Test Using Seat Back Test Fixture

Three IFE monitor designs (Configurations #1, #5, and #6) were tested in this investigation. Test results are provided in Appendix E. Head component testing was performed similar to the parameters outlined in 4.2.

The first tests used small aluminum blocks to mount the monitor to the seat back fixture instead of a typical sheet metal bracket. The idea was that the aluminum blocks have minimal energy attenuation in this test condition. Therefore, this test setup would be considered a conservative representation of seat back monitor installations currently in use. Testing showed that using rigid monitor mounts is too conservative, with monitors exhibiting damage significantly greater than damage due to HIC dynamic testing (see Figure 7). Further work is required to find a test configuration (seat back test fixture and monitor mounting) that is conservative enough to cover a wide range of monitor installations on seat backs but is not so conservative as to cause acceptable monitor designs to fracture into unacceptable sharp edges and loose pieces.

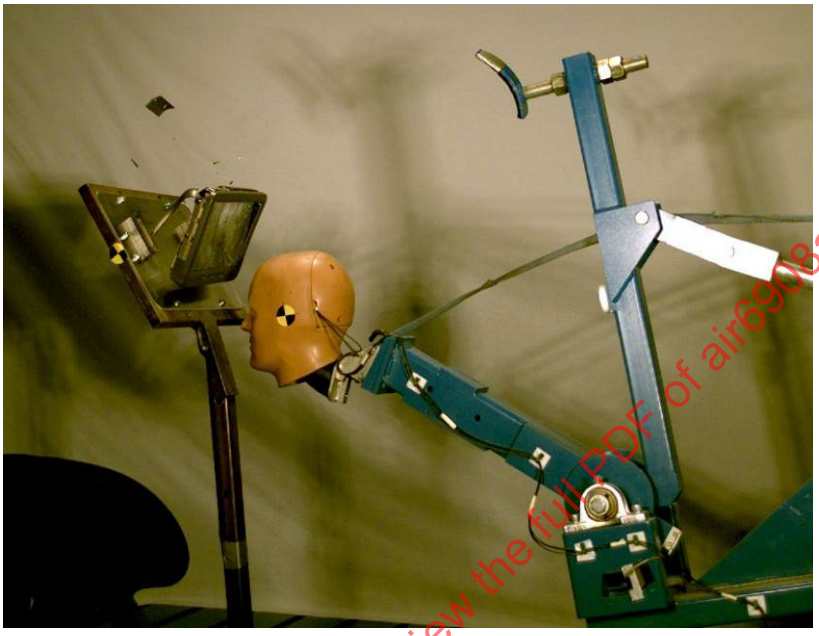

Figure 7 - Head component test using seat back test fixture

Conclusion: Head component testing using the seat back fixture as currently defined requires additional refinement and validation.

4.4 Three-Point Static Bend Tests

Five IFE monitor designs were tested (four production monitors, one “mass equivalent” monitor) to assess the consistency of the test method and to determine general force-displacement patterns. Test results are provided in Appendix F. Test parameters varied from those described in 3.4 and ARP6330 Section 5.3 (load application speed, applicator shape, etc.) due to different labs running tests at different times; however, these testing variations did not affect the consistency or general response of monitor designs. A “mass equivalent” monitor is a dummy part that has the same external dimensions, attachment points, mass, and c.g. as a production monitor and is typically used as ballast during a seat dynamic test. As this “mass equivalent” monitor design is known to be stiffer than a production monitor (plastic screen, metal plates instead of electronics), the mass equivalent monitor was also tested to validate that the three-point static bend test could discern between obviously different monitor stiffnesses.

Test results clearly show the effect of glass failure variability, where the monitor will fail at different points along the force-displacement curve and create a sawtooth pattern. An example of this behavior is provided in Figure 8. However, the monitor force-displacement curve before and after subcomponent failure is sufficiently consistent to be able to make a comparison between two monitor configurations.

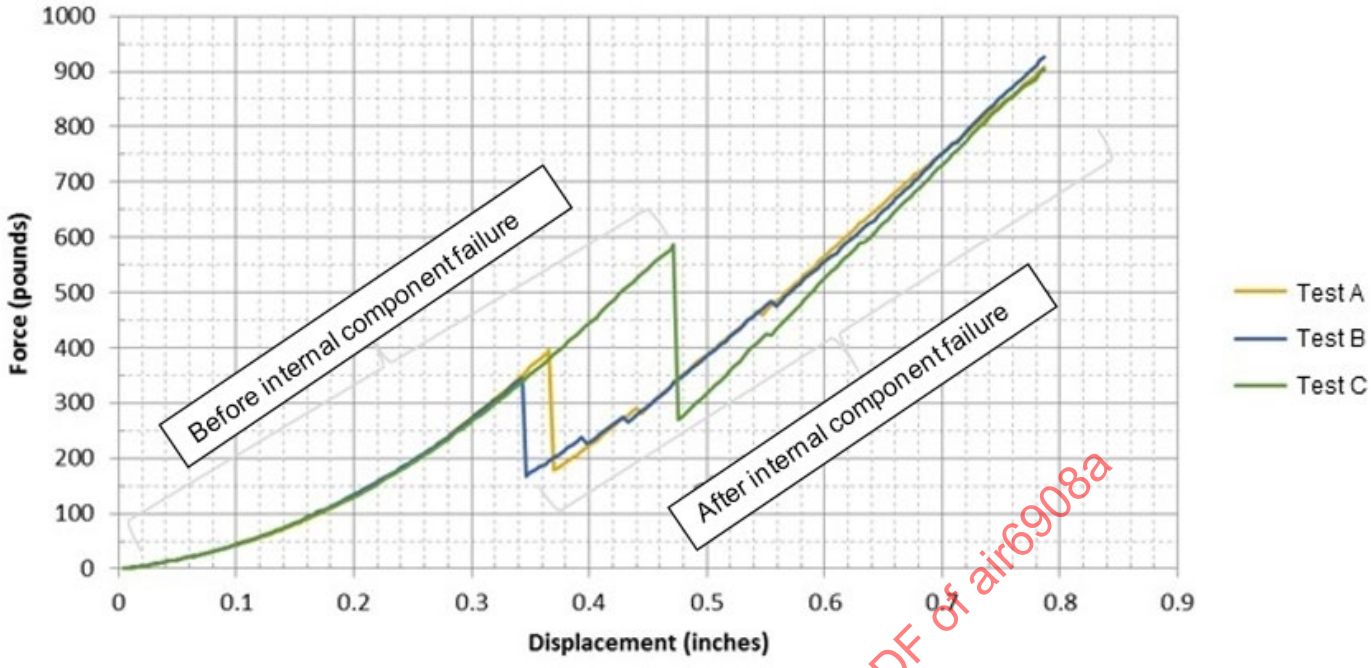

Figure 8 - Example IFE monitor force-displacement curve

While static bending tests can measure the change in stiffness of the IFE monitor, the results do not directly translate to a change in blunt trauma (head acceleration and HIC). Some type of head impact testing (seat dynamic HIC testing, head component testing) was considered in developing a transfer function to correlate the significance of a variation in monitor static test performance to a variation in HIC results; however, the variation in head impact test results made correlating static and dynamic test results doubtful. To determine the sensitivity of HIC results to variations in monitor stiffness, a parametric study was undertaken using analytical modeling techniques defined in ARP5765. This approach allows variation of one monitor parameter (touch screen stiffness, for example) while all other parameters are held constant. Although measuring head acceleration and HIC in absolute terms using analytical methods is not currently an accepted means of demonstrating compliance, measuring the general trends and sensitivities of a seat back monitor change in terms of HIC and head acceleration is feasible.

To reduce the number of variations to be analyzed in the HIC sensitivity study, one monitor design was chosen for analysis: the Panasonic 10.6-inch seat back monitor tested in seat/IFE Configuration #1. The monitor design is representative of the seat back IFE monitors currently being produced: a layered construction of a touch screen, display panel, and electronics packaged in a boxlike structure. The monitor design also includes a polymer protective film on the touch screen that functions to protect the glass from damage and to retain glass fragments if the glass fractures. The monitor is attached to the seat structure by way of threaded mounting holes on the back surface of the monitor. Figure 9 illustrates the typical construction of an IFE monitor.

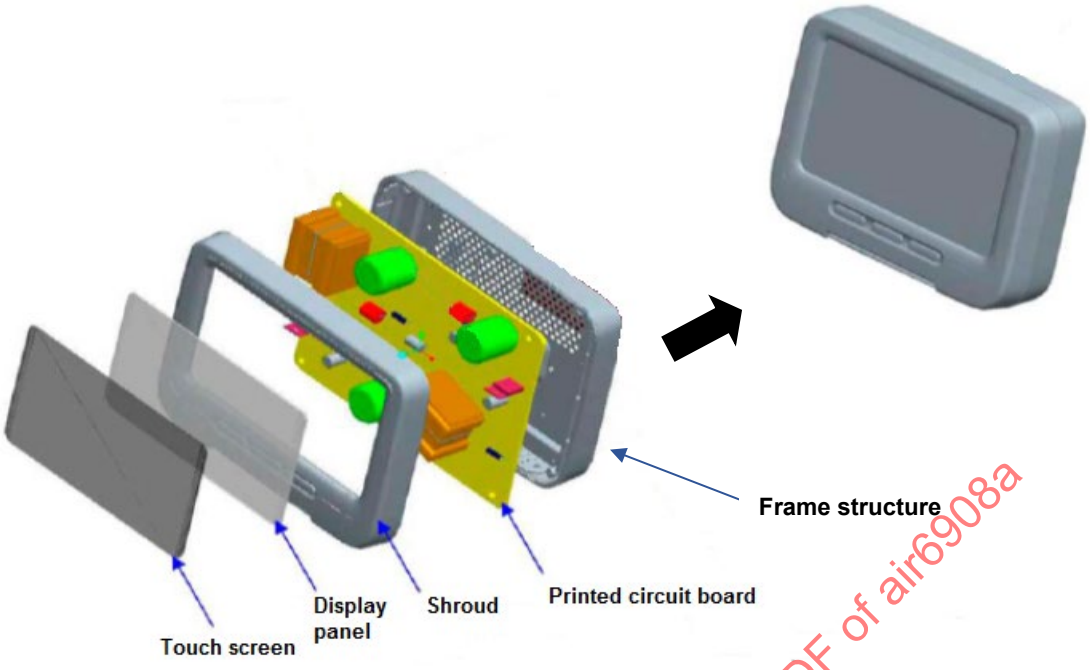

Figure 9 - Exploded view of IFE monitor (example)

Internal components of current monitor constructions, such as the touch screen and display panel, primarily consist of glass materials, which, for this application, are considered non-rate sensitive based on discussions with a major glass manufacturer and literature found on the subject (see 2.1.3).

NOTE: IFE monitor designs where the internal panels deviate from a primarily glass-based construction will need further evaluation to determine whether the new panel component constructions can be considered non-rate sensitive during head impact.

The overall approach to the HIC sensitivity study is shown in Figure 10.

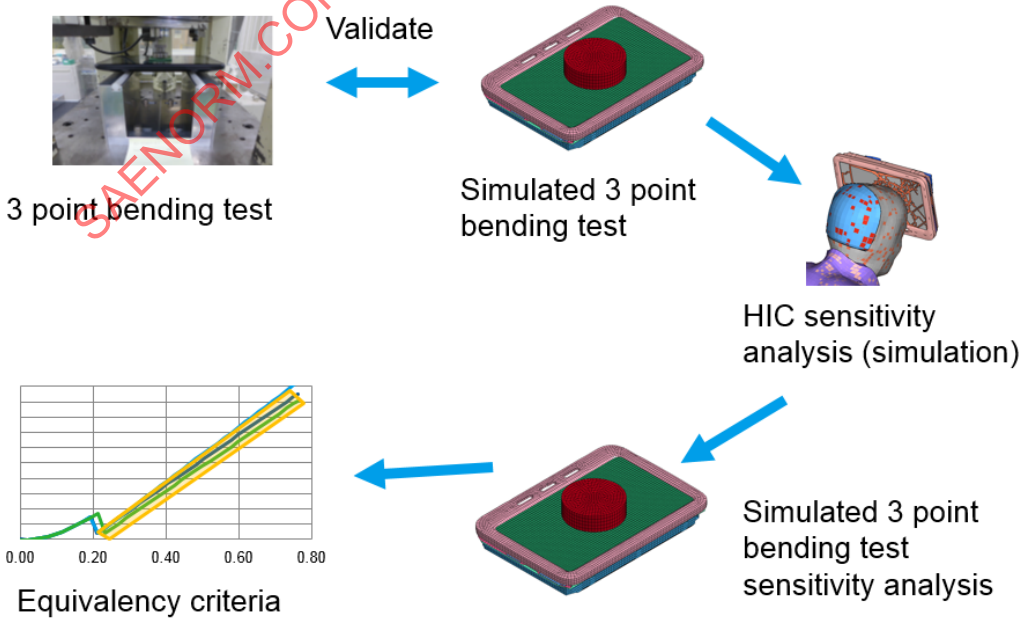

Figure 10 - HIC sensitivity analysis approach

4.4.1 Development of Seat Back Monitor Finite Element Model

The first step was to create a finite element model (FEM) of the Panasonic 10.6-inch monitor from 3D geometry and material properties. The monitor FEM was then calibrated by simulating a three-point bend test using LS-DYNA and correlating results to monitor static bend test data. Correlation results are shown in Figure 11. While the display panel is slightly stiffer than the production monitor, the difference was determined to be negligible for this application.

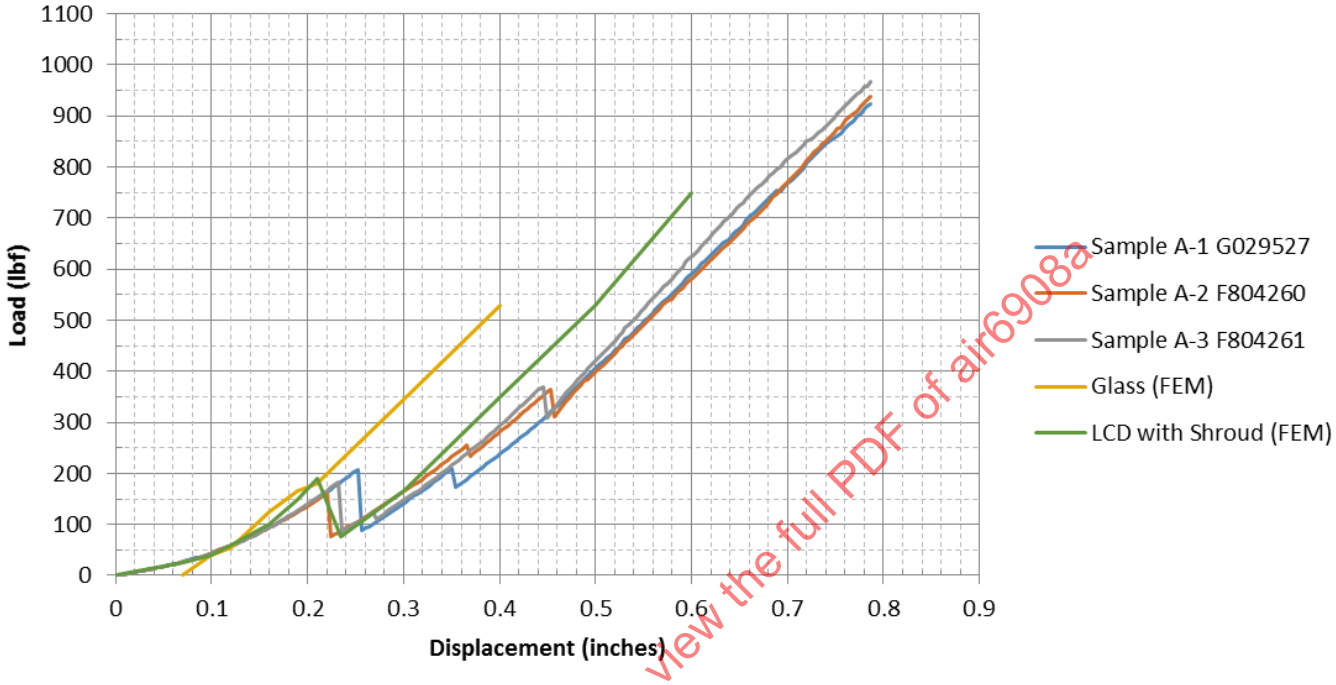

Figure 11 - 10.6-inch Panasonic monitor FEM correlation

4.4.2 HIC Sensitivity Analyses

HIC sensitivity analyses were then performed by Collins Aerospace, Recaro, and Safran of the integrated seat/10.6-inch Panasonic monitor using LS-DYNA. As with the evaluations of head component testing methods, the seat designs analyzed were typical HIC-compliant economy class seat designs currently in production. Separate analyses were performed by the three companies using their engineering teams to develop and analyze models for this sensitivity analysis. This was purposely done to take into account differing design philosophies, approaches to head impact energy attenuation in the seat back design, and modeling techniques.

The analyses concentrated on modifications to the touch screen and display panel, which are the most common monitor subcomponents to be changed. The modulus of elasticity of these subcomponents was adjusted by ±50% to determine whether a change of that magnitude will significantly alter the energy attenuation properties and HIC result of the seat. Variance in the onset of glass fracturing was also analyzed. See Table 2 for a list of the monitor parameters modified. Initially, the stiffness variation to be analyzed was ±25%, but the first few analyses performed did not result in a noticeable change in HIC results, so the variation was increased to ±50%. Collins Aerospace provided additional parametric studies with a range of stiffness values to supplement the ±50% variance dataset.

Table 2 - HIC sensitivity study modified parameters

Configuration	Description	Curve #1 (Glass)	Curve #2 (Internal)	Glass Breakage
1	Baseline	E=10.0×10^6 psi	E=10.0×10^6	Low-range
2	Stiffer touch screen	E=15.0×10^6 psi	Unchanged	Unchanged
3	Less stiff touch screen	E=5.0×10^6 psi	Unchanged	Unchanged
4	Stiffer display panel	Unchanged	E=15.0×10^6 psi	Unchanged
5	Less stiff display panel	Unchanged	E=5.0×10^6 psi	Unchanged
6	Glass breaks later	Unchanged	Unchanged	Largest deflection

Analysis results are provided in Appendix G. Head impacts from both head component test and dynamic test methods were simulated to assess a range of head impact severities.

Most of the analyzed monitor variations did not result in a change in HIC greater than 200, which, as mentioned in 4.1, is the general estimate of HIC variance for seat dynamic testing. Collins Aerospace had two analyses around the HIC of 200 variance, the analysis with the 50% stiffer touch screen (HIC increased by 212) and the analysis with the 50% stiffer display panel (HIC increased by 194). For the other analyses simulating dynamic test conditions, the changes in HIC did not exceed 144. The analyses simulating a head component test did not result in a change in HIC greater than 60 except for one analysis that resulted in a HIC increase of 162. This outlier is especially curious as the same combination of monitor change (stiffer display panel) and seat design (Safran) were also analyzed using seat dynamic test conditions, which resulted in a HIC increase of only 104. Varying the monitor FEM glass material erosion parameters that control the glass fracturing function did not result in significant changes to HIC. This is likely due to the consistency of the glass fracturing function in the model, unlike the glass material itself where fracturing is defined by the random sizes and locations of flaws.

Based on the analysis provided by Collins Aerospace, the acceptable stiffness variance of monitor subcomponents was decreased from 50 to 30%.

Conclusion: Most of the analyzed variations in seat HIC performance due to the changes in monitor component stiffness were below the estimated variance in full scale HIC testing. Therefore, limited changes to monitor component stiffness do not have a significant effect on the integrated seat HIC performance.

4.4.3 Three-Point Bending Sensitivity Analysis

To assess the change in force-displacement curves due to the variations analyzed in the HIC sensitivity study, a three-point bend test of the monitor FEM was simulated using a 30% monitor subcomponent stiffness variation. Results are provided in Figures 12 and 13.

As these variations in monitor stiffness were determined not to have a significant effect on seat HIC performance, a monitor configuration within the range of analyzed force-displacement curve variations is considered similar to the baseline monitor configuration in terms of blunt trauma. The similarity criteria slope variance of ±17.5% for the part of the force-displacement curve before monitor subcomponent failure was determined to be acceptable, as this matches closely to the slope variances calculated for the 30% touch screen stiffness changes (both less and more stiff). For the post-failure portion of the force-displacement curve, all the HIC parametric studies performed consistently showed that the less stiff display panel did not have a significant effect on the HIC performance of a seat design; therefore, even though the calculated slope change in force-displacement curves for less stiff display panels was quite small (-3.9% change), the similarity criteria for the lower bound of the slope range was kept the same as the pre-failure part of the curve (-17.5%) for consistency. Display panels that were stiffer did have a noticeable effect on HIC for the seat design analyzed; therefore, the similarity criteria upper slope change limit of +10% for the post-failure part of the curve is used, based on rounding up the calculated force-displacement slope change of +7.8%.

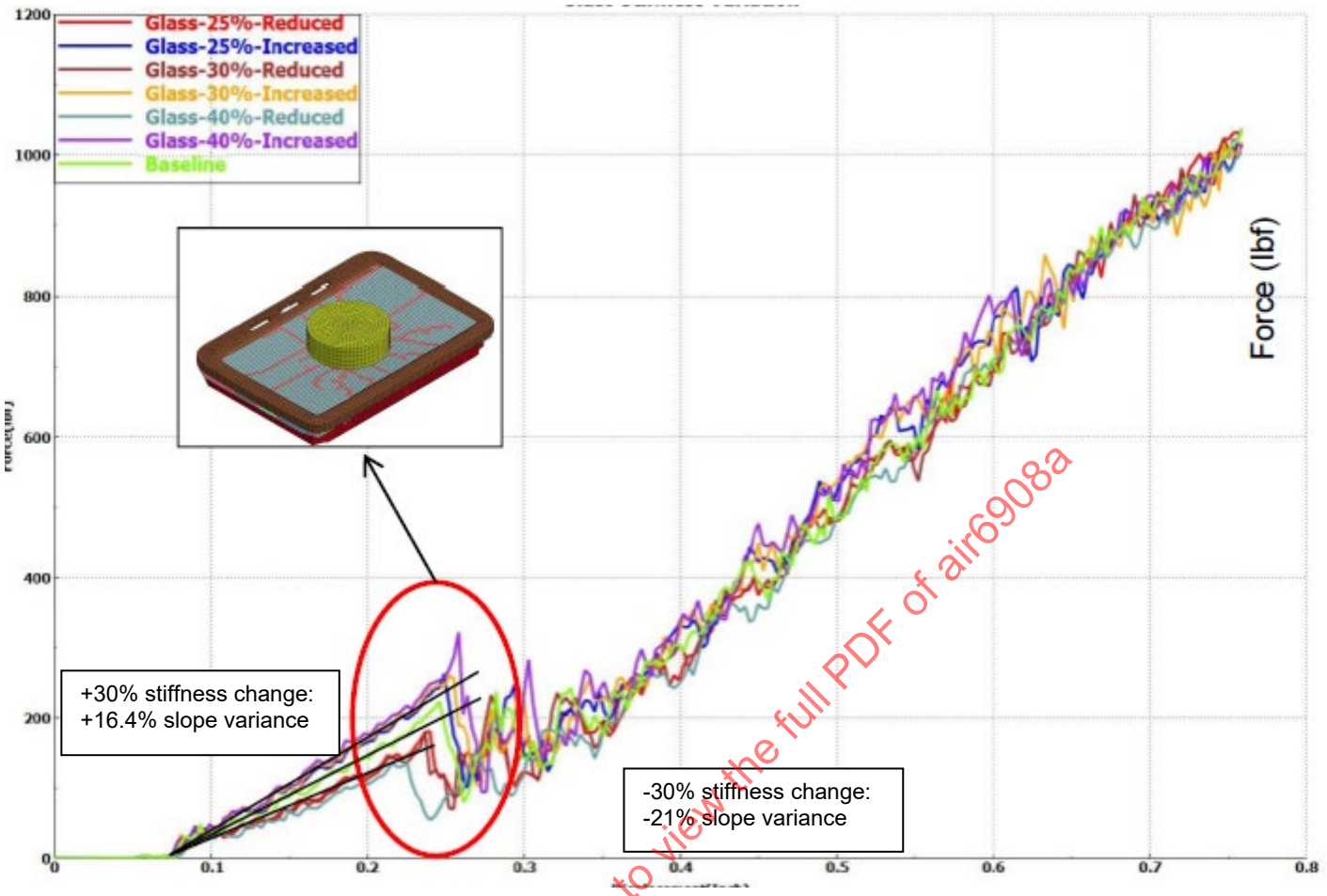

Figure 12 - Three-point bend test simulation - touch screen modulus of elasticity variance

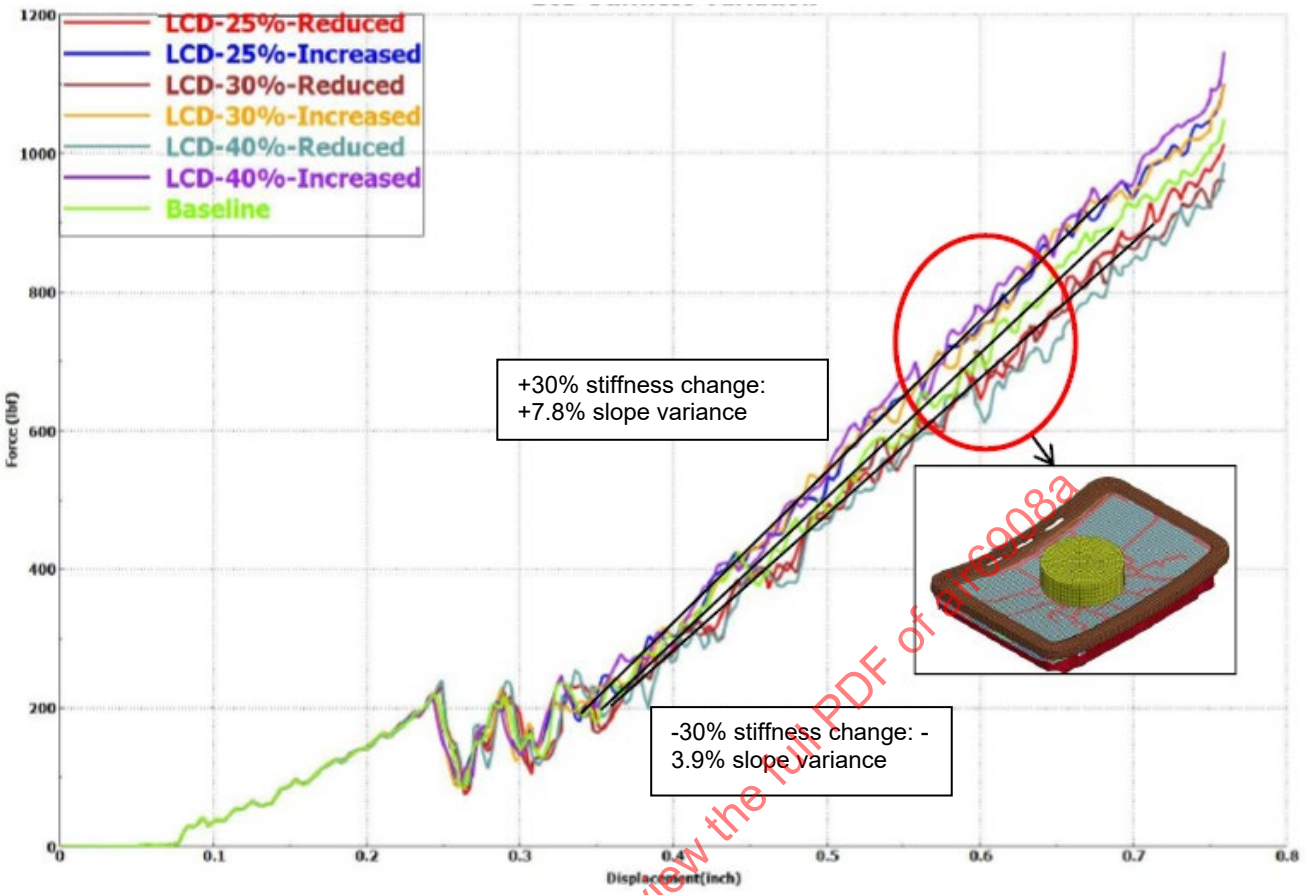

Figure 13 - Three-point bend test simulation - display panel modulus of elasticity variance

4.4.4 Similarity Criteria and Limitations

In addition to the stiffness variations calculated by the three-point bending sensitivity analysis described in 4.4.3, the range where the averaged baseline and revised force-displacement curves are evaluated was limited to (a) avoid comparing curves where initial subcomponent failure is occurring and (b) allow a “settle in” displacement distance at the start of the test.

Initial subcomponent failure has been shown in multiple monitor designs (see Appendix F) to vary primarily due to the use of glass material in the subcomponent panels. As noted earlier, flaws present in glass will be the sites for fracture propagation and significantly affect how the subcomponent (and, therefore, the monitor) will perform under load. As the flaw locations, number, and severity are variable, the load at which initial failure occurs will also vary. It was determined that attempting to compare force-displacement curves within the range of where initial failure occurs (which then results in a step change in load) would likely not be able to accurately assess the effect of the design change. Therefore, portions of the curve before and after initial failure were chosen for comparison. The displacement comparison point of half or three quarters of monitor thickness (depending on overall thickness of monitor) was chosen, as it typically falls between initial subcomponent failure and monitor catastrophic failure. A more complex method of determining a comparison point based on the range of initial failures was discussed; however, it was decided a simpler method based on monitor thickness would provide for a sufficient comparison criteria.

A displacement distance of 0.1 inch (2.54 mm) from initial load application was chosen as the “settle in” displacement because it is typically less than the displacement at the initial subcomponent failure and allows the force applied to the monitor to reach a level where comparing curves with a 17.5% variance was not overly restrictive. For example, the allowable stiffness variance at 30 lbf (133 N) would only be ±5.25 lbf (23.4 N).

Limiting the ARP6330 similarity criteria to IFE monitors with attachment locations on the monitor back surface was due to the scope of the analyses performed. Similar analyses for monument mounted monitors or monitors with different attachment locations could be performed to define a similar criteria for those monitor installation parameters.

The applicability limitation based on the integrated seat HIC value is included in ARP6330 to provide an additional level of conservatism in the use of the three-point bend test similarity criteria. HIC parametric studies generally show a higher sensitivity to touch screen changes than display panel changes. The average HIC variance due to a 50% increase or decrease in touch screen modulus of elasticity was +130 and +43, respectively, while a similar variance in the display panel resulted in an average HIC variance of +117 and -22. The ±30% variance in monitor subcomponent modulus of elasticity for the Collins seat design showed that the touch screen still had a noticeable variance in HIC (+71 and +144), while the display panel HIC variance decreased significantly (+63 and +3). A reduction in monitor component stiffness variation is expected to have similar results in the Recaro and Safran designs (display panel HIC variance will be reduced more than the touch screen variance).

The display panel variance shows more consistency as the HIC increases with increasing display panel stiffness. Since the Collins analysis of a ±30% results in a maximum HIC variance of +63, the HIC applicability limitation for the display panel similarity criteria is 940 (1000 - 63 = 937 rounded up to 940). The overall HIC variance range of the Collins seat due to ±30% stiffness change to the touch screen is +71 (more stiff) to +144 (less stiff). Therefore, using the +144 variance, the HIC applicability limitation for the touch screen similarity criteria is 860 (1000 - 144 = 856 rounded up to 860).

5. ENERGY ATTENUATION STUDY

To further analyze what is happening during an ATD head impact with an integrated seat back, a study on how the monitor contributes to the overall energy attenuation of the seat back system was undertaken by Recaro and Safran. The same FEMs and dynamic loading conditions used in the HIC sensitivity study were used for this study. Results are provided in Appendix H.

Total head impact energy dissipated by the integrated seat back is equivalent in both simulations (Recaro = 353.9 J, Safran = 346.4 J). The Recaro integrated seat design attenuates head impact energy primarily by internal strain energy (material deformation), while the Safran integrated seat design attenuates head impact energy primarily by kinetic energy (transference of momentum). Changes to a monitor typically do not significantly change monitor mass or c.g. (kinetic energy); therefore, the primary concern is whether the internal strain energy characteristics of the integrated seat are affected. Study results show internal strain energy attenuation is accomplished by the seat back structure (≈60%), followed by the monitor (≈30%) and monitor tilt bracket (≈10%). See Figures 14 and 15 for the distribution of energy dissipation in Safran and Recaro analyzed integrated seat backs. Plots of seat back internal strain energy over time are provided in Figure H1 (Recaro) and Figure H4 (Safran).

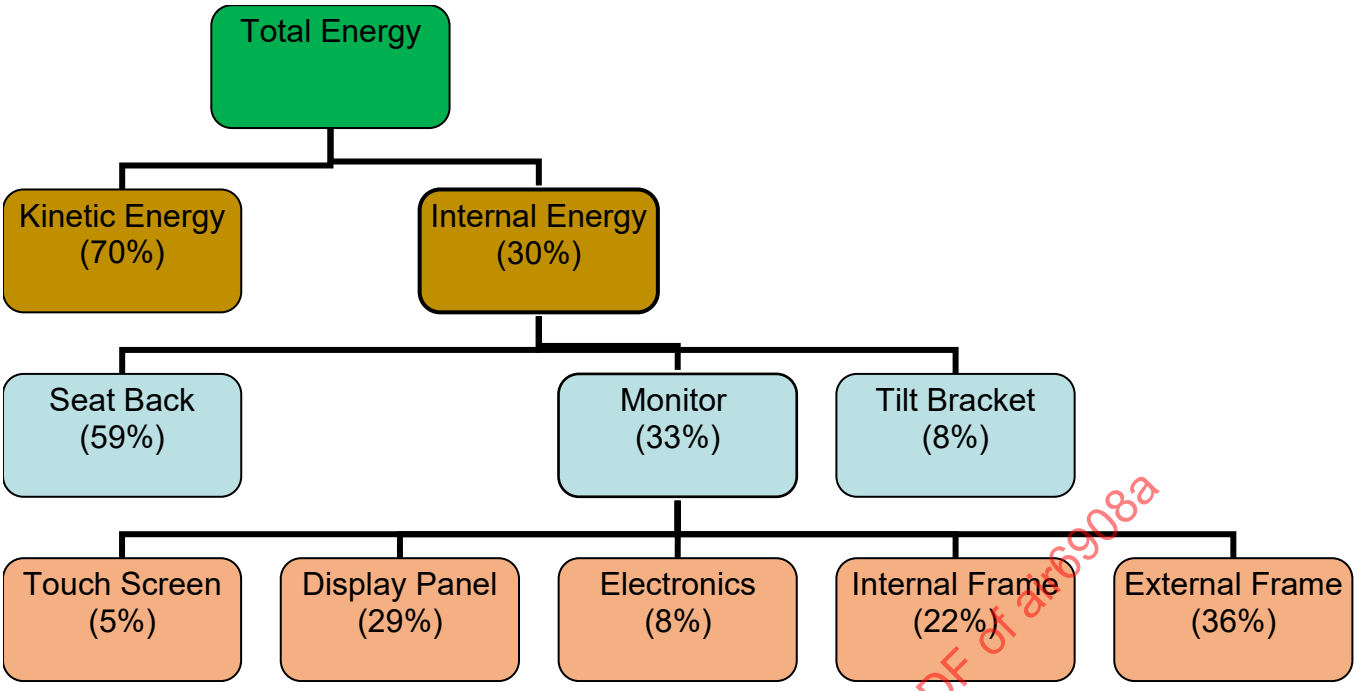

Figure 14 - Summary of seat back energy attenuation - Safran

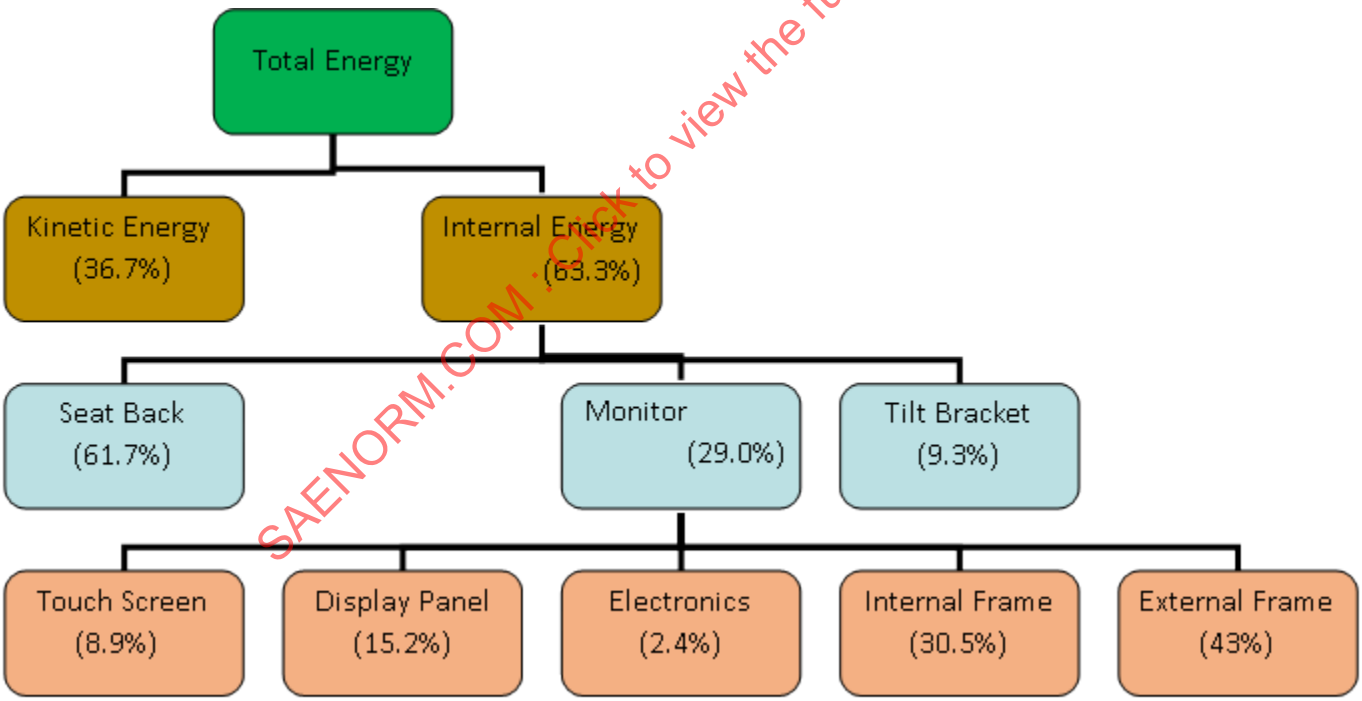

Figure 15 - Summary of seat back energy attenuation - Recaro

Of the various components that make up an IFE monitor, the monitor frame structure (internal and external) dissipates most of the internal strain energy being attenuated by the monitor. The monitor components prone to design changes or obsolescence (touch screen, display [LCD] panel, and electronics) contribute significantly less. This is due to the construction of current IFE monitor designs.

a. The frame structure is primarily aluminum (ductile), while the internal components are primarily glass (brittle).

b. The internal components are attached to the monitor frame; therefore, load imparted to the internal components are being reacted by the frame.

c. The glass material in the monitor internal components will fracture, significantly reducing further energy attenuation by the component.

Plots of monitor internal strain energy over time are provided in Figure H2 (Recaro) and Figure H5 (Safran). The monitor components experience loading at initial head contact, with the electronics lagging by around 1 ms. This is due to the electronic components positioned in the back of the monitor. The contribution of the display panel (LCD panel) to seat back energy attenuation differs between FEM analyses, with the Safran seat design seeing a larger contribution by the display panel than the Recaro design. However, the overall contribution of the display panel for both seat designs is less than 3%. Other panel components, such as the electronics and touch screen, have a lower overall contribution to energy attenuation.

Analysis results also showed the effect of touch screen and display panel stiffness changes on seat back and monitor internal strain energy distribution is minimal. Analysis results are provided in Tables H4, H5, H9, and H11. Safran also calculated the effect of eliminating glass fracturing (no glass erosion) in the touch screen, and for their seat design, the effect was also minimal (see Table H10). This could be due to the already small contribution of the touch screen in attenuating head impact energy.

6. SURROGATE TARGET EVALUATION

Currently, if the IFE monitor is being contacted by the ATD head during HIC testing, the IFE monitor needs to be representative of the production part. This subjects the monitor design to repeated evaluation of frangibility characteristics, even though the monitor design has previously shown an acceptable level of robustness through previous head impact testing. FAA policy memorandum ANM-03-115-28 describes the use of a surrogate target in blunt trauma tests, where a 1/4-inch aluminum plate may be used as a substitute for the production monitor. The aluminum plate is much more rigid than seat back monitors and does not provide the impact energy attenuation of a seat back monitor, particularly in the first few milliseconds of head contact. Therefore, meeting the HIC < 1000 criterion using an aluminum plate is highly unlikely. The policy does allow the use of surrogate parts less rigid than an aluminum plate; however, additional substantiation is necessary.

One potential method of using the FAA surrogate part policy is to adapt the production monitor to be less frangible while still retaining its impact energy attenuating capability. The working team explored the idea of applying a polymer tape or wrap to the external surface of the monitor to make it a type of non-frangible surrogate part. The general concept is similar to the AC 25.562-1B Change 1 guidance for retention of mass items under dynamic loads, where once the retention of a mass item is already demonstrated, the design aspect has been validated and, therefore, subsequent tests may be conducted with the mass secured.

To evaluate the possible change to monitor impact energy attenuation performance with the addition of tape, Panasonic tested three monitor configurations using the seat back test fixture described in 4.3: no tape added (baseline configuration), duct tape added, and mover's stretch wrap added. Additional layers were added for conservatism. See Figure 16 for pictures of test samples.

Figure 16 - Panasonic 10.6-inch monitor with duct tape and mover's wrap added

Two locations on the monitor were impacted: center of viewing screen and the bottom edge of the monitor. Head impacts to the bottom edge of the monitor shroud were added to the testing as there were questions whether the addition of tape would affect how the ATD head would slide over the shroud edge. See Figures 17, 18, and 19 for pictures of the head strike locations tested.

Figure 17 - Seat back test fixture head strike locations

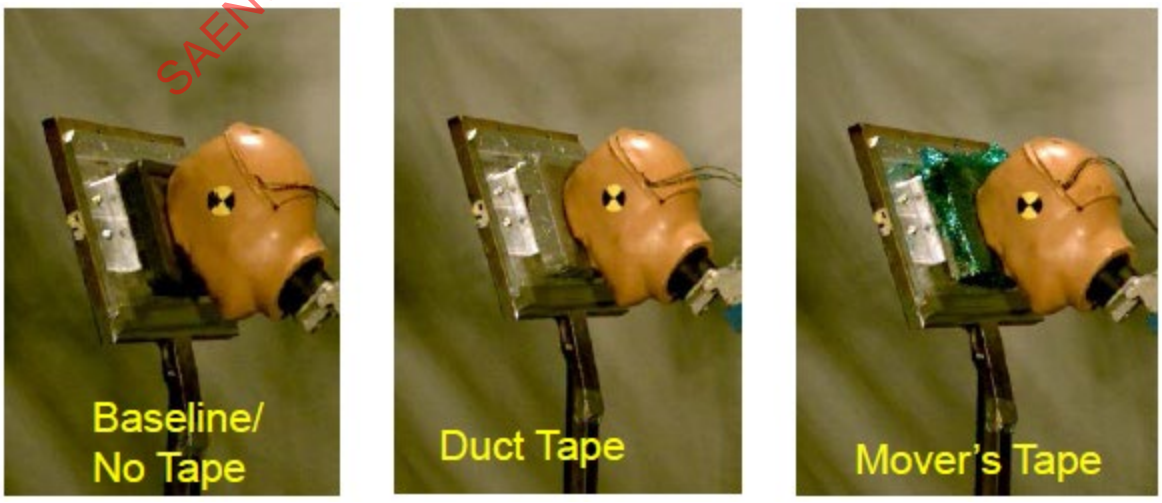

Figure 18 - Head component testing with added tape - center of view screen

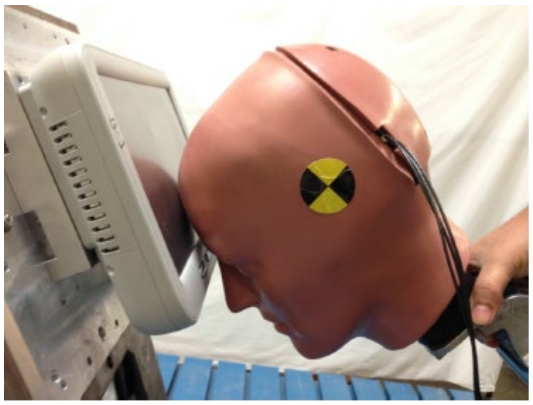

Figure 19 - Head component testing - bottom edge

Test results area provided in Appendix I and show HCTD HIC results did not vary by more than 10%, which is within the normal variance seen in this type of impact testing. Head strikes on the bottom edge showed lower HIC numbers for the taped monitors but did not vary by more than 10%.

Conclusion: The addition of a thin layer of tape (<0.010 inch [10 mils]) does not affect head contact or the energy attenuation properties of the monitor and, therefore, would not alter the HIC results of the integrated seat.

7. DEVELOPMENT OF IMPACT TEST TO ASSESS MONITOR FRANGIBILITY

The following goals were used in developing a test method for monitor frangibility.

a. The monitor is allowed to bend during the impact.

b Test method is conservative enough to cover a wide range of seat back installations but not so conservative as to significantly overestimate head impact severity.

c. Impact energy is attenuated in a similar fashion as a seat back:

   1. Monitor alone attenuates impact energy at initial head contact.

   2. Monitor + structure attenuates the rest of the impact energy.

d. The test method allows for adjustment of impact characteristics and severity.

e The test is simple to set up and run.

f. Consistent results.

As stated earlier, older monitor designs were thicker and more rigid, and the typical design issues experienced were due to compressive loading, unlike the thinner and more flexible monitors, which undergo bending. Therefore, standoffs, brackets, or some other way of spacing the monitor aft surface away from fixture surfaces was needed.

Developing an approach on how to define the impact severity on the monitor was challenging, and multiple ideas were proposed, such as:

- A test fixture and test method defined to represent a seat back with a HIC = 1000.
- A test fixture and test method that matched a “generic” seat energy attenuation profile.
- Test with a “generic” seat back.
- A test matching the head deceleration of 1-inch (25.4-mm) thick padding typically used for head impact protection.

Because each seat design has its specific way of attenuating head impact energy (see Section 5), it was decided to not try and define the behavior of a “generic” seat, or how a seat can meet the HIC ≤ 1000, but focus on the monitor behavior itself.

From initial investigations of seat back reactions to head impact during seat dynamic testing (see Appendix G) plus discussions within the SAE SEAT Committee, it was desired to replicate the general behavior of how monitor installations attenuate energy when installed on a seat; first the monitor and then the monitor + mounting structure (brackets, seat back, etc.). This goal plus the other goals expressed by the committee (adjustable, simple, and consistent) resulted in a test fixture that is primarily rigid, with the only impact energy attenuating features being the monitor and an aluminum sheet. Aluminum has been used in the past as an impact attenuator when researching HIC compliance with bulkheads. It is also easy to procure, easy to work with, provides repeatable results, and different thicknesses are available.

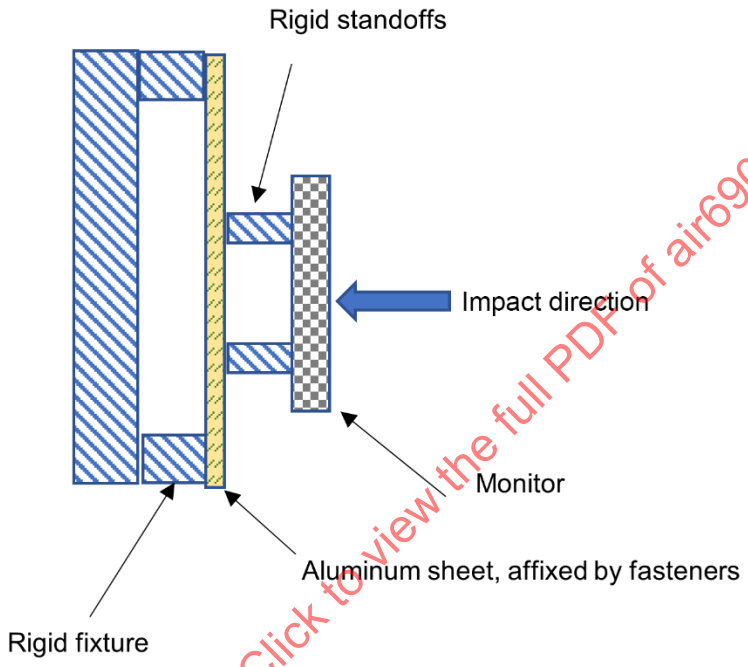

Figure 20 - Monitor impact test fixture

7.1 Initial Assessments Using Simulation

To assess the proposed test fixture, simulations using different impactors (free motion headform and pendulum impactor), aluminum thickness, and impact velocity were performed. The monitor model used was the baseline Panasonic 10.6-inch model used in the previous three-point bend test simulations. Findings were the following.

a. The test method generates an impactor deceleration curve with an initial short duration pulse followed by a longer duration second pulse, which is a general pattern seen in seat back HIC testing.

b. Aluminum thickness primarily alters the impactor second deceleration pulse.

c. Impact speed alters amplitudes of both peaks in the impactor deceleration.

d. The pendulum impactor, due to the larger mass, creates a larger secondary deceleration pulse.

Results of these simulations are provided in Appendix J. Based on these results, the decision was made to perform physical testing to assess the test method and test fixture for consistency and ease of use and to gather additional data. For the initial round of testing, a linear metallic hemispherical impactor per FMVSS 201 was used due to its impact consistency and ability to easily derive impactor energy during an impact.

7.2 Impact Testing

The first few impact tests were performed with strain gages installed on the aluminum sheet with the idea that by measuring the behavior of the aluminum sheet, the contribution of the sheet in attenuating the impact could be quantified. This data could also be used in assessing the accuracy of the simulations previously created. The post-test condition of the aluminum sheets was also scanned to measure deformation. While these efforts yielded additional data, it became clear this made the testing burdensome and that a more straightforward method would be to use the impactor acceleration data to assess energy attenuation of the monitor.

Test parameters for the first series of tests (three with the same monitor, one test without monitor) are provided in Table 3. The monitor used in all tests was a Panasonic 9-inch designed for seat back installations.

Table 3 - Monitor frangibility impact test parameters

Parameter	Value	Why?
Impactor	Linear hemisphere	• Industry standard • One axis
Aluminum sheet thickness	1/16 inch (1.58 mm)	Simulations show thinner sheet represents head deceleration better than a thicker sheet (higher initial peak, lower secondary peak).
Impactor velocity	22 ft/s (6.7 m/s)	Highest impact velocity where simulations show that the aluminum sheet would not deflect into the fixture.
Impactor angle	Perpendicular with screen surface	Keep load condition simple (one axis)
Impactor contact location	Center of monitor screen	• Maximum bending of monitor • Loading monitor area of change (glass, plastic film, etc.)

Test results showed the following.

a. An impact with the behavior desired, with the first 5 ms of the impact being attenuated by the monitor, followed by another peak involving the monitor mounting. See Figure 21.

b. The same test parameters resulted in similar results.

c. The contribution of the monitor to attenuate the impact was noticeable in the test data. Adding a monitor to the impact load path reduced the impactor peak force while the impact duration increased. See Figures 22 and 23.

Feedback from the test lab is that the test setup is straightforward after elimination of the strain gages.

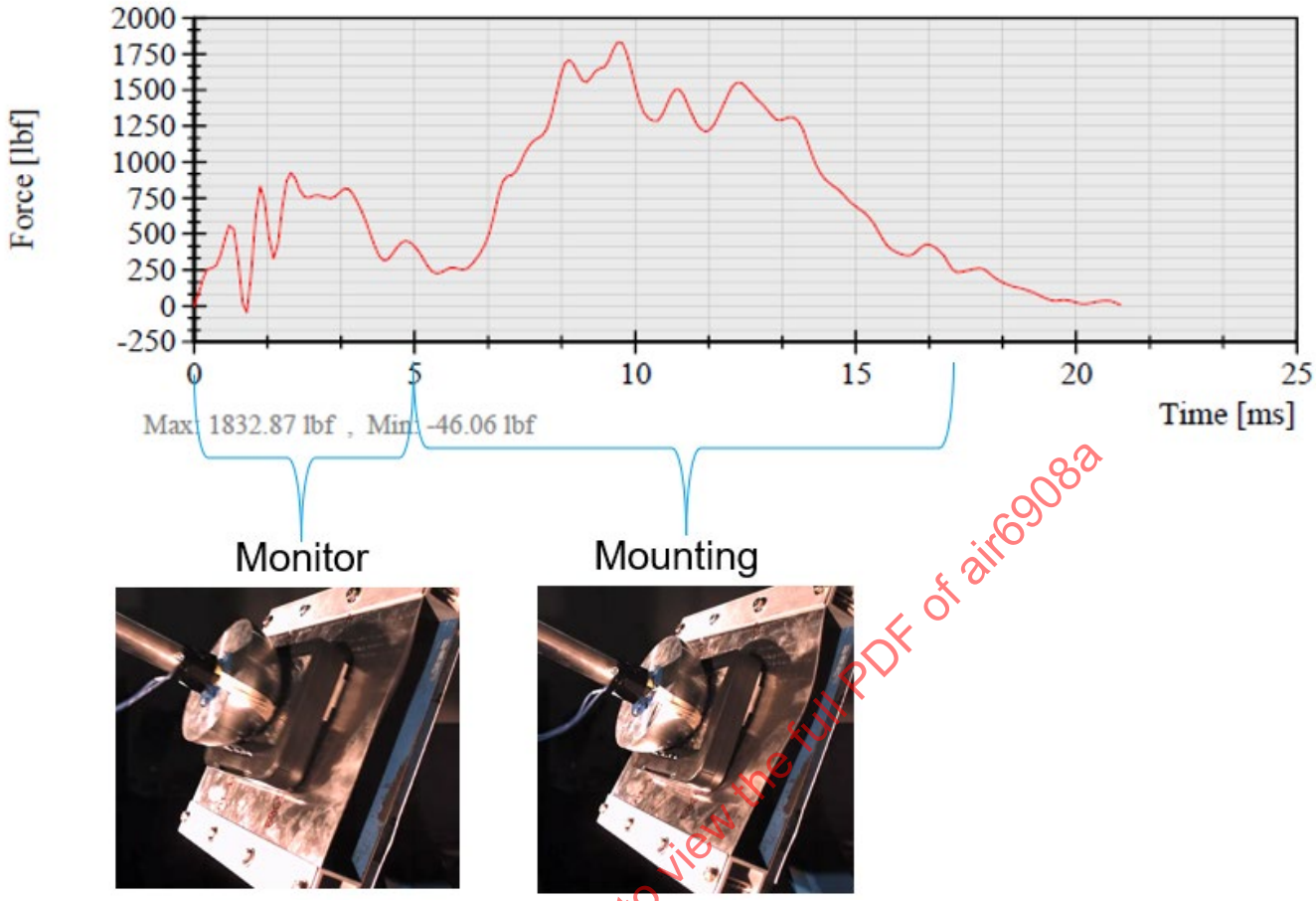

Figure 21 - Frangibility testing - general characteristics

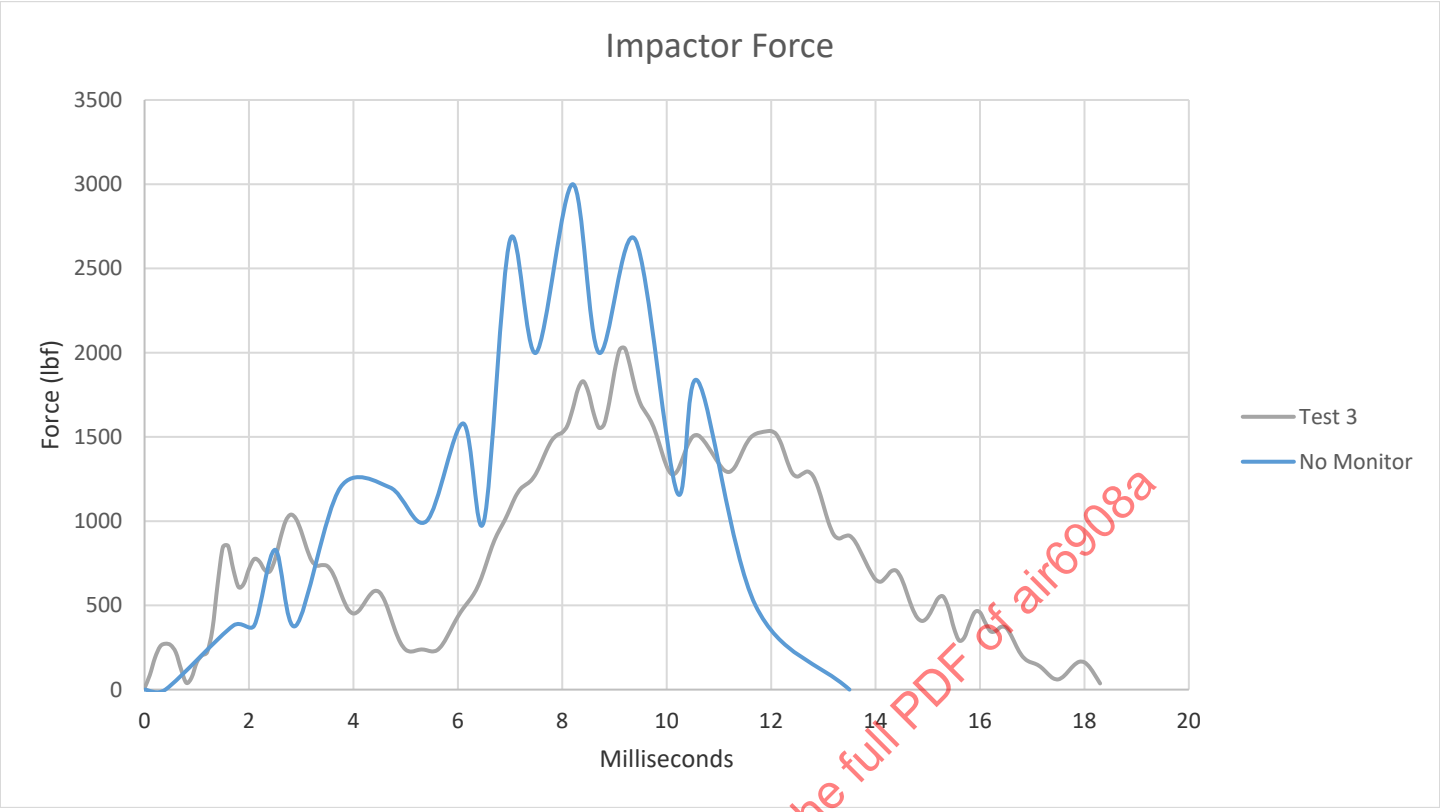

Figure 22 - Frangibility test impactor force - with and without monitor

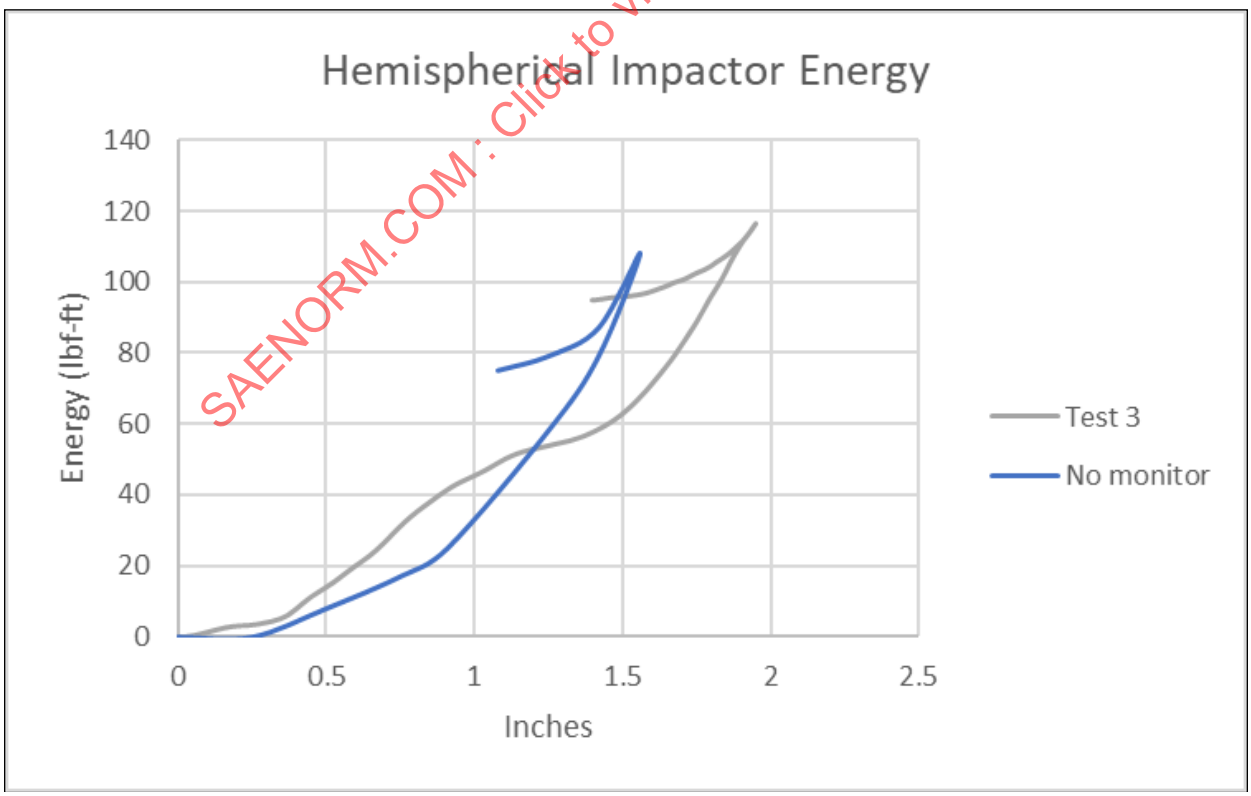

Figure 23 - Frangibility test impactor energy - with and without monitor

Another series of tests were performed with a higher impact velocity of 35 ft/s (10.7 m/s) to see how an increase in impactor velocity would be reflected in the test data. As expected, the peak force and impact duration increased relative to the tests performed at 22 ft/s (6.7 m/s).

Test data is provided in Appendix K. In all tests, the lab personnel verified there was no contact between the aluminum sheet and the test fixture.

8. NOTES

8.1 Revision Indicator

A change bar (I) located in the left margin is for the convenience of the user in locating areas where technical revisions, not editorial changes, have been made to the previous issue of this document. An (R) symbol to the left of the document title indicates a complete revision of the document, including technical revisions. Change bars and (R) are not used in original publications, nor in documents that contain editorial changes only.

PREPARED BY SAE AIRCRAFT SEAT COMMITTEE

APPENDIX A - SEAT/IFE MONITOR CONFIGURATIONS INVESTIGATED

Table A1 lists the integrated seat configurations being investigated, the associated IFE monitor change, and the type of test data gathered.

Table A1 - Seat/IFE monitor configurations investigated

Configuration (Seat/IFE)	IFE Monitor (Baseline)	Monitor Modification	HIC Testing	HCTD Testing (Seat)	HCTD Testing (Fixture)	Three-Point Bend Testing
1. Safran Seats USA / Panasonic	10.6 inch	Display panel replacement	X		X	X
2. Safran Seats USA / Thales	10.6 inch	Display panel change	X	X		X
3. Safran Seats USA / Thales	8.9 inch	Display panel replacement	X	X		X
4. Collins / Thales	10.6 inch	Display panel change	X			X
5. Recaro / Panasonic	11.1 inch	Touch screen change	X	X	X	X
6. None / Panasonic	9-inch mass equivalent	N/A			X	X

APPENDIX B - SEAT DYNAMIC TEST HIC RESULTS

HIC results for the five integrated seat configurations investigated are provided in Tables B1, B2, and B3. The “HIC zone” referred to is the location of the seat back being struck by the ATD head as defined in FAA AC 25.562-1B, Appendix 4. Figures B1 and B2 provide photos of monitors in their post-test condition.

Table B1 - Safran Seats USA HIC test data

			Baseline Monitor		Modified Monitor		
Configuration	**HIC Zone**	**Seat Pitch (inches)**	**Test #**	**HIC**	**Test #**	**HIC**	**Δ HIC**
1	C	--	K06013	855	N/A(1)		
2	C	--	K09042	772	K14137	817	+45
3	C	--	K10060	817	K14112	738	-79

(1) HIC test data was not available for this seat/IFE monitor configuration.

Table B2 - Collins Aerospace HIC test data

			Baseline Monitor		Modified Monitor		
Configuration	**HIC Zone**	**Seat Pitch (inches)**	**Test #**	**HIC**	**Test #**	**HIC**	**Δ HIC**
4	C	30	WS4372	940	WS5891	641	-299
4	A	34	V12-890	735	V14-458	719	-16
4	A	32	WS5690	842	WS5845	817	-25

Figure B1 - Collins Aerospace HIC test post-test photos - modified monitors (Zones C and A)

Table B3 - Recaro HIC test data

			Baseline Monitor		Modified Monitor		
Configuration	**HIC Zone**	**Seat Pitch (inches)**	**Test #**	**HIC**	**Test #**	**HIC**	**Δ HIC**
5	C	--	--	660	--	805	+145

Figure B2 - Recaro HIC test post-test photos - baseline and modified monitor

APPENDIX C - INTEGRATED SEAT HEAD COMPONENT TEST DATA

C.1 CONFIGURATION #2: SAFRAN SEATS USA/THALES 10.6-INCH MONITOR

Head component test data for Configuration #2 is provided in Table C1. ATD head velocity and acceleration are provided in Figures C1 and C2. Post-test photographs of the monitors are provided in Figures C3 to C7.

Table C1 - Configuration #2 test results - baseline monitor only

Test #	Impact Head Velocity (ft/s)	Max Resultant Head Acceleration (g)	HIC	HIC Duration (ms)	Δ Max Head Acceleration From Average (g)	Δ HIC From Average
H14089	34.6	221	665		+13	+117
H14090	35.2	144	335		- 64	-213
H14126	35.4	199	410		- 9	-138
H14127	35.4	238	705		+ 30	+157
H14128	34.2	236	624		+ 28	+76
Average		208	548			
Variance		94	370			

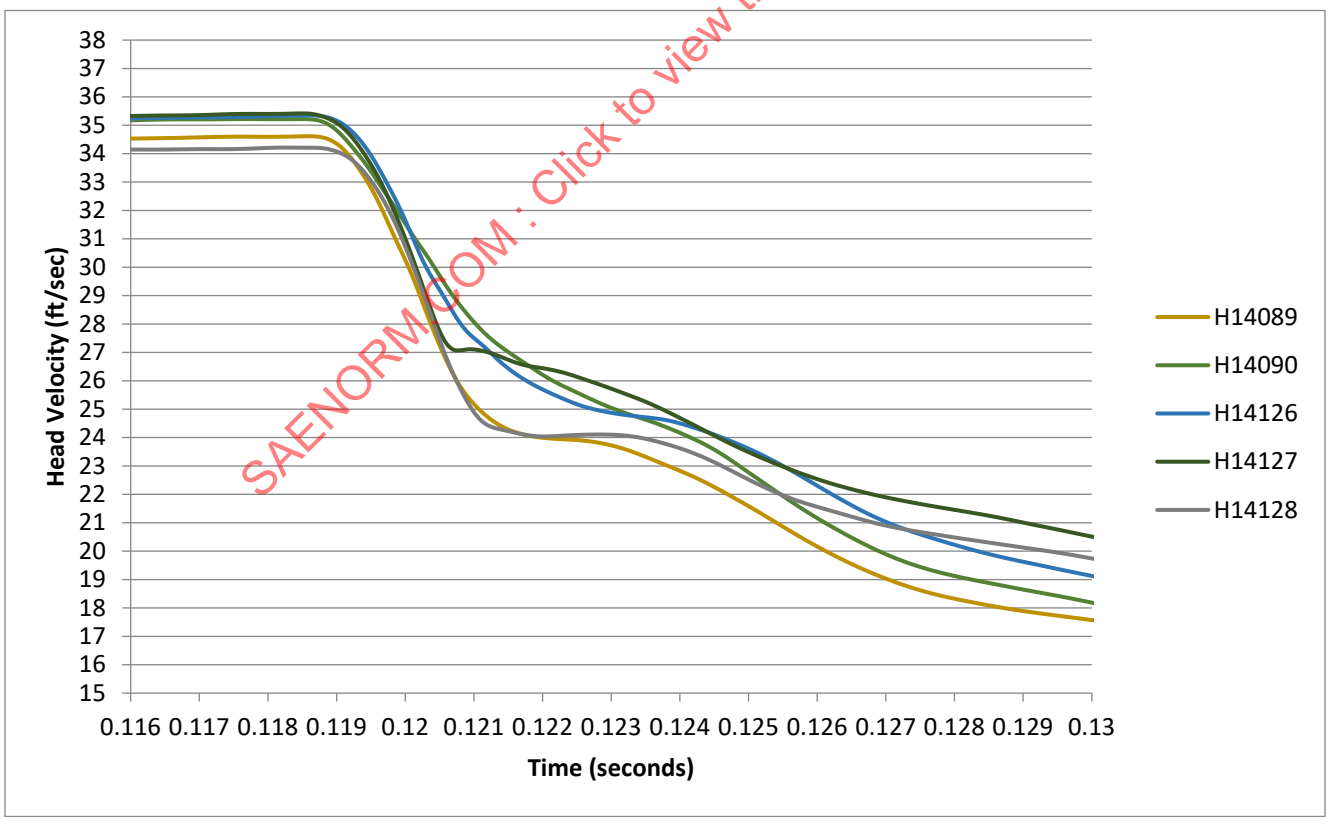

Figure C1 - Configuration #2 ATD head velocity during impact test

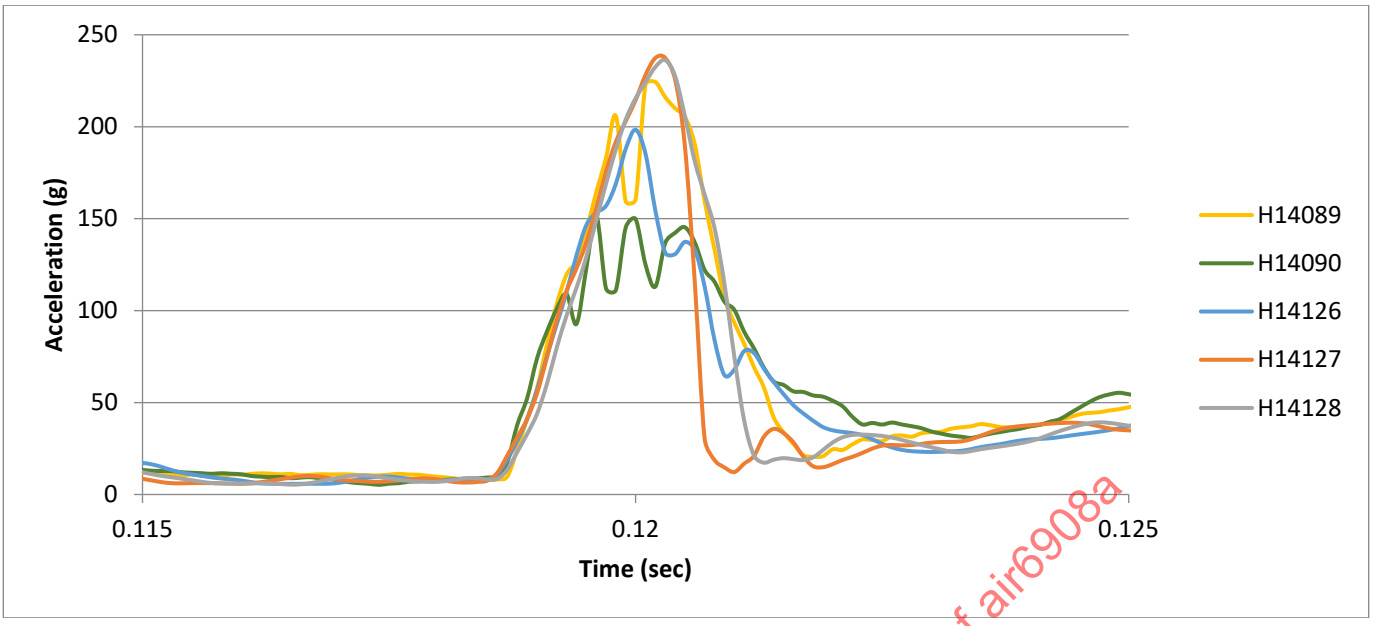

Figure C2 - Configuration #2 ATD head c.g. resultant acceleration

Figure C3 - H14089 post-test photo

Figure C4 - H14090 post-test photo

Figure C5 - H14126 post-test photo

Figure C6 - H14127 post-test photo

Figure C7 - H14128 post-test photo

C.2 CONFIGURATION #3: SAFRAN SEAT USA/THALES 8.9-INCH MONITOR

Head component test data for Configuration #3 is provided in Table C2. ATD head velocity and acceleration are provided in Figures C8 and C9. Post-test photographs of the monitors are provided in Figures C10, C11, and C12.

Table C2 - Configuration #3 test results - baseline monitor only

Test #	Impact Head Velocity (ft/s)	Max Resultant Head Acceleration (g)	HIC	HIC Duration (ms)	Δ Max Head Acceleration From Average (g)	Δ HIC From Average
H14133	34.9	177	500		-8	-47
H14134	35.2	183	556		-2	+9
H14135	34.5	196	584		+11	+37
Average		185	547			
Variance		18	84			

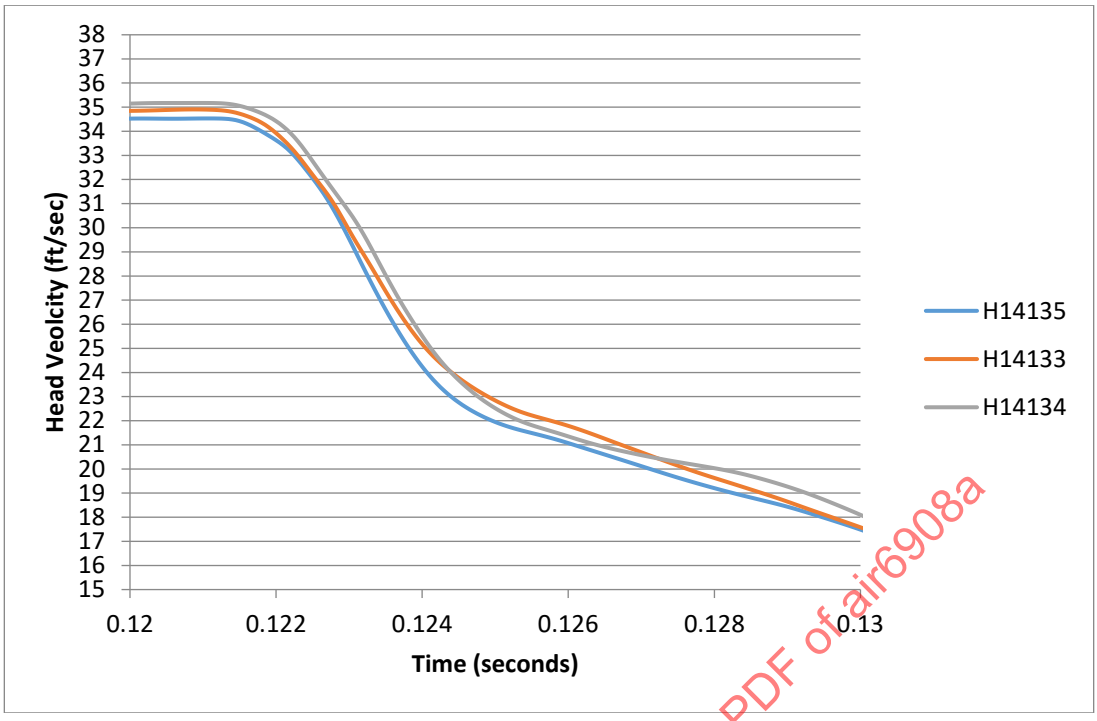

Figure C8 - Configuration #3 ATD head velocity

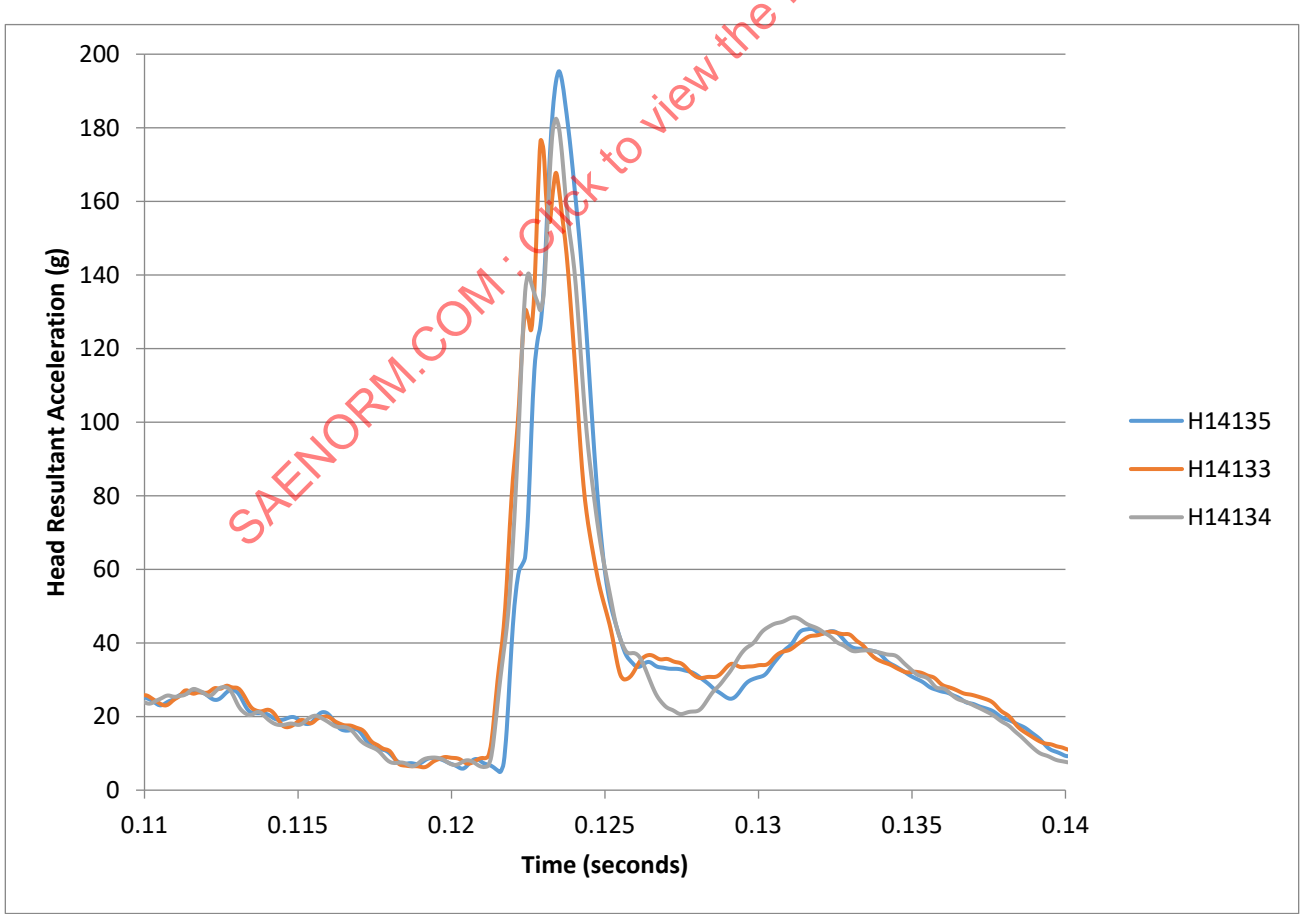

Figure C9 - Configuration #3 ATD head c.g. resultant acceleration

Figure C10 - H14133 post-test photo

Figure C11 - H14134 post-test photo

Figure C12 - H13135 post-test photo

C.3 CONFIGURATION #5: RECARO/PANASONIC 11.1-INCH MONITOR

Head component test data for Configuration #5 is provided in Table C3. ATD head acceleration is provided in Figure C13. Post-test photographs of the monitors are provided in Figures C14 and C15. Test series 17-# is with the baseline monitor installed in the seat, and test series 15-# is with the revised monitor installed in the seat. Test 17-1 had an instrumentation issue and did not collect head acceleration data.

Table C3 - Configuration #5 test results

Test #	Impact Head Velocity (ft/s)	Max Resultant Head Acceleration (g)	HIC	HIC Duration (ms)	Δ Max Head Acceleration From Average (g)	Δ HIC From Average
17-2 / H14119	34.0	155	254	11.5	+4	-15
17-3 / 14120	34.7	147	283	10.4	-4	+15
Average		151	268	11.0		
Variance		7	29	1.1		
15-1 / H14121	34.5	164	286	1.4	+9	-1
15-2[(1)] / H14122	34.4	140	325	10.8	-15	+38
15-3 / H14123	34.7	160	251	10.9	+5	-36
Average		155	287	7.7		
Variance		24	74	9.5		
Δ Averages		4	19	2.3		

(1) Touch screen fractured.

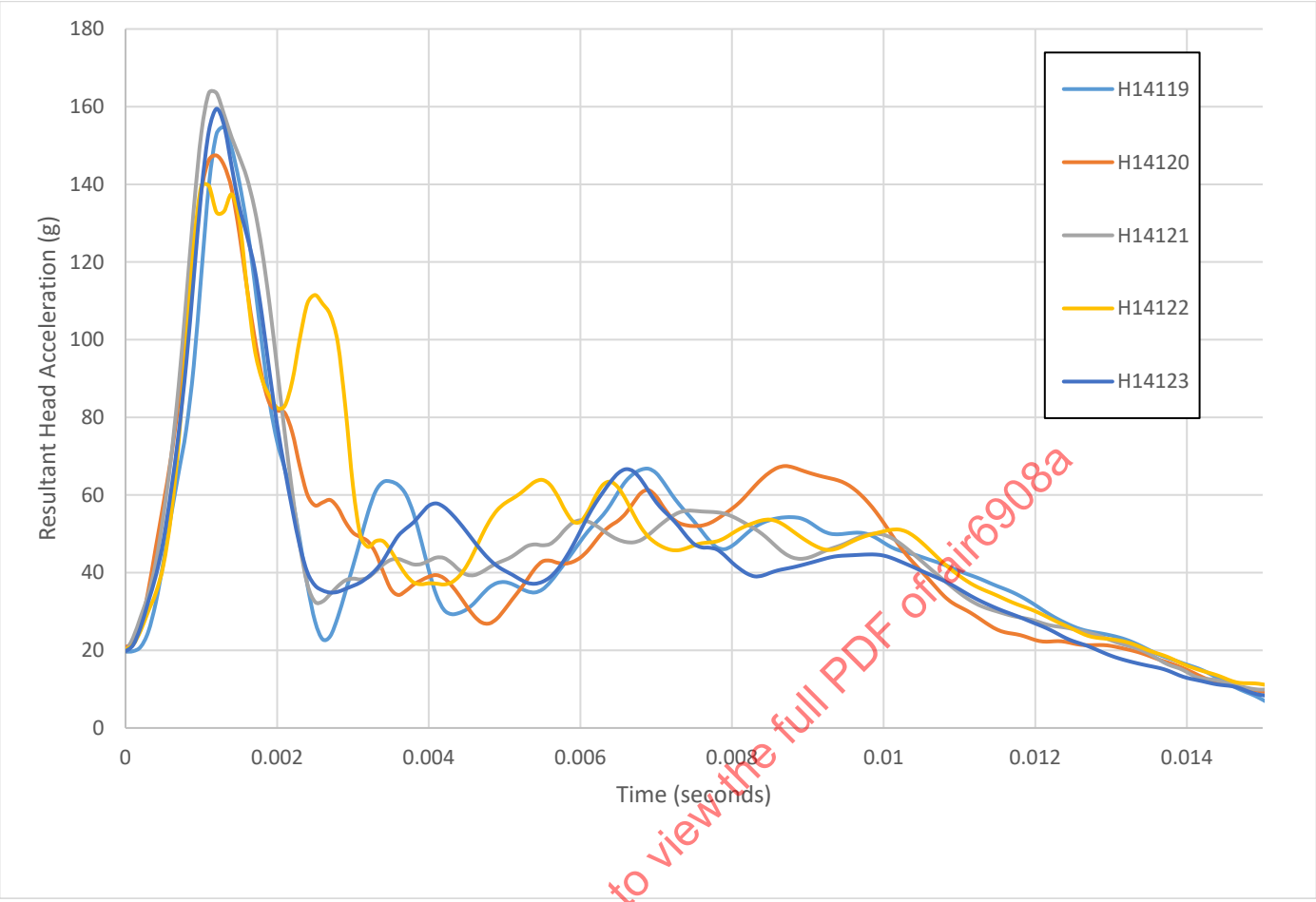

Figure C13 - Configuration #5 ATD head c.g. resultant acceleration

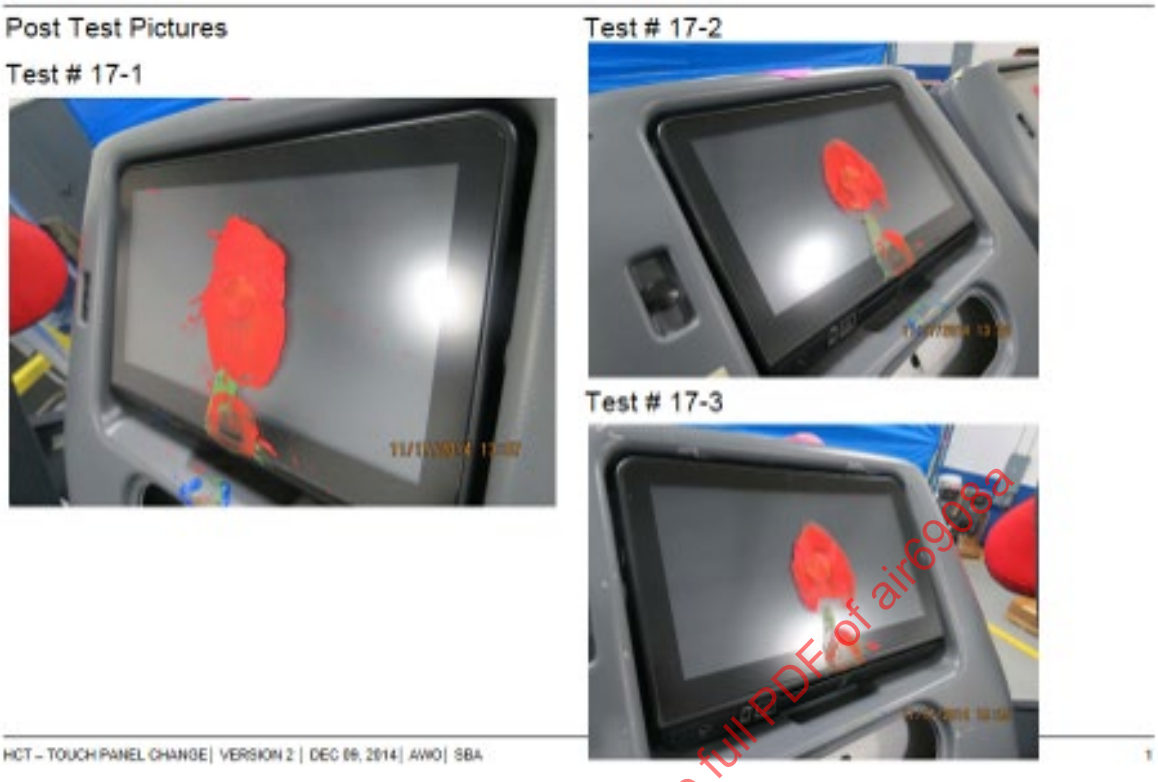

Figure C14 - Test 17-1, 17-2, and 17-3 post-test photos

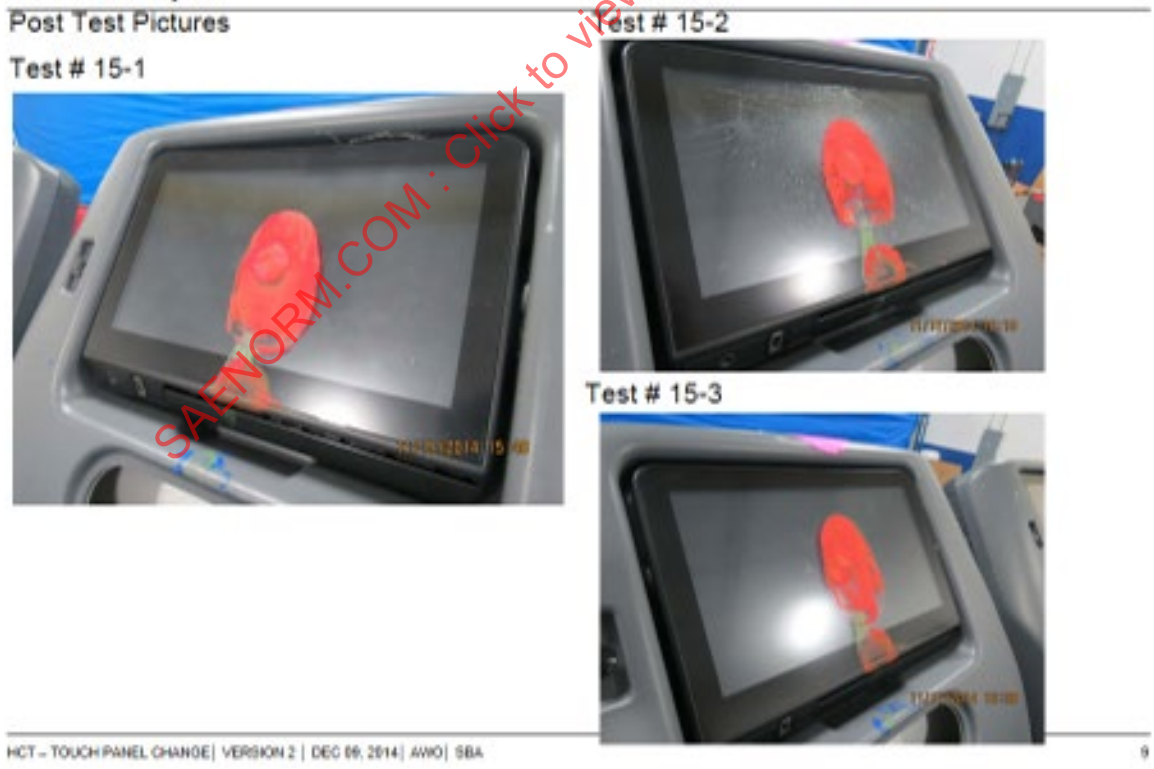

Figure C15 - Test 15-1, 15-2, and 15-3 post-test photos

APPENDIX D - ROW-TO-ROW HIC TESTING HEAD IMPACT VELOCITY ANALYSIS

Safran Seats USA analyzed a variety of their economy class (E/C) and business class (B/C) HIC dynamic test results. The specific seat model has been denoted as a sequential number due to the proprietary nature of the data. As expected, the shorter seat pitches typically resulted in lower head impact velocities due to the ATD head making contact with the seat back before reaching a maximum head velocity. Shorter pitches typical of E/C seats had a head impact velocity from 18 to 25 ft/s, while longer pitches typical of B/C seats had a head impact velocity from 25.7 to 43.2 ft/s. While the seat design and its reaction to the forward acceleration loads defined in AS8049 will affect the head impact velocity, in general, the trends and magnitude of the head velocity ranges measured by Safran Seats USA can be considered applicable to a range of seat designs.

Since the 34 ft/s head strike velocity defined in FAA policy memorandum ANM-03-115-31 is higher than the velocities measured for all E/C dynamic tests and many B/C seats tests, using 34 ft/s for impact testing of seat back mounted video monitors is appropriate for this investigation.

Table D1 - Initial head impact velocity with seat back during HIC testing

Count	Seat Pitch	Yaw	Seat Class	Seat Model	Left Seat HIC	Right Seat HIC	Left Seat Velocity at T1 (ft/s)	Right Seat Velocity at T1 (ft/s)
1	32	0	E/C	#1	550	724	**19.36**	**21.62**
2	31	0	E/C	#1	706	--	**24.86**	--
3	31	0	E/C	#1	834	--	**24.12**	--
4	30	0	EC	#2	821	--	**25.29**	--
5	31	0	E/C	#1	--	924	--	**20.41**
6	30	0	E/C	#2	605	--	**19.66**	--
7	30	0	E/C	#2	556	--	**20.70**	--
8	31	0	E/C	#1	904	680	**18.46**	**17.95**
9	30	0	E/C	#2	711	--	**19.79**	
10	30	0	E/C	#2	618	--	**21.02**	
11	40	10	B/C	#3	862	698	**35.51**	**33.52**
12	36	0	B/C	#3	727	--	**25.77**	--
13	36	0	B/C	#3	624	743	**27.64**	**25.35**
14	36	0	B/C	#4	718	--	**43.16**	--
15	33	0	B/C	#4	650	--	**28.83**	--
16	34	10	B/C	#5	594	--	**27.04**	--
17	40	10	B/C	#3	804	893	**32.10**	**35.81**
18	40	10	B/C	#3	978	749	**42.17**	**37.77**
19	40	10	B/C	#3	903	768	**40.85**	**37.88**
20	36	0	B/C	#3	785	--	**36.82**	--
		Average ATD Head Velocity at Initial Head Contact = 28 ft/s						

APPENDIX E - SEAT BACK TEST FIXTURE HEAD COMPONENT TEST DATA

E.1 CONFIGURATION #5: PANASONIC 11.1-INCH MONITOR

Six monitors in total were tested. The first three tests were with the baseline monitor configuration, and the final three tests were with the revised touch screen.

E.1.1 Test Configuration

The vertical stand was held in place before head impact by a 75-pound capacity (333 N) cable tie. A 1.5-mm 6061-T6 aluminum plate and aluminum block spacers were used to mount the IFE monitor to the test fixture. See Figure E1 for pictures of the monitor mounting.

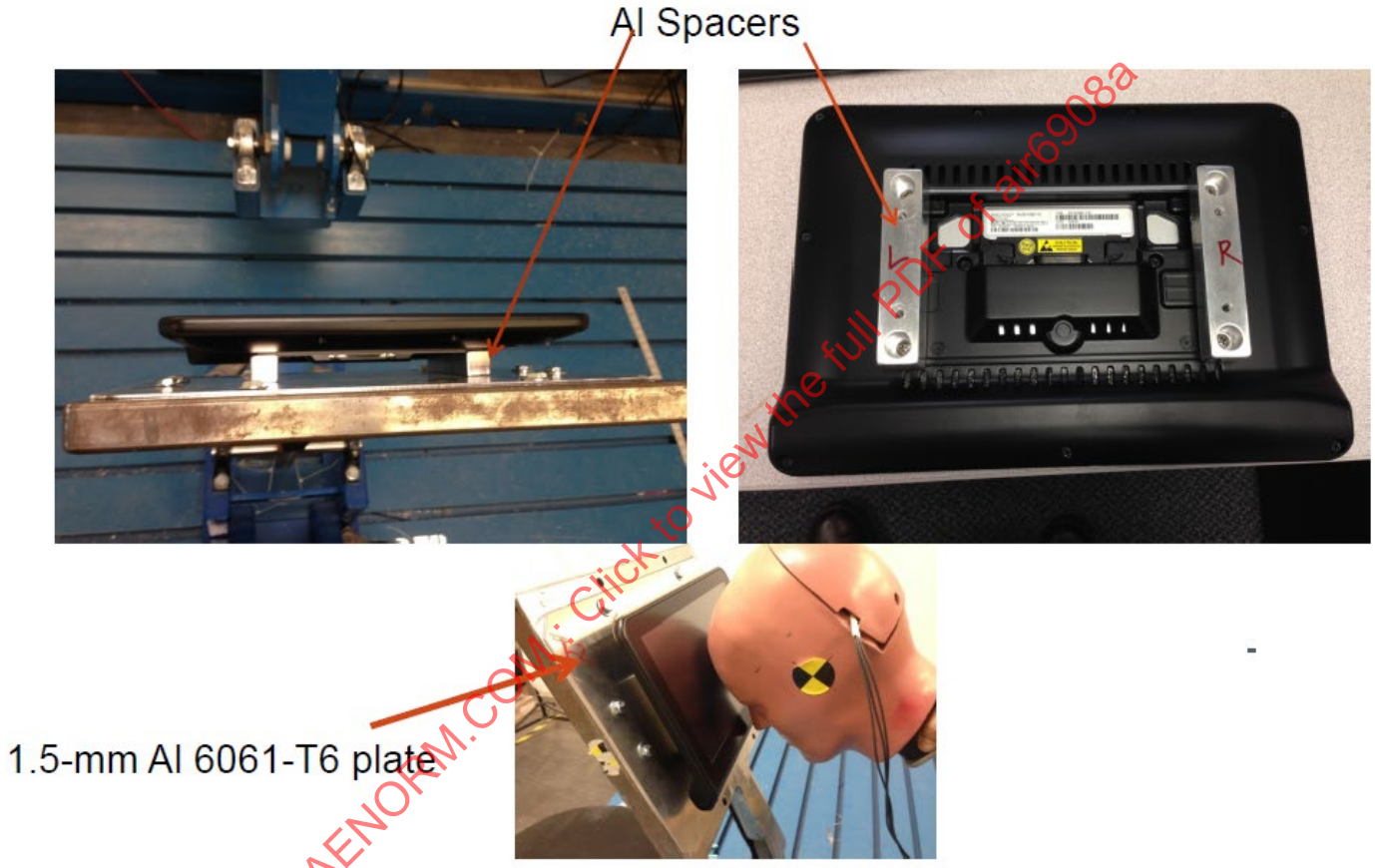

Figure E1 - Panasonic 11.1-inch monitor mounted to test fixture

E.1.2 Test Results

Head component test data for Configuration #5 is provided in Table E1. ATD head acceleration is provided in Figure E2. Test #5 was the only one where the touch screen fractured, resulting in a noticeable drop in head acceleration and the lowest HIC score of either monitor configuration. Figure E3 shows the difference between tests 4, 5, and 6 in the condition of the touch screen after initial head impact.

Post-test photographs of the monitors are provided in Figures E4 and E5. Video analysis indicates that the rebound of the seat back test fixture into the ATD head (secondary head impact) after initial head contact increased the severity of the monitor damage.

Table E1 - Configuration #5 test results

Test #	Impact Head Velocity (ft/s)	Max Resultant Head Acceleration (g)	HIC	HIC Duration (ms)	Δ Max Head Acceleration From Average (g)	Δ HIC From Average
1 (Jan. 28, 2015)	35.6	175	877	6.3	+3	-24
2 (Jan. 28, 2015)	34.7	167	923	6.2	-5	+22
3 (Jan. 28, 2015)	34.9	174	902	6.1	+2	+1
Average		172	901	6.2		
Variance		8	46	0.2		
4 (Jan. 29, 2015)	34.6	180	955	6.1	-4	+33
5 (Jan. 29, 2015)	34.7	186	873	6.0	+2	-49
6 (Jan. 29, 2015)	34.9	186	939	5.9	+2	+17
Average		184	922	6.0		
Variance		6	82	0.2		
Δ Averages (Different touch screens)		12	21	0.2		

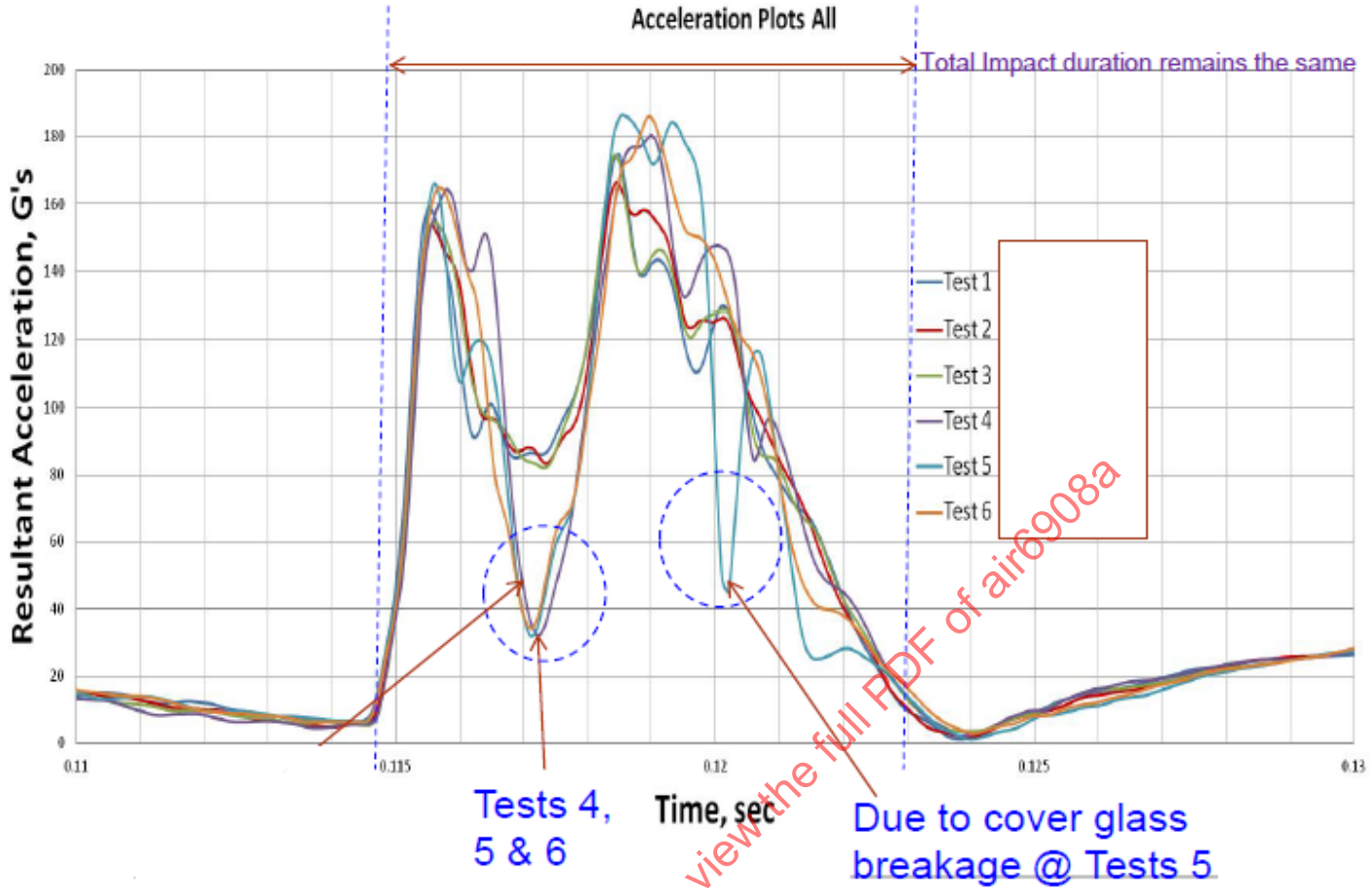

Figure E2 - Configuration #5 ATD head c.g. resultant acceleration

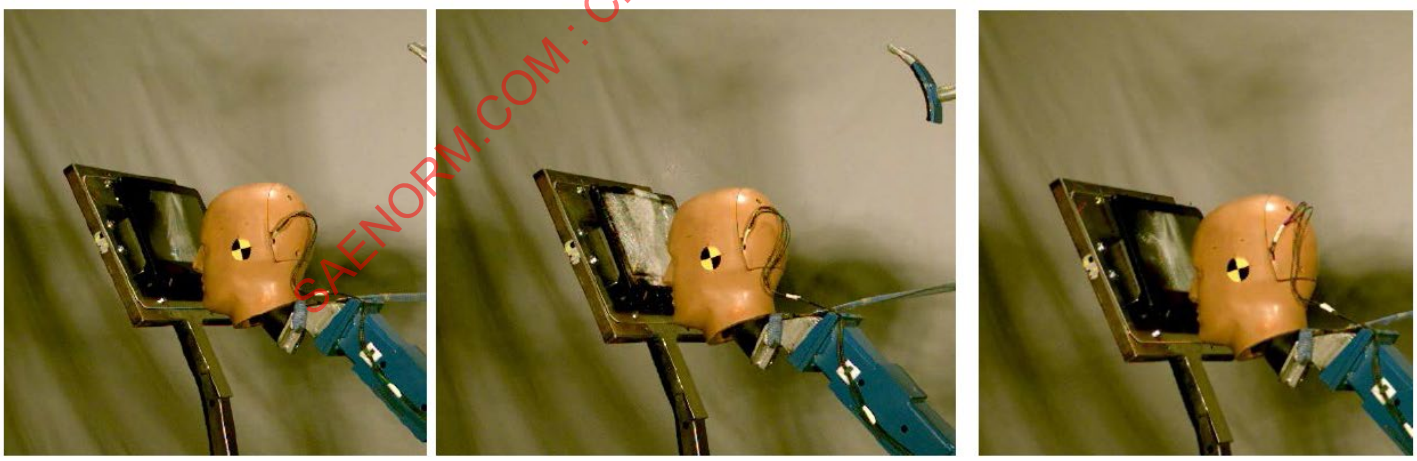

Figure E3 - Configuration #5 photos of tests 4, 5, and 6 ATD head contact

Figure E4 - Configuration #5 post-test photos of test 1, 2, and 3 monitors

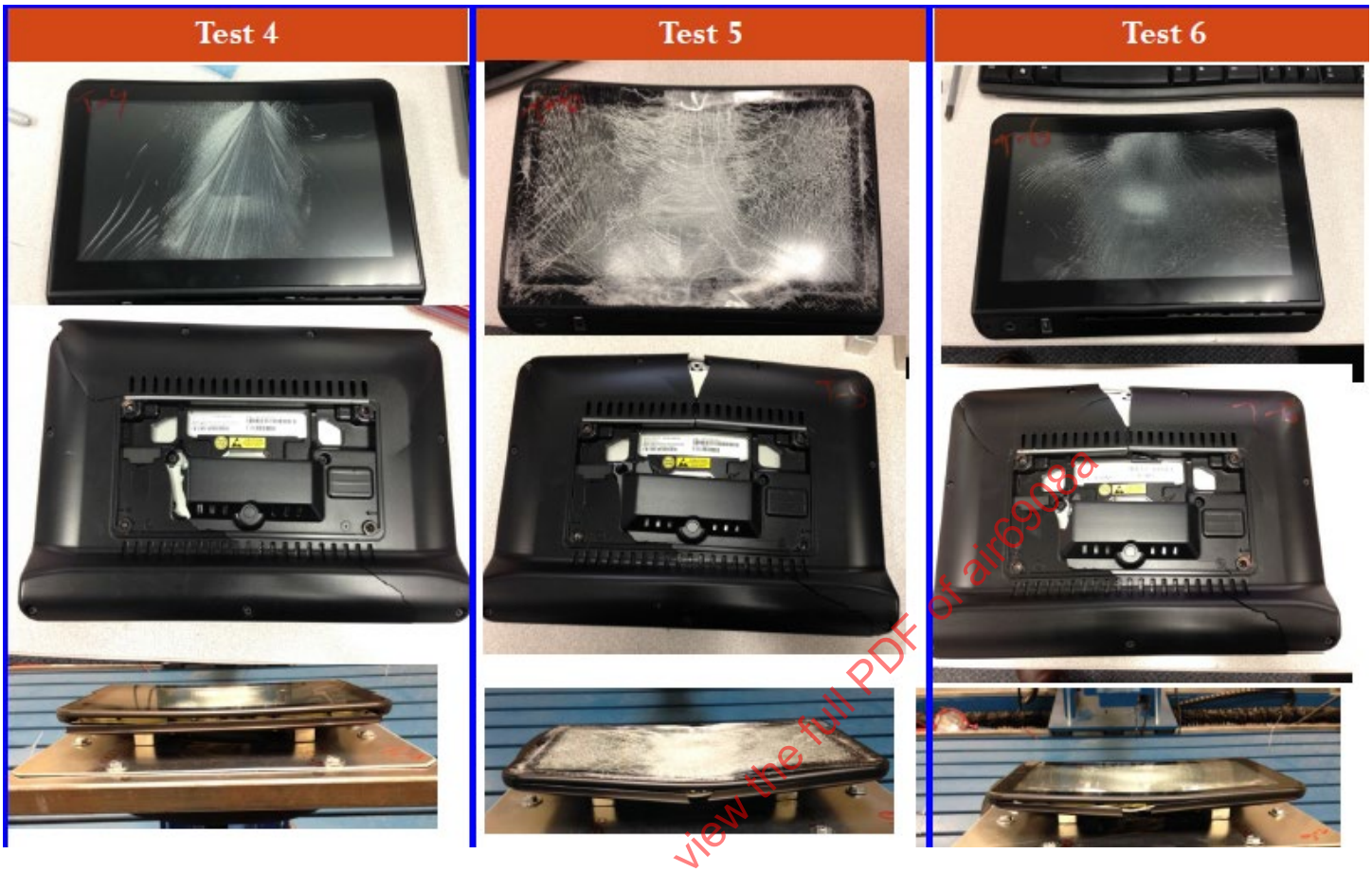

Figure E5 - Configuration #5 post-test photos of test 4, 5, and 6 monitors

E.2 CONFIGURATION #1: PANASONIC 10.6-INCH MONITOR

One baseline monitor was tested as described in seat/IFE Configuration #1.

E.2.1 Test Configuration

Test configuration was similar to the one described in E.1.1.

E.2.2 Test Results

Head component test data for Configuration #1 is located in Table E2. ATD head c.g. acceleration is provided in Figure E6.

Post-test photographs of the monitors are provided in Figure E7, showing damage significant enough to dislodge the monitor from its mounting.

Table E2 - Configuration #1 test results

Test #	Impact Head Velocity (ft/s)	Max Resultant Head Acceleration (g)	HIC	HIC Duration (ms)	Δ Max Head Acceleration From Average (g)	Δ HIC From Average
1	34.3	161	596	7.4	--	--

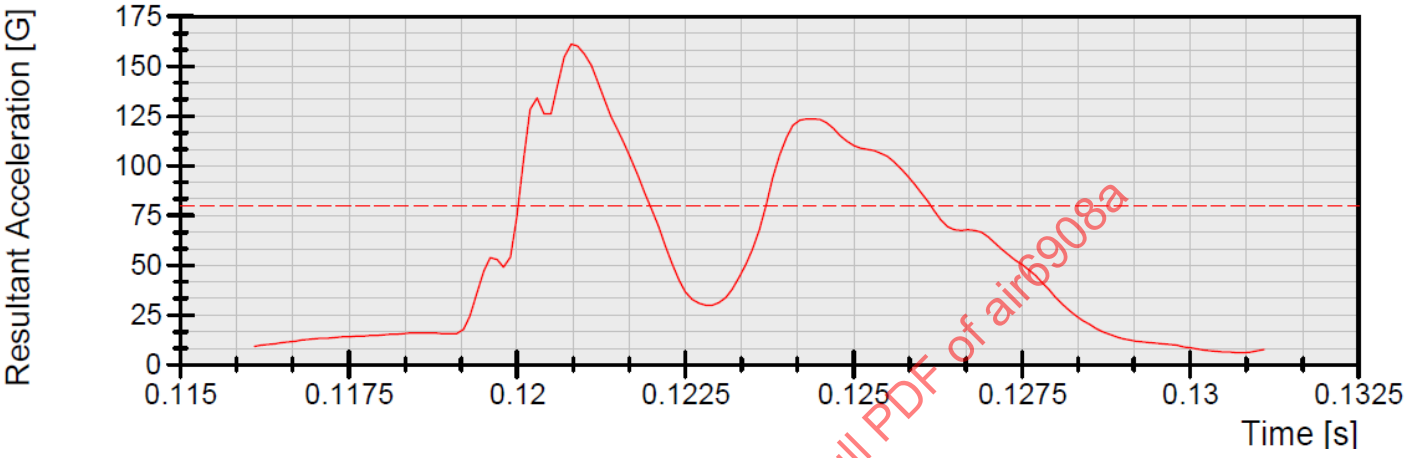

Figure E6 - Configuration #1 ATD head c.g. resultant acceleration

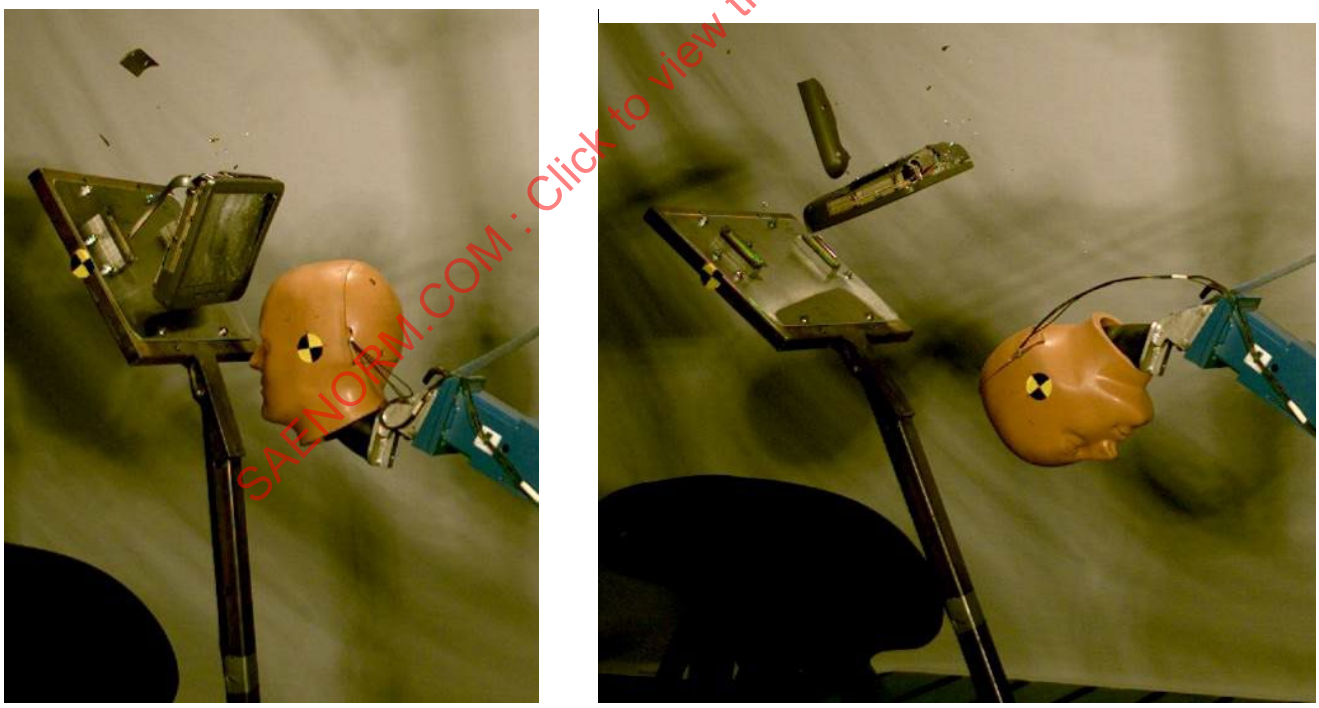

Figure E7 - Configuration #1 test photos

E.3 CONFIGURATION #6: PANASONIC 9-INCH MASS EQUIVALENT MONITOR

Six monitors in total were tested. The first three tests were with the 9-inch mass equivalent monitor, while the final three tests were with the 9-inch production monitor.

E.3.1 Test Configuration

The vertical stand was held in place before head impact by a 75-pound capacity (333 N) cable tie. An 18-mm hardwood plywood sheet and aluminum blocks were used to mount the IFE monitor to the test fixture. See Figure E8 for pictures of the monitor mounting.

Figure E8 - Configuration #6 test setup

E.3.2 Test Results

Head component test data is located in Table E3. ATD head acceleration plots are provided in Figure E9. Test #1 results noticeably deviated from tests #2 and #3. Lab personnel noted that the head impact angle and location could have varied slightly due to the time between tests (over 2 months) and inadequate control of the test setup. Post-test photographs of the monitors are provided in Figure E10.

Table E3 - Configuration #6 test results

Test #	Impact Head Velocity (ft/s)	Max Resultant Head Acceleration (g)	HIC	HIC Duration (ms)	Δ Max Head Acceleration From Average (g)	Δ HIC From Average
1 (July 2, 2014)	34.5	734	2993	2.6	+113	+166
2 (Sept. 8, 2014)	34.8	575	2773	2.6	-46	-54
3 (Sept. 8, 2014)	34.8	555	2716	2.7	-66	-111
Average		621	2827	2.6		
Variance		179	277	0.1		
4 (June 30, 2014)	34.7	277	1959	3.9	-20	-192
5 (June 30, 2014)	34.9	289	2195	3.5	-8	+44
6 (July 1, 2014)	34.9	324	2298	3.4	+27	+147
Average		297	2151	3.6		
Variance		47	339			
Δ Averages (ME versus production monitor)		324	676	1.0		

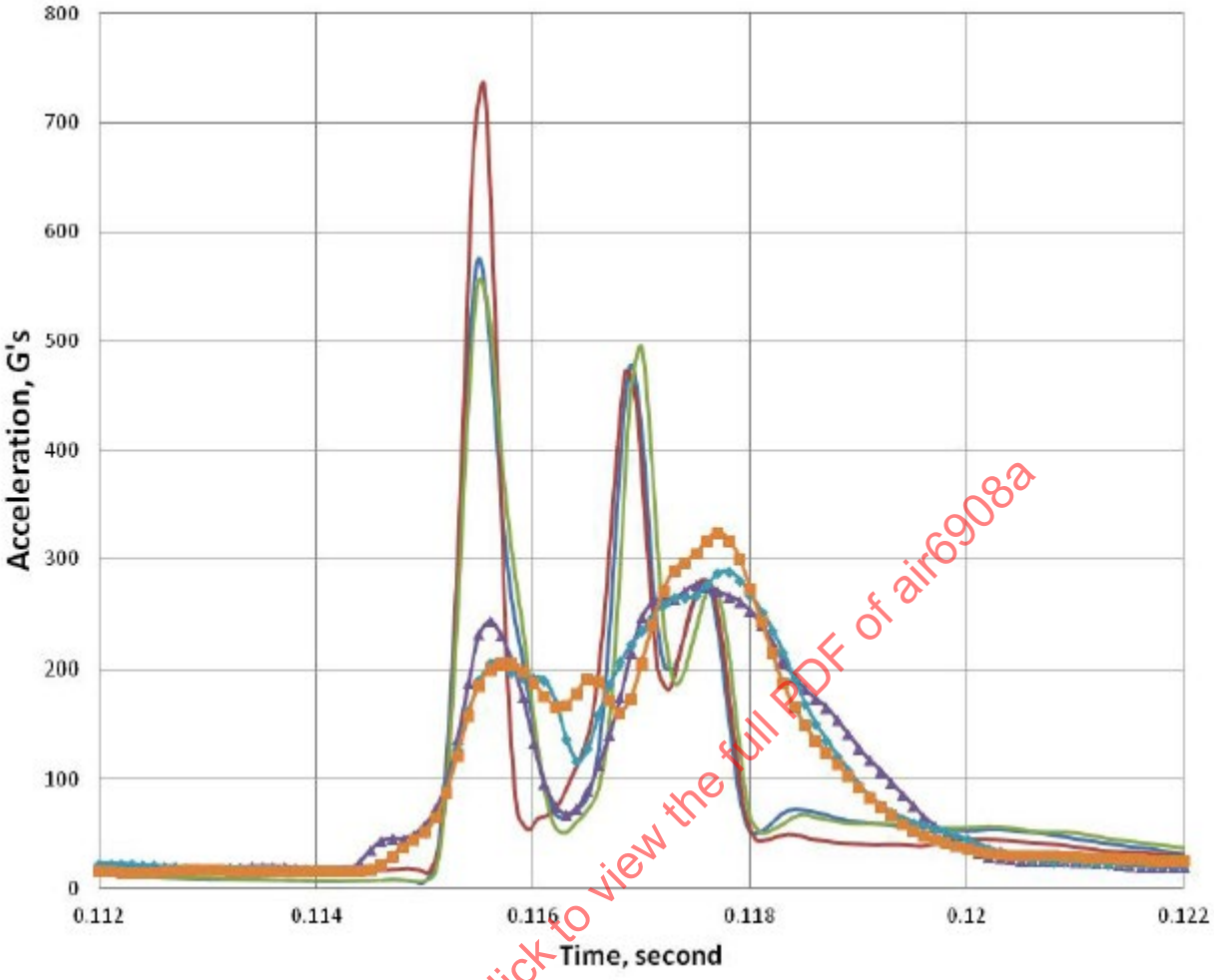

Figure E9 - Configuration #6 ATD head c.g. resultant acceleration

Figure E10 - Configuration #6 post-test photos of mass equivalent monitor

APPENDIX F - THREE-POINT BEND TEST DATA

Figure F1 shows the results of the Panasonic 10.6-inch monitor three-point static bend testing (see Appendix A, Configuration #1). The “A” samples are the baseline configuration of the monitor, and the “B” samples are the monitor configuration with a revised display panel subcomponent.

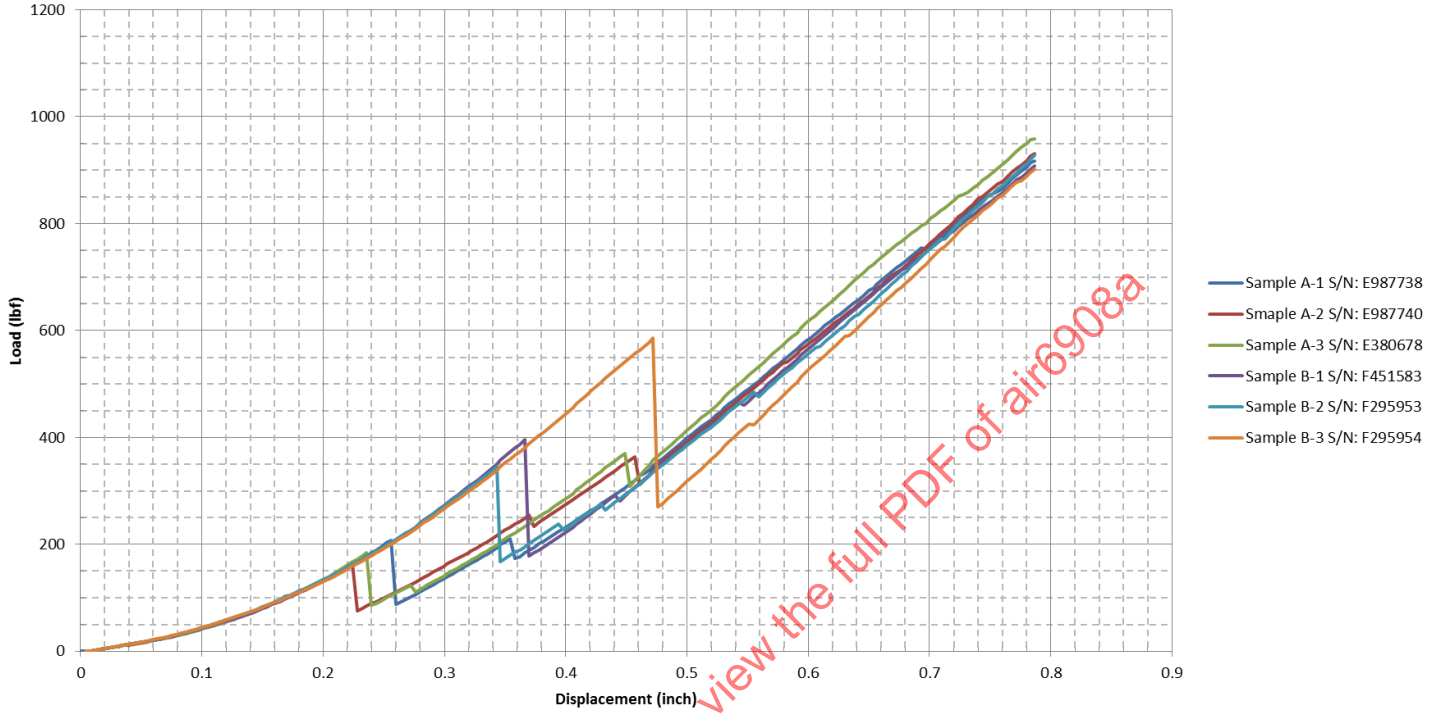

Figure F1 - Panasonic 10.6-inch monitor three-point bend test data

Figure F2 shows the results of the Thales 10.6-inch monitor three-point static bend testing (see Appendix A, Configurations #2 and #4). The test data shown is only for the baseline configuration of the monitor.

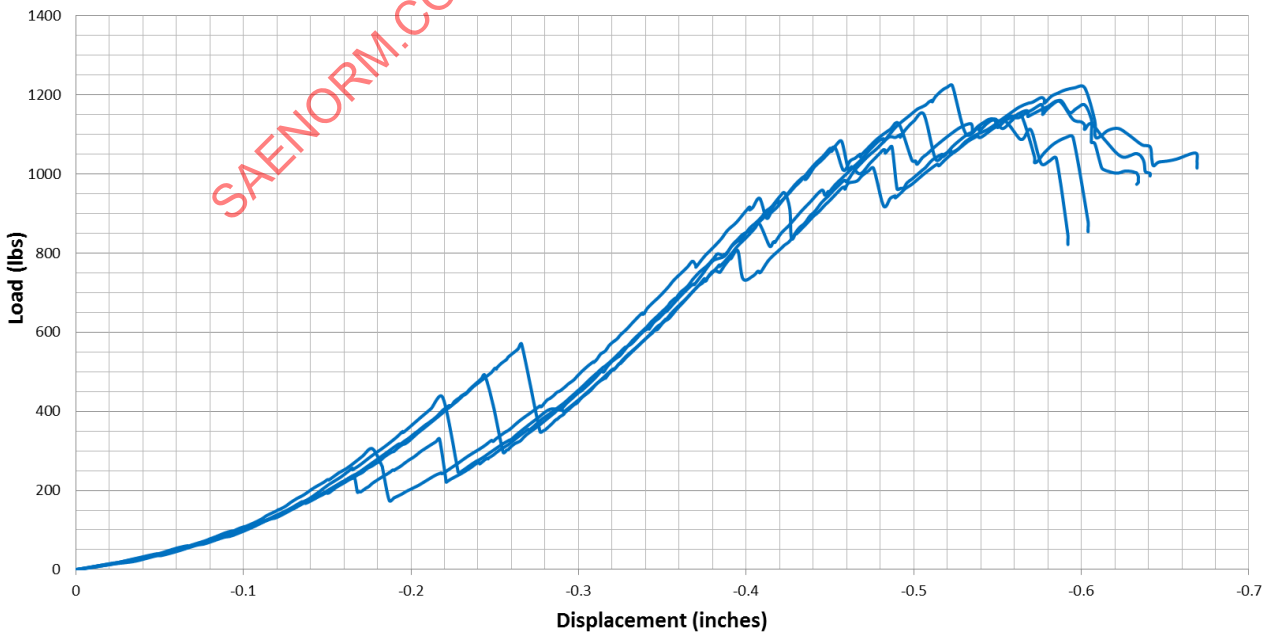

Figure F2 - Thales 10.6-inch monitor three-point bend test data

Figure F3 shows the results of the Thales 8.9-inch monitor three-point static bend testing (see Appendix A, Configuration #3). The test data shown is only for the baseline configuration of the monitor.

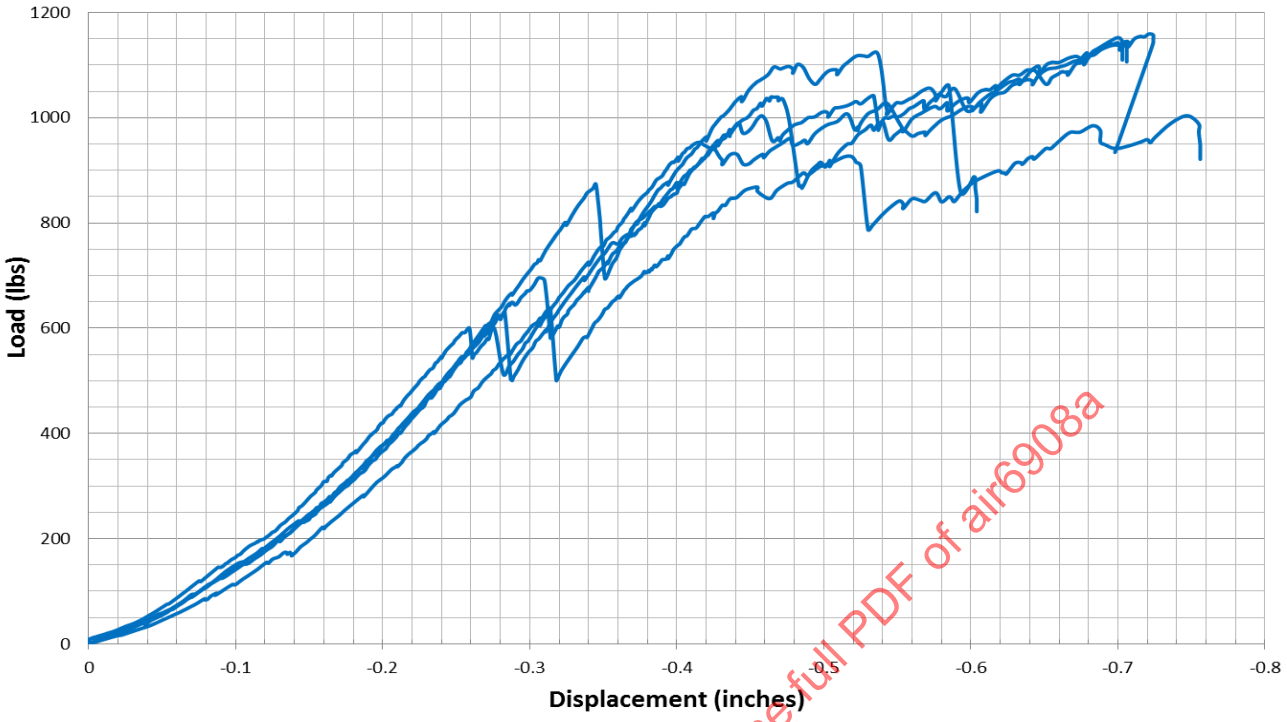

Figure F3 - Thales 8.9-inch monitor three-point bend test data

Figure F4 shows the results of the Panasonic 11.1-inch monitor three-point static bend testing (see Appendix A, Configuration #5). The “A” samples are the baseline configuration of the monitor, and the “B” samples are the monitor configuration with the revised touch screen subcomponent.

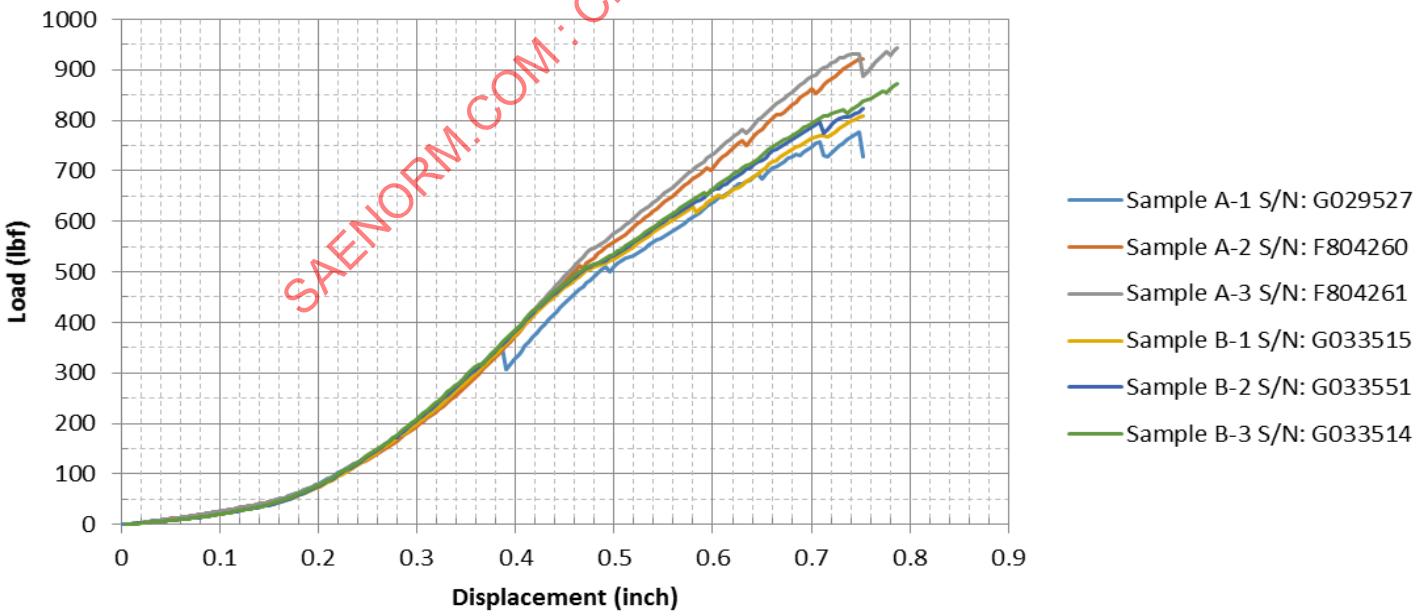

Figure F4 - Panasonic 11.1-inch monitor three-point bend test data

Figure F5 shows the results of three-point static bend testing of a Panasonic 9-inch mass equivalent (or dummy) monitor (see Appendix A, Configuration #6). Figures F6 and F7 show photos of the testing in progress.

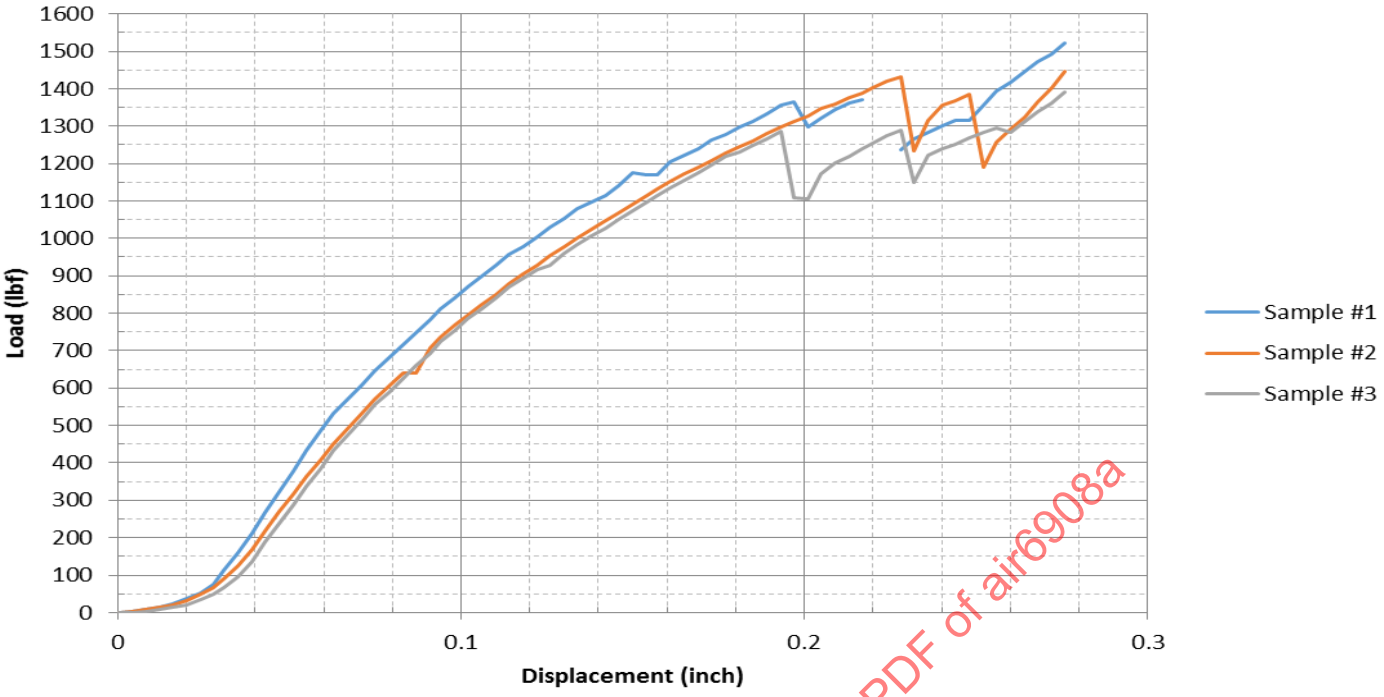

Figure F5 - Panasonic 9-inch mass equivalent monitor three-point bend test data

Figure F6 - Panasonic 9-inch mass equivalent monitor test - photo #1

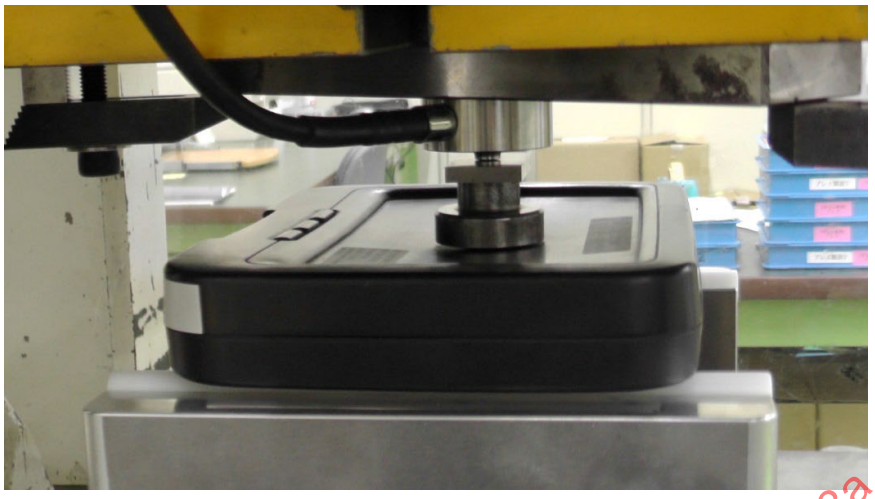

Figure F7 - Panasonic 9-inch mass equivalent monitor test - photo #2

APPENDIX G - HIC SENSITIVITY ANALYSIS RESULTS

This appendix provides the results of HIC sensitivity analyses performed by various seat suppliers and some general details about the seat FEMs used. Details as to the seat design and how it attenuates a head impact to achieve acceptable HIC results are proprietary and are not available for publication. However, some information has been provided to document the validity of the integrated seat models used.

G.1 COLLINS AEROSPACE

G.1.1 Seat FEM Construction

The target seat FEM is identical to the seat design with regard to:

- Seat spreaders.
- Seat back structure, including monitor mounting.
- HIC attenuation mechanism about the seat back pivot.

The launch seat used in the row-to-row HIC simulations had the following characteristics:

- Hybrid II ATD installed on a rigid seat structure using a lap belt.
- The seat pitch is adjusted to facilitate a head strike to the center of the monitor.
- Glass erosion function was included in the simulations to emulate the effect of glass fracturing.

Material properties were from the following sources:

- Aluminum: Metallic Materials Properties Development and Standardization (MMPDS)
- Steel: MMPDS
- Seat back hoop composite: Material coupon test (internal)
- Lap belt webbing: Material coupon test (internal)
- Plastics: Supplier specification and Matweb database, and material coupon testing[1]
- Diaphragm: Supplier specification and material coupon testing[1]
- Foam cushion: The seat cushion model was validated by performing static and dynamic compression tests for each seat type, and the test data was converted to the material properties of the solver foam material card.

Collins Aerospace used their resident software tools, procedures, and model documentation/archival processes in the development and execution of their models used in this study. Processes are based on the analytical modeling techniques defined in ARP5765.

The starting seat FEM did not have an installed monitor and had to be modified to integrate the Panasonic 10.6-inch monitor model and monitor attachment for this analysis. Before being modified, the seat FEM had been refined to the point where the HIC results of the FEM compared favorably with dynamic test results of the same seat model and no IFE monitor installed (see Table G1). Figure G1 provides screenshots of the row-to-row HIC simulation before load is applied and at head initial contact with the seat back.

[1] Coupon testing by another company, with conformed samples from Collins.

Table G1 - Comparison of Collins Aerospace FEM model and dynamic test HIC results

	HIC	HIC Duration
Simulation	748	<5 ms
Dynamic test	700 (average)	5 ms ± 1 ms

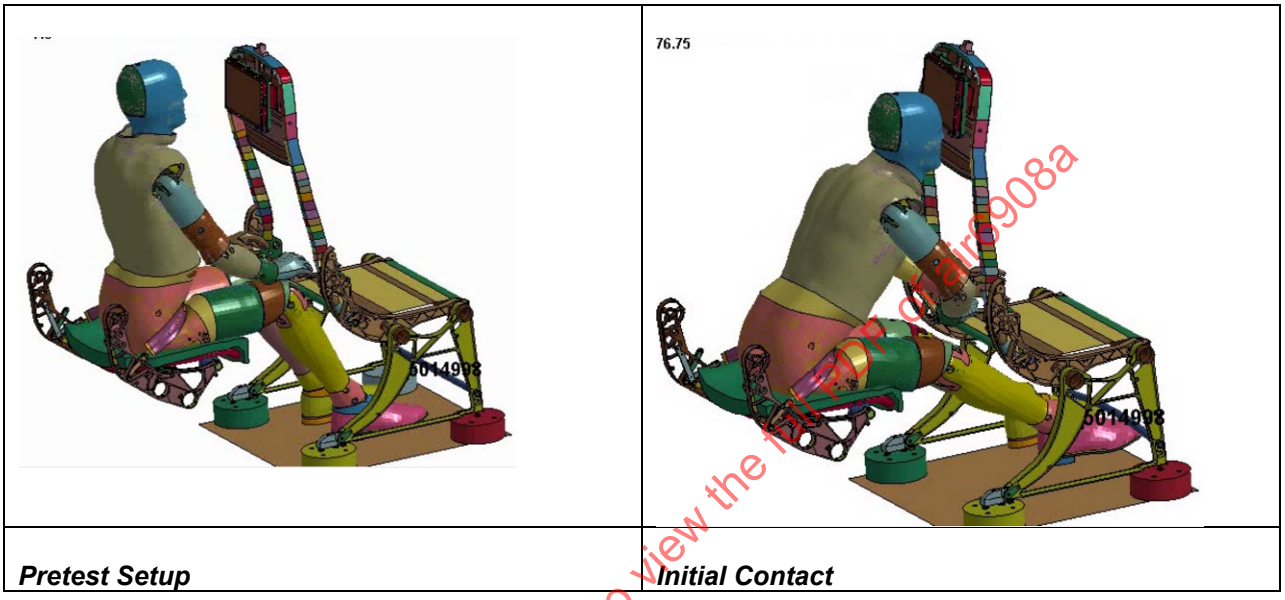

Pretest Setup ***Initial Contact***

Figure G1 - Collins Aerospace row-to-row HIC simulation screenshots

G.1.2 Analysis Results

Collins Aerospace decided to simulate head impacts using an FEM of the head component test device first in order to expedite simulation results (run time greatly reduced) and to improve consistency of the head impact (no arm/leg interaction with the seat back). Initial head contact was the center of the monitor viewing screen, with a head impact velocity of 34 ft/s. Glass erosion function was included in the simulations to emulate the effect of glass fracturing. Head acceleration results are provided in Table G2 and Figure G2.

Table G2 - Collins Aerospace HCTD parametric study results

Configuration	Curve #1 (Glass)	Curve #2 (Internal)	Glass Breakage	HIC	Δ HIC to Baseline	HIC Duration (ms)	Δ HIC Duration to Baseline
#1 Baseline	Unchanged	Unchanged	Low-range	536	--	5.0	--
#2 Stiffer touch screen	E=15.0×10^6 psi	Unchanged	Unchanged	553	+17	4.9	-0.01
#3 Less stiff touch screen	E=5.0×10^6 psi	Unchanged	Unchanged	547	+11	4.8	-0.02
#4 Stiffer display panel	Unchanged	E=15.0×10^6 psi	Unchanged	548	+12	4.9	-0.01
#5 Less stiff display panel	Unchanged	E=5.0×10^6 psi	Unchanged	522	-14	5.0	0.0
#6 Glass breaks late	Unchanged	Unchanged	Largest deflection	519	-17	4.9	-0.01

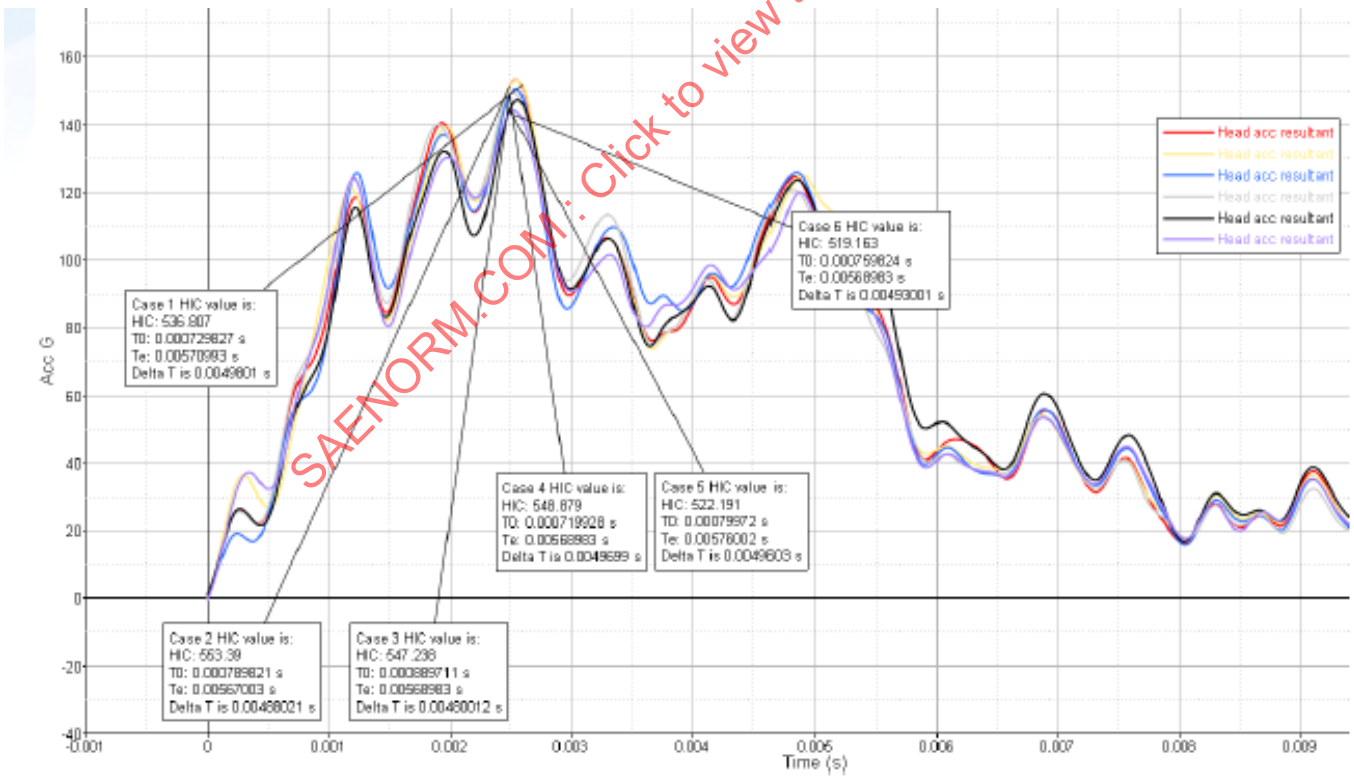

Figure G2 - Collins Aerospace HCTD parametric study ATD head c.g. resultant acceleration

Collins Aerospace then proceeded to run multiple row-to-row dynamic test simulations with a ±50% and ±30% modulus of elasticity change. See results in Table G3.

Table G3 - Collins Aerospace row-to-row dynamic test parametric study results

Configuration	Curve #1 (Glass)	Curve #2 (Internal)	Glass Breakage	HIC	Δ HIC to Baseline	HIC Duration (ms)	Δ HIC Duration to Baseline
#1 Baseline	Unchanged	Unchanged	Low-range	655	--		
#2 Stiffer touch screen	E=15.0×10^6 psi	Unchanged	Unchanged	867	+212		
#3 Less stiff touch screen	E=5.0×10^6 psi	Unchanged	Unchanged	766	+111		
#4 Stiffer display panel	Unchanged	E=15.0×10^6 psi	Unchanged	849	+194		
#5 Less stiff display panel	Unchanged	E=5.0×10^6 psi	Unchanged	690	+35		
#2 Stiffer touch screen	E=13.0×10^6 psi	Unchanged	Unchanged	726	+71		
#3 Less stiff touch screen	E=7.0×10^6 psi	Unchanged	Unchanged	799	+144		
#8 Stiffer display panel	Unchanged	E=13.0×10^6 psi	Unchanged	718	+63		
#9 Less stiff display panel	Unchanged	E=7.0×10^6 psi	Unchanged	658	+3		

G.2 RECARO

G.2.1 Seat FEM Construction

The seat FEM is identical to the seat design with regard to:

- Seat spreaders.
- Seat back structure, including monitor mounting.
- HIC attenuation mechanism about the seat back pivot.

The HIC attenuation mechanism has been validated by component test, where the mechanism force versus displacement was recorded and used accordingly in the seat model.

Material properties were from the following sources:

- Aluminum: Coupon testing (internal)
- Steel: Metallic Materials Properties Development and Standardization (MMPDS) and coupon testing (internal)
- Lap belt webbing: Coupon testing (internal)
- Plastics: Supplier specification and coupon testing (internal)
- Foam cushion: Coupon testing (internal)
- Diaphragm: Coupon testing (internal)

Recaro used their resident software tools, procedures, and model documentation/archival processes in the development and execution of their models used in this study. Processes are based on the analytical modelling techniques defined in ARP5765.

G.2.2 Analysis Results

Recaro simulated a row-to-row HIC test with the following test parameters:

- The IFE monitor mounting bracket tilt rotation mechanism was locked to eliminate variability due to monitor tilt.
- Head contact at the center of the monitor viewing screen.
- Row-to-row seat pitch set at 35 inches (63.5 cm) to facilitate a direct ATD head strike on the monitor.
- Glass erosion function was included in the simulations to emulate the effect of glass fracturing.

Head acceleration results are provided in Table G4 and Figure G3.

Table G4 - Recaro row-to-row dynamic test parametric study results

Configuration	Curve #1 (Glass)	Curve #2 (Internal)	Glass Breakage	HIC	Δ HIC to Baseline	HIC Duration (ms)	Δ HIC Duration to Baseline
#1 Baseline	Unchanged	Unchanged	Low-range	1127	--	8.5	--
#2 Stiffer touch screen	$E=15.0\times10^6$ psi	Unchanged	Unchanged	1253	+126	9.4	+0.9
#3 Less stiff touch screen	$E=5.0\times10^6$ psi	Unchanged	Unchanged	1103	-24	8.5	0.0
#2 Stiffer touch screen	Unchanged	$E=15.0\times10^6$ psi	Unchanged	1180	+53	9.2	+0.7
#3 Less stiff touch screen	Unchanged	$E=5.0\times10^6$ psi	Unchanged	1086	-41	9.3	+0.8

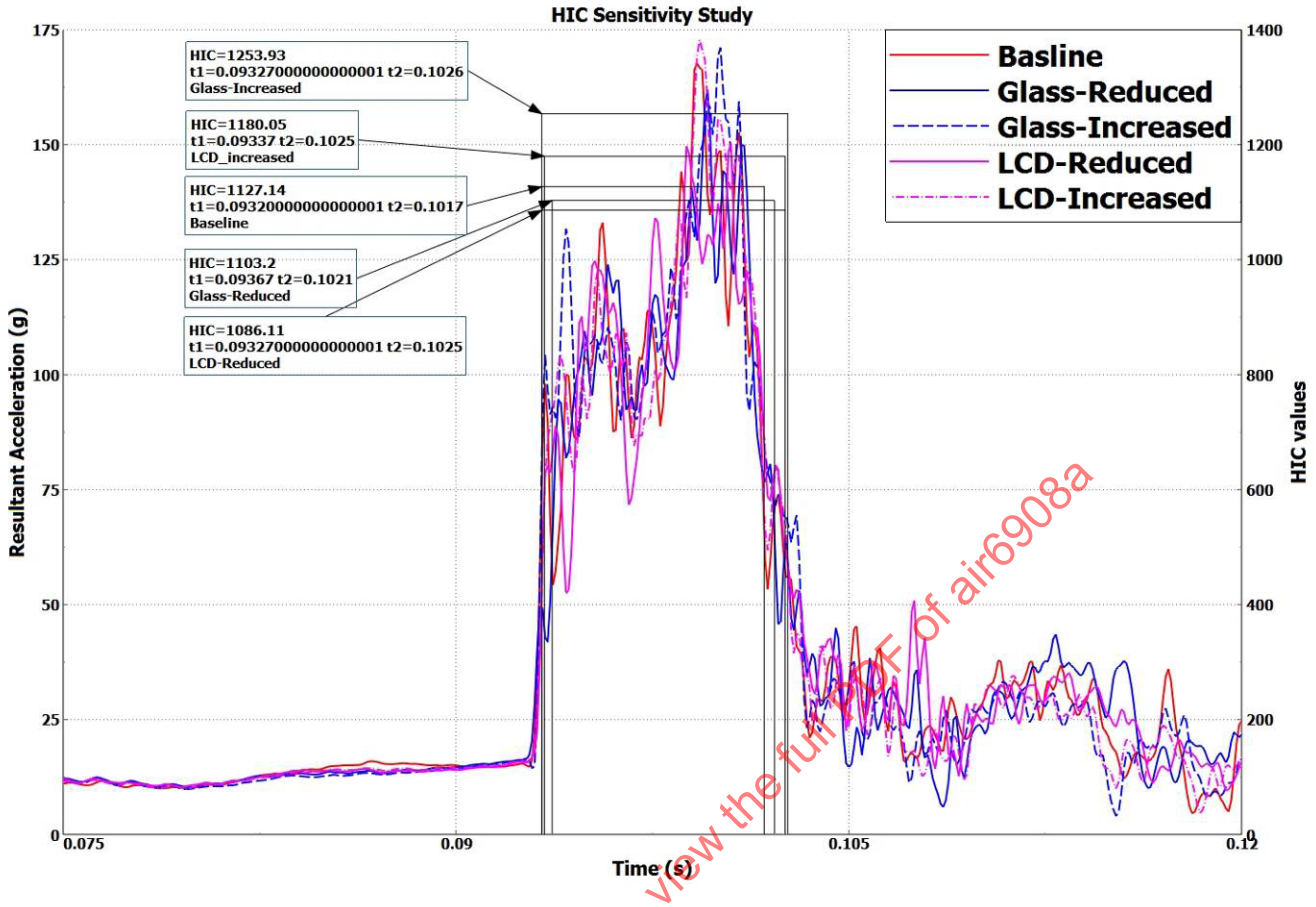

Figure G3 - Recaro dynamic test parametric study ATD head c.g. resultant acceleration

G.3 SAFRAN AEROSPACE

G.3.1 Seat FEM Construction

The seat FEM is identical to the seat design with regard to:

- Seat base frame.
- Seat back structure.
- HIC attenuation mechanism about the seat back pivot.

A model of a production monitor mounting bracket was scaled to attach the baseline 10.6-inch monitor model to the production seat back model. The HIC number and duration were comparable to the test data for this seat model.

The Hybrid II ATD model used had been validated by the ATD manufacturer Humanetics.

Material properties were from the following sources:

- Aluminum: Metallic Materials Properties Development and Standardization (MMPDS)-07
- Steel: MMMPDS-07
- Plastics: Supplier material data[2]

Safran used their resident software tools, procedures, and model documentation/archival processes in the development and execution of their models used in this study. Processes are based on the analytical modeling techniques defined in ARP5765.

G.3.2 Analysis Results

Safran performed three different head strike analyses.

a. Head component test device (HCTD) impact with a rigid IFE mounting bracket.

b. HCTD impact with the production IFE mounting bracket tilt function locked out.

c. Row-to-row dynamic test with the seats at a 35-inch (63.5-cm) pitch, with the production IFE mounting bracket tilt function locked out.

The initial head contact was at the center of the monitor viewing screen. Head impact velocity for the HCTD simulations was 34 ft/s. Glass erosion was included in most of the simulations, except for the results reported in Table G7. For their seat design, Safran determined that eliminating touch screen glass fracturing in the model would lead to expected HIC trends (stiffer touch screen results in higher HIC).

Analysis results are provided in Tables G5, G6, G7, and G8 and Figures G4, G5, and G6.

Table G5 - Safran HCTD parametric study results with rigid bracket

Configuration	Curve #1 (Glass)	Curve #2 (Internal)	Glass Breakage	HIC	Δ HIC to Baseline	HIC Duration (ms)	Δ HIC Duration to Baseline
#1 Baseline	Unchanged	Unchanged	Low-range	1155	--	2.18	--
#2 Stiffer touch screen	E=15.0×10^6 psi	Unchanged	Unchanged	1109	-46	1.86	-0.32
#3 Less stiff touch screen	E=5.0×10^6 psi	Unchanged	Unchanged	1155	-00	2.02	-0.16
#2 Stiffer touch screen	Unchanged	E=15.0×10^6 psi	Unchanged	1213	+58	2.22	+0.04
#3 Less stiff touch screen	Unchanged	E=5.0×10^6 psi	Unchanged	1143	-12	2.02	-0.16
#6 Glass breaks late	Unchanged	Unchanged	Largest deflection	1097	-58	2.18	+0.00

[2] Plastic materials were not in the primary load path of the head impact and, therefore, were not as critical for analysis accuracy as the metallic components.

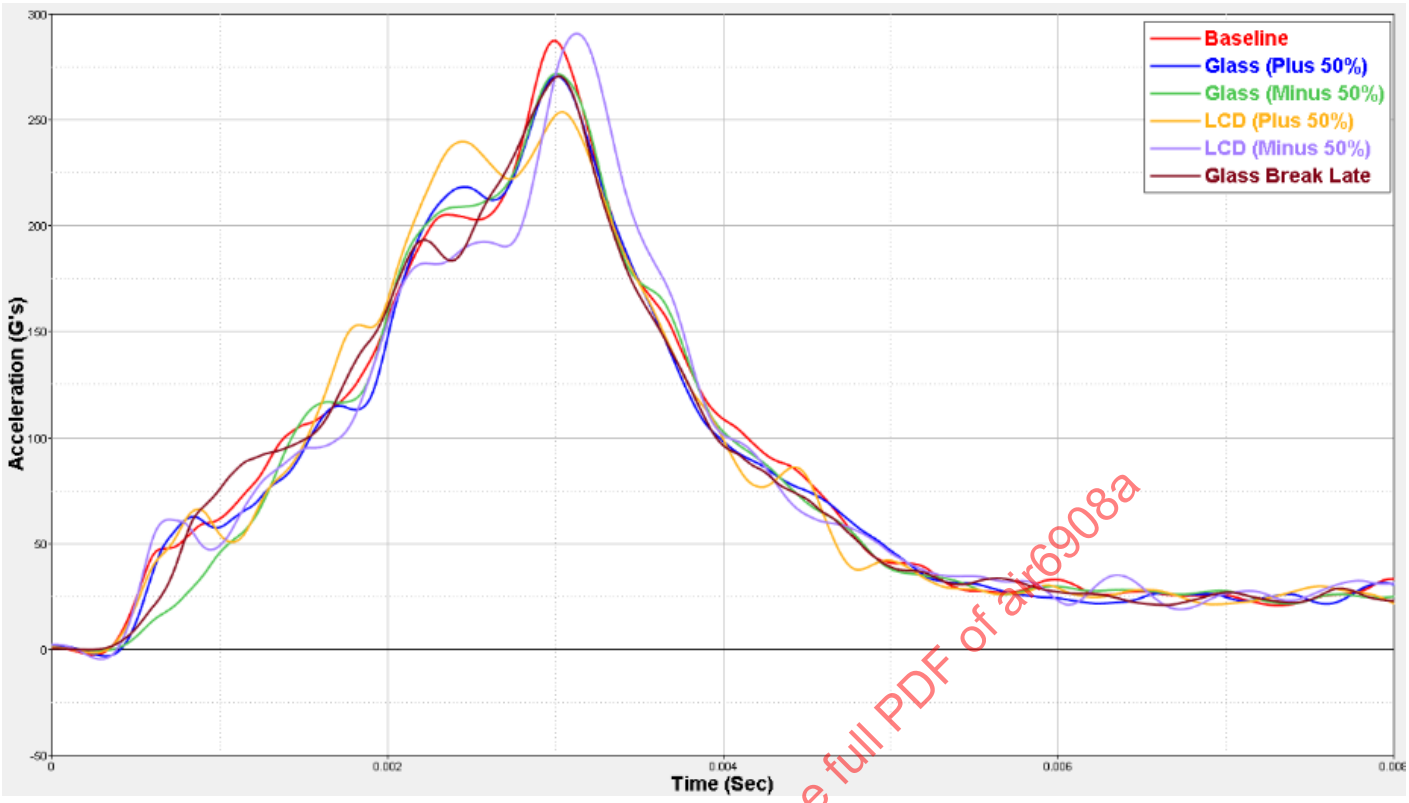

Figure G4 - Safran HCTD parametric study ATD head c.g. resultant acceleration with rigid bracket

Table G6 - Safran HCTD parametric study results with bracket tilt locked

Configuration	Curve #1 (Glass)	Curve #2 (Internal)	Glass Breakage	HIC	Δ HIC to Baseline	HIC Duration (ms)	Δ HIC Duration to Baseline
#1 Baseline	Unchanged	Unchanged	Low-range	474	--	2.12	--
#2 Stiffer touch screen	E=15.0×10^6 psi	Unchanged	Unchanged	487	+13	2.08	-0.04
#3 Less stiff touch screen	E=5.0×10^6 psi	Unchanged	Unchanged	513	+49	2.20	+0.08
#2 Stiffer touch screen	Unchanged	E=15.0×10^6 psi	Unchanged	636	+162	2.04	-0.08
#3 Less stiff touch screen	Unchanged	E=5.0×10^6 psi	Unchanged	439	-35	2.04	-0.08
#6 Glass breaks late	Unchanged	Unchanged	Largest deflection	460	-14	2.52	+0.40

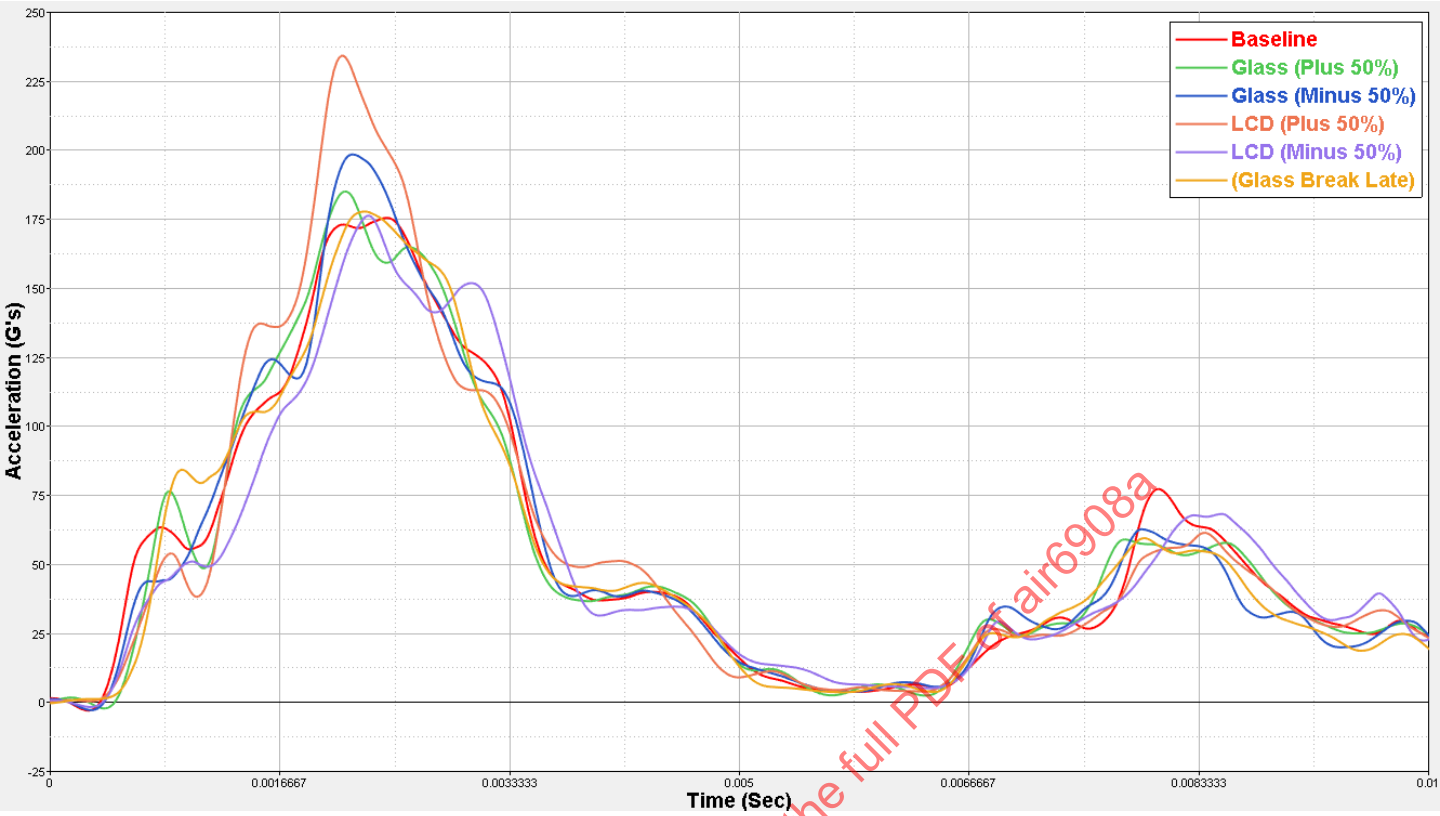

Figure G5 - Safran HCTD parametric study ATD head c.g. resultant acceleration with bracket tilt locked

Table G7 - Safran row-to-row dynamic test parametric study results

Configuration	Curve #1 (Glass)	Curve #2 (Internal)	Glass Breakage	HIC	Δ HIC to Baseline	HIC Duration (ms)	Δ HIC Duration to Baseline
#1 Baseline	Unchanged	Unchanged	Low-range	573	--	2.25	--
#2 Stiffer touch screen	E=15.0×10^6 psi	Unchanged	Unchanged	626	+53	2.32	+0.07
#3 Less stiff touch screen	E=5.0×10^6 psi	Unchanged	Unchanged	616	+43	2.24	-0.01
#2 Stiffer touch screen	Unchanged	E=15.0×10^6 psi	Unchanged	677	+104	2.18	-0.07
#3 Less stiff touch screen	Unchanged	E=5.0×10^6 psi	Unchanged	557	-16	2.20	-0.05
#6 Glass breaks late	Unchanged	Unchanged	Largest deflection	584	+11	2.20	-0.05

Table G8 - Safran row-to-row dynamic test parametric study results (no glass erosion)

Configuration	Curve #1 (Glass)	Curve #2 (Internal)	Glass Breakage	HIC	Δ HIC to Baseline	HIC Duration (ms)	Δ HIC Duration to Baseline
#1 Baseline (no glass erosion)	Unchanged	Unchanged	Low-range	743	--	1.74	--
#2 Stiffer touch screen (no glass erosion)	E=15.0×10^6 psi	Unchanged	Unchanged	766	+23	1.64	-0.10
#3 Less stiff touch screen (no glass erosion)	E=5.0×10^6 psi	Unchanged	Unchanged	664	-79	2.28	+0.54

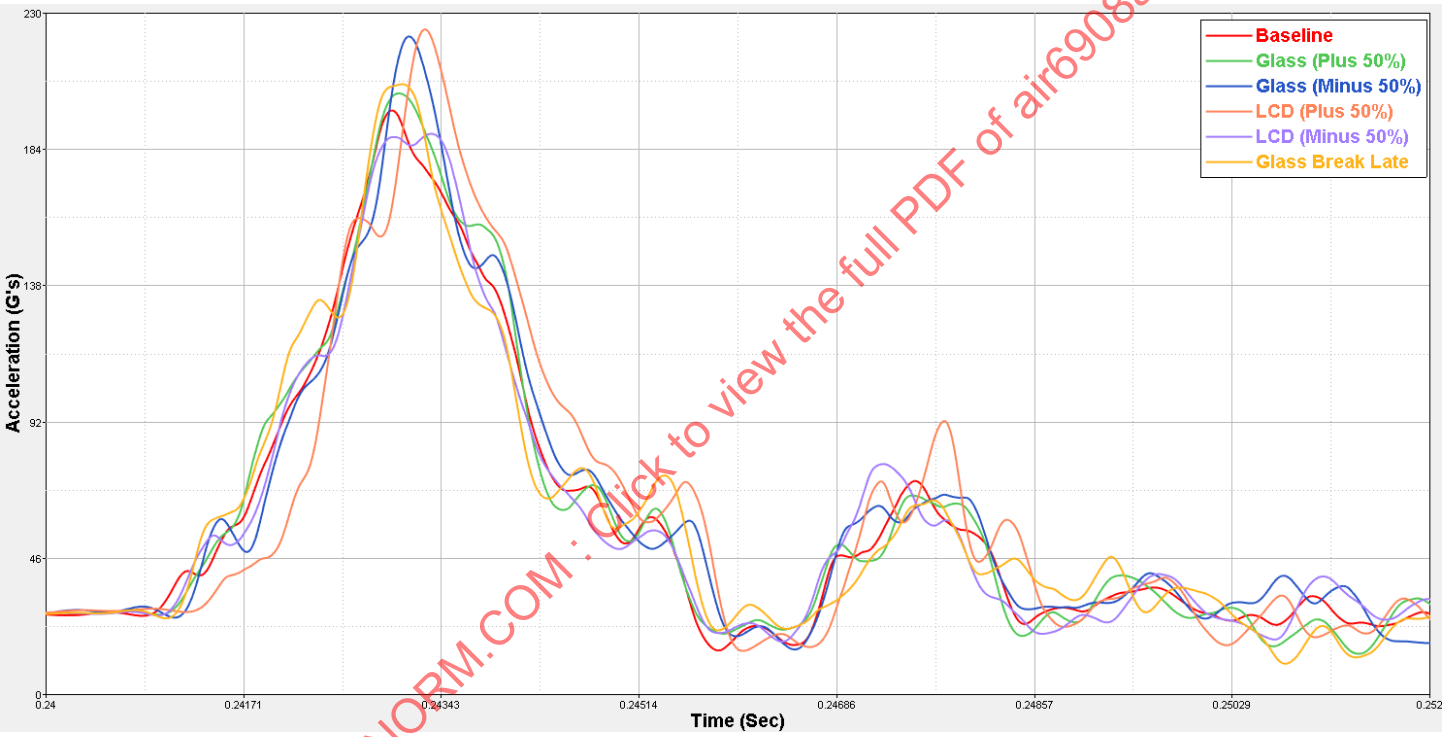

Figure G6 - Safran parametric study ATD head c.g. resultant acceleration for row-to-row dynamic tests

APPENDIX H - ENERGY ATTENUATION ANALYSIS RESULTS

H.1 RECARO

The Recaro seat model energy attenuation analysis results presented are for the “baseline” seat back configuration. Tables H1, H2, and H3 and Figures H2, H3, and H4 provide detailed data on the energy attenuation distribution of the integrated seat back during head impact. Tables H4 and H5 provide results of a parametric study as to the effect a component change would have on overall seat back energy attenuation properties (magnitude and distribution).

Hourglass energy was insignificant for this analysis, with backrest structure at 0.35 J and no hourglass energy for the monitor and tilt bracket.

Table H1 - Kinetic/internal strain energy attenuation - Recaro

Type of Energy	Energy (Joules)	Percentage Contribution
Kinetic	130.0	36.7%
Internal	223.9	63.3%

Table H2 - Seat back internal strain energy distribution - Recaro

Seat Component	Energy (Joules)	Percentage Contribution
Seat back	138.0	61.7%
Monitor	65.0	29.0%
Tilt bracket	20.9	9.3%

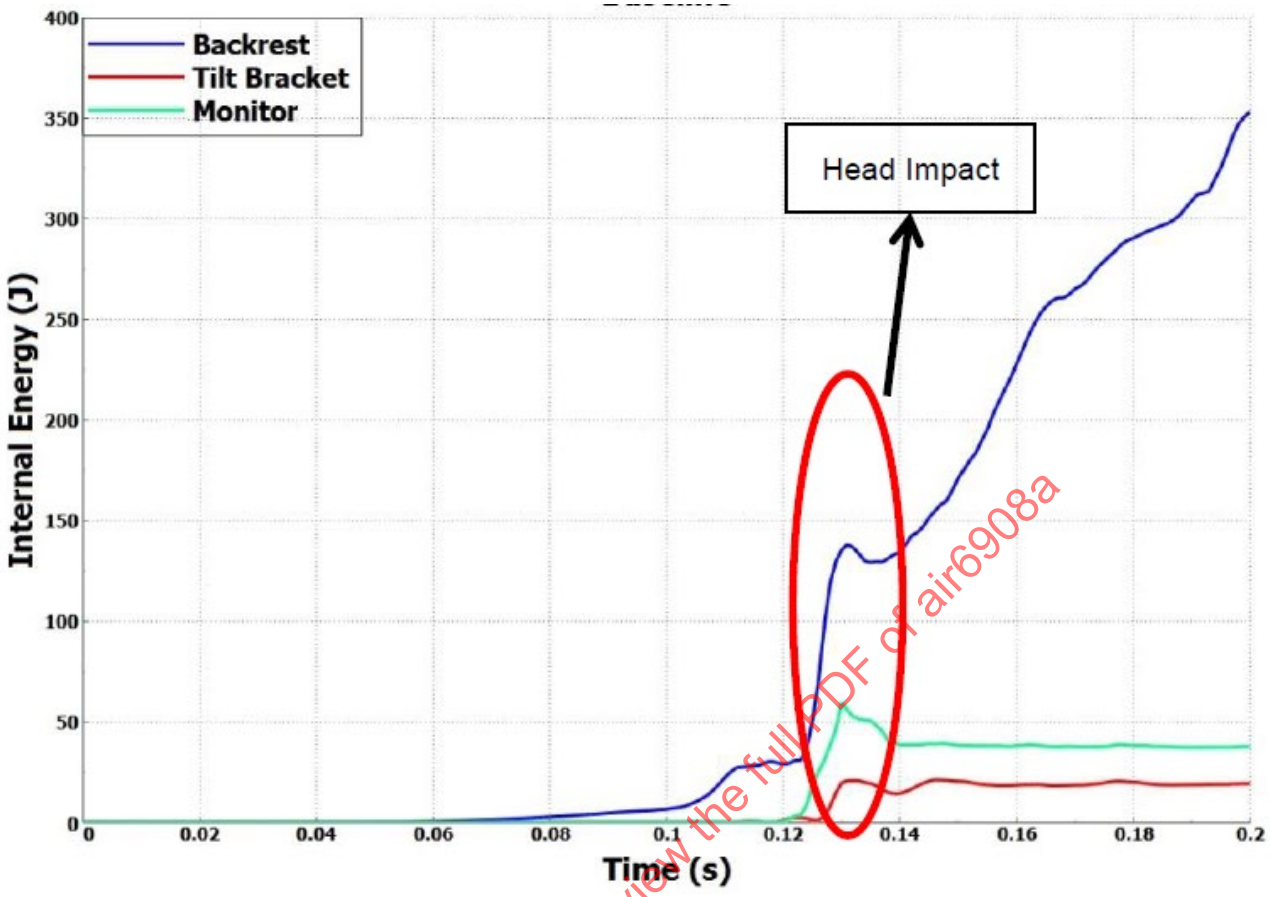

Figure H1 - Seat back internal strain energy distribution over time - Recaro

Table H3 - Monitor internal strain energy distribution - Recaro

Monitor Subcomponent	Energy (Joules)	Percentage Contribution
Touch screen	5.8	8.9%
Display panel (LCD)	9.9	15.2%
Electronics	1.6	2.4%
Internal frame	19.8	30.5%
External frame	28.0	43.0%

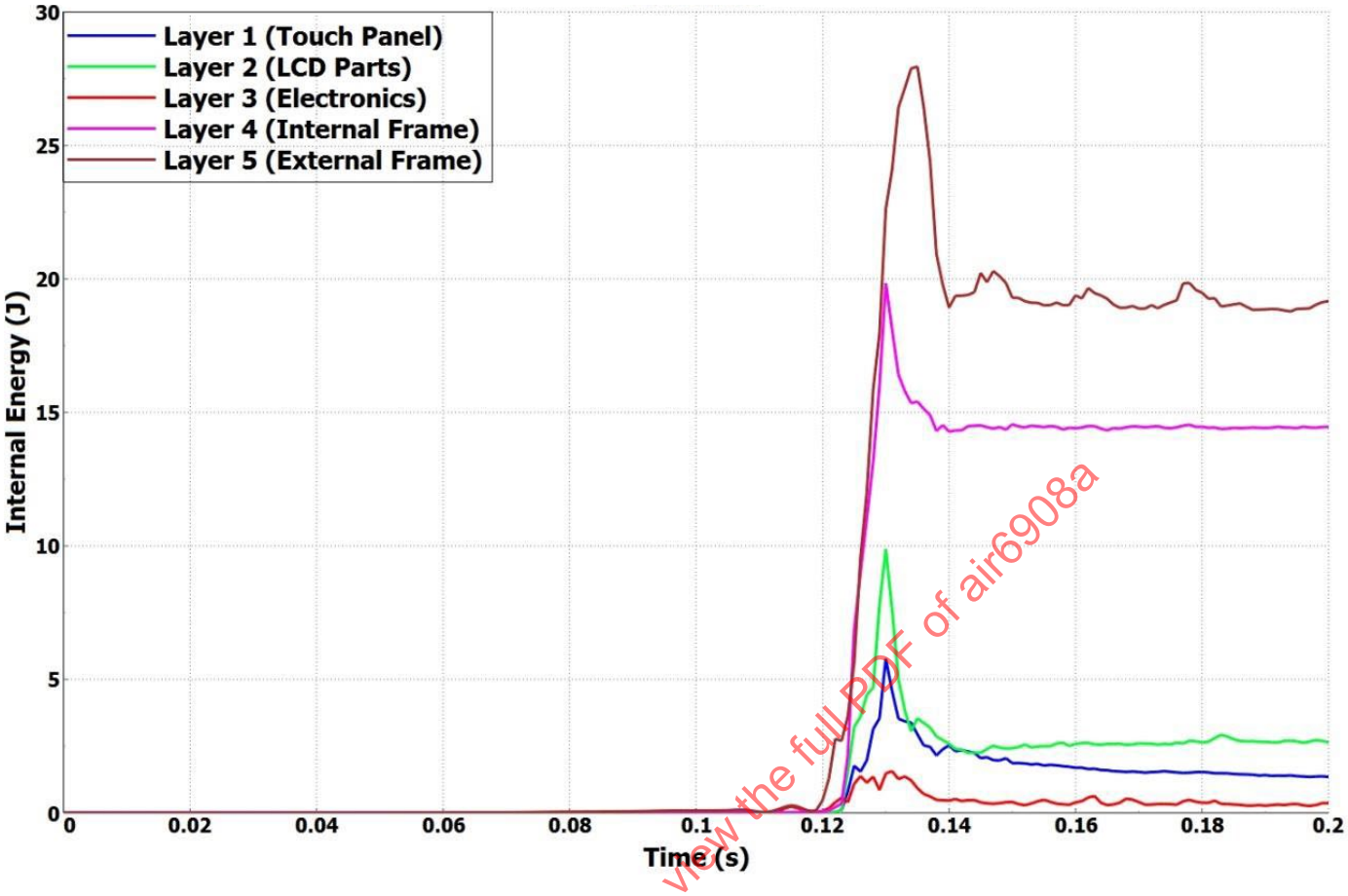

Figure H2 - Monitor internal strain energy distribution over time - Recaro

Table H4 - Effect of monitor change on seat back internal strain energy distribution - Recaro

Configuration	Curve #1 (Glass)	Curve #2 (Internal)	Seat Back (J) (% Contribution)	IFE Monitor (J) (% Contribution)	Tilt Bracket (J) (% Contribution)
#1 Baseline	Unchanged	Unchanged	138 (61.7%)	65.0 (29.0%)	20.9 (9.3%)
#2 Stiffer touch screen	E=15.0×10^6 psi	Unchanged	140.5 (61.7%)	65.5 (28.8%)	21.7 (9.5%)
#3 Less stiff touch screen	E=5.0×10^6 psi	Unchanged	138 (62.0%)	60.6 (27.2%)	24.1 (10.8%)
#4 Stiffer display panel	Unchanged	E=15.0×10^6 psi	139 (61.8%)	63.8 (28.4%)	22 (9.8%)
#5 Less stiff display panel	Unchanged	E=5.0×10^6 psi	142 (60.9%)	65.4 (28.0%)	25.9 (11.1%)

Table H5 - Effect of monitor change on monitor internal strain energy distribution - Recaro

Configuration	Curve #1 (Glass)	Curve #2 (Internal)	Touch Screen (J) (% Contribution)	Display Panel (J) (% Contribution)	Electronics (J) (% Contribution)	Internal Frame (J) (% Contribution)	External Frame (J) (% Contribution)
#1 Baseline	Unchanged	Unchanged	5.8 (8.9%)	9.9 (15.2%)	1.6 (2.4%)	19.8 (30.5%)	28.0 (43.0%)
#2 Stiffer touch screen	$E=15.0\times10^6$ psi	Unchanged	7 (10.7%)	10.3 (15.7%)	1.7 (2.6%)	20.9 (31.9%)	25.6 (39.1%)
#3 Less stiff touch screen	$E=5.0\times10^6$ psi	Unchanged	3.7 (6.2%)	9 (14.9%)	1.6 (2.6%)	18.8 (30.9%)	27.5 (45.4%)
#4 Stiffer display panel	Unchanged	$E=15.0\times10^6$ psi	6.6 (10.4%)	10.3 (16.1%)	1.5 (2.4%)	19.5 (30.5%)	25.9 (40.6%)
#5 Less stiff display panel	Unchanged	$E=5.0\times10^6$ psi	4.8 (7.3%)	6.8 (10.5%)	1.5 (2.3%)	21.2 (32.4%)	31 (47.5%)

H.2 SAFRAN

The Safran seat model energy attenuation analysis results presented are for the “baseline” seat back configuration. Tables H6, H7, and H8 and Figures H6, H7, and H8 provide detailed data on the energy attenuation distribution of the integrated seat back during ATD head impact. Tables H9, H10, H11, and H12 provide results of a parametric study as to the effect a component change would have on overall seat back energy attenuation properties (magnitude and distribution).

Hourglass energy was insignificant for this analysis.

Table H6 - Kinetic/internal strain energy attenuation - Safran

Type of Energy	Energy (Joules)	Percentage Contribution
Kinetic	244.2	70%
Internal	113.4	30%

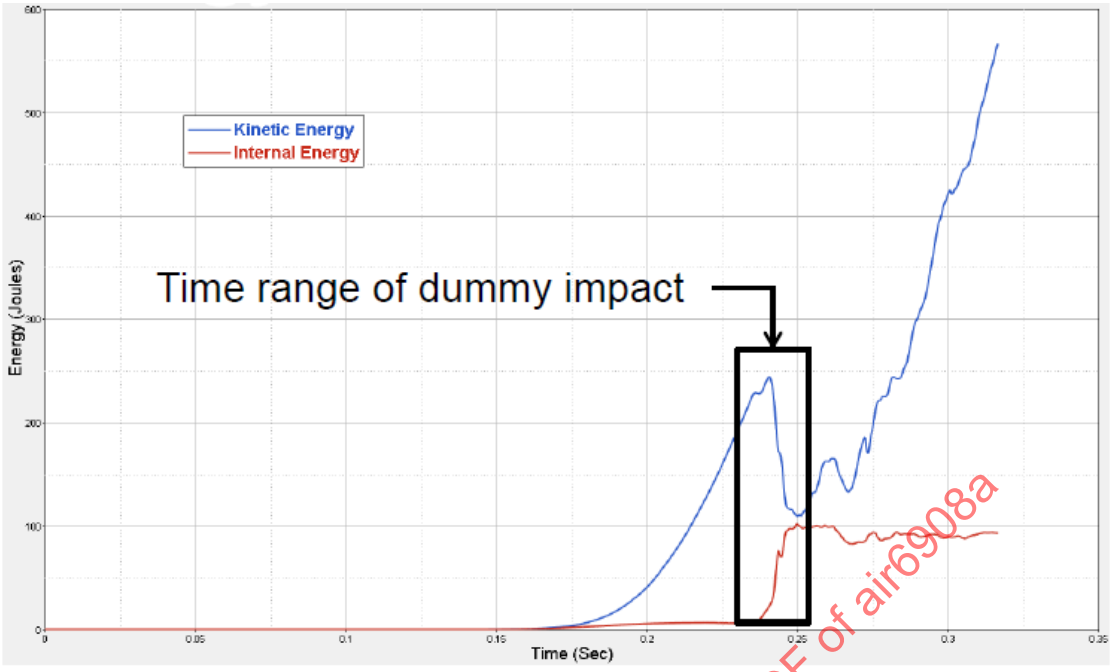

Figure H3 - Kinetic/internal strain energy attenuation over time - Safran

Table H7 - Seat back internal strain energy distribution - Safran

Seat Component	Energy (Joules)	Percentage Contribution
Seat back	66.6	59%
Monitor	37.2	33%
Tilt bracket	9.6	8%

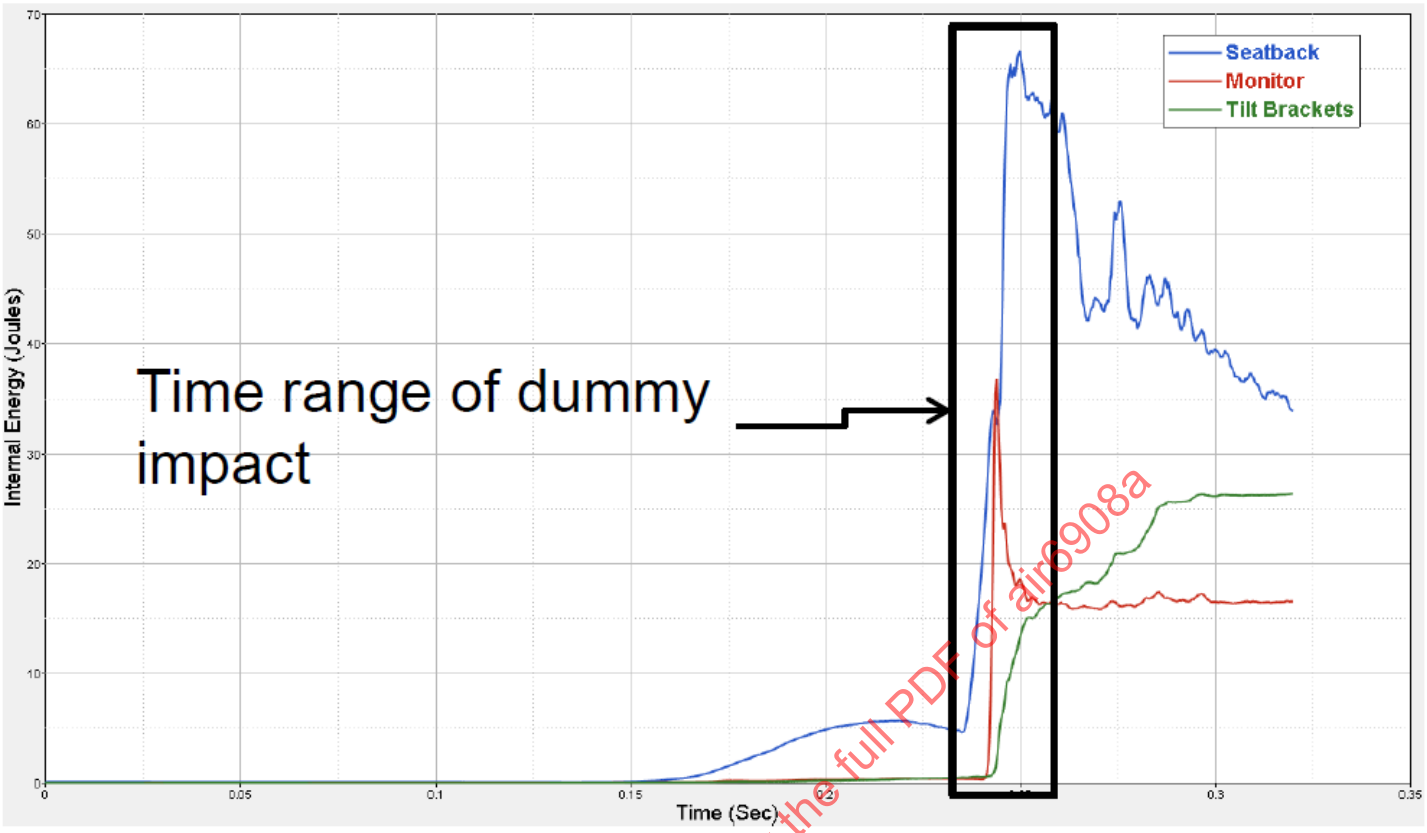

Figure H4 - Seat back internal strain energy distribution over time - Safran

Table H8 - Monitor internal strain energy distribution - Safran

Monitor Subcomponent	Energy (Joules)	Percentage Contribution
Touch screen	1.8	5%
Display panel (LCD)	10.9	29%
Electronics	3.1	8%
Internal frame	8.0	22%
External frame	13.4	36%

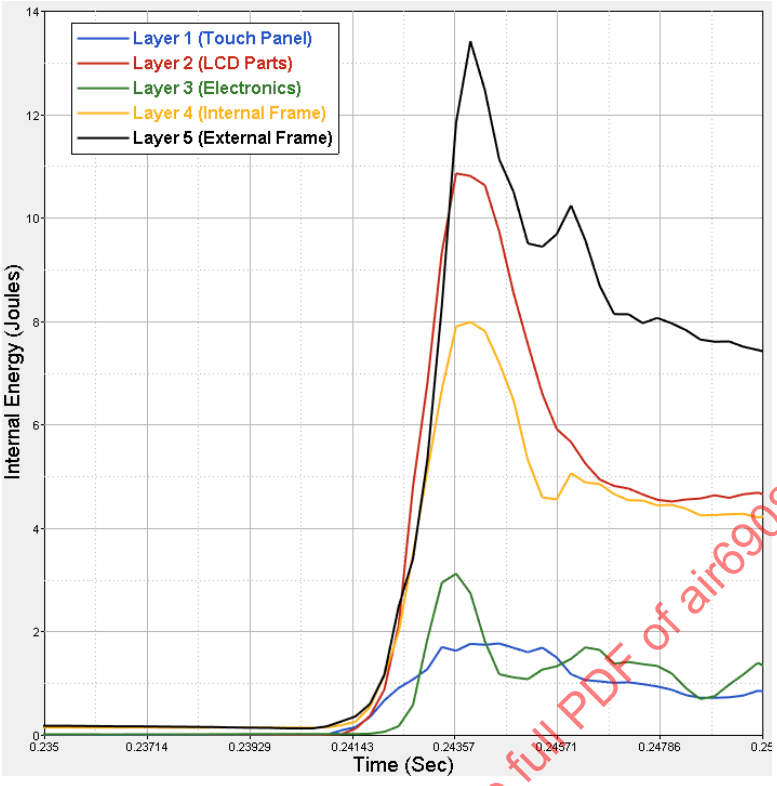

Figure H5 - Monitor internal strain energy distribution over time - Safran

The parametric study of the seat back monitor internal strain energy distribution was done with and without the glass erosion function to determine whether the variability seen due to glass failure would affect the overall energy distribution through the seat back system. Results show that changing the glass stiffness and not including glass erosion has negligible effect on the internal strain energy dissipation from the monitor assembly. Hence, the analyses for display panel variations were not performed.

Table H9 - Effect of monitor change on seat back internal strain energy distribution (with glass erosion function) - Safran

Configuration	Curve #1 (Glass)	Curve #2 (Internal)	Seat Back (J) (% Contribution)	IFE Monitor (J) (% Contribution)	Tilt Bracket (J) (% Contribution)
#1 Baseline	Unchanged	Unchanged	66.6 (59%)	37.2 (33%)	9.6 (8%)
#2 Stiffer touch screen	$E=15.0\times10^6$ psi	Unchanged	66.8 (58%)	38.5 (33%)	10.1 (9%)
#3 Less stiff touch screen	$E=5.0\times10^6$ psi	Unchanged	68.4 (57%)	41.8 (35%)	10.1 (8%)
#4 Stiffer display panel	Unchanged	$E=15.0\times10^6$ psi	73.7 (60%)	40.2 (32%)	9.1 (8%)
#5 Less stiff display panel	Unchanged	$E=5.0\times10^6$ psi	66.3 (58%)	38.5 (33%)	9.6 (9%)

Table H10 - Effect of monitor change on seat back internal strain energy distribution (without glass erosion function) - Safran

Configuration	Curve #1 (Glass)	Curve #2 (Internal)	Seat Back (J) (% Contribution)	IFE Monitor (J) (% Contribution)	Tilt Bracket (J) (% Contribution)
#1 Baseline	Unchanged	Unchanged	66.5 (54%)	45.0 (37%)	11.6 (9%)
#2 Stiffer touch screen	$E=15.0\times10^6$ psi	Unchanged	64.8 (53%)	44.7 (37%)	12.1 (10%)
#3 Less stiff touch screen	$E=5.0\times10^6$ psi	Unchanged	66.8 (56%)	41.8 (35%)	11.5 (9%)

Table H11 - Effect of monitor change on monitor internal strain energy distribution - Safran

Configuration	Curve #1 (Glass)	Curve #2 (Internal)	Touch Screen (J) (% Contribution)	Display Panel (J) (% Contribution)	Electronics (J) (% Contribution)	Internal Frame (J) (% Contribution)	External Frame (J) (% Contribution)
#1 Baseline	Unchanged	Unchanged	1.8 (5%)	10.9 (29%)	3.1 (8%)	8.0 (22%)	13.4 (36%)
#2 Stiffer touch screen	$E=15.0\times10^6$ psi	Unchanged	2.0 (5%)	11.0 (29%)	3.1 (8%)	8.6 (22%)	13.8 (36%)
#3 Less stiff touch screen	$E=5.0\times10^6$ psi	Unchanged	3.2 (8%)	11.2 (27%)	3.1 (7%)	11.1 (26%)	13.2 (32%)
#4 Stiffer display panel	Unchanged	$E=15.0\times10^6$ psi	1.6 (4%)	12.3 (31%)	2.9 (7%)	8.0 (20%)	15.4 (38%)
#5 Less stiff display panel	Unchanged	$E=5.0\times10^6$ psi	2.3 (6%)	10.1 (26%)	3.0 (8%)	9.8 (25%)	13.3 (35%)

Table H12 - Effect of monitor change on monitor internal strain energy distribution - Safran (no glass erosion)

Configuration	Curve #1 (Glass)	Curve #2 (Internal)	Touch Screen (J) (% Contribution)	Display Panel (J) (% Contribution)	Electronics (J) (% Contribution)	Internal Frame (J) (% Contribution)	External Frame (J) (% Contribution)
#1 Baseline	Unchanged	Unchanged	11.8 (27%)	5.2 (12%)	3.1 (7%)	8.3 (19%)	15.6 (35%)
#2 Stiffer touch screen	$E=15.0\times10^6$ psi	Unchanged	13.2 (29%)	4.7 (11%)	3.3 (8%)	8.2 (18%)	15.3 (34%)
#3 Less stiff touch screen	$E=5.0\times10^6$ psi	Unchanged	9.2 (22%)	6.1 (15%)	3.1 (7%)	8.3 (20%)	15.1 (36%)

APPENDIX I - WRAPPED MONITOR RESULTS

Information provided in this appendix was not used in the development of ARP6330 and is included for possible future uses.

I.1 IMPACT LOCATION #1

Test data is located in Table I1. Head acceleration plots for the three monitor configurations tested (baseline, duct tape added, mover's wrap added) are shown Figures I1, I2, and I3. Pictures of the tested monitors post-test are provided in Figure I4.

Table I1 - Impact location #1 test data

Test Number and Date	Head Velocity (ft/s)	Peak g (Resultant)	Δ From Average	HIC	Δ From Average	Delta T, ms	Average Acceleration (Resultant)	%Δ From Average
No Tape (baseline)								
BT1 (June 30, 2014)	34.68	277	-20 (-7%)	1959	-192 (-9%)	3.90	191	-14 (-7%)
BT2 (June 30, 2014)	34.91	289	-8 (-3%)	2195	+44 (+2%)	3.50	208	+3 (+2%)
BT3 (June 30, 2014)	34.89	324	27 (+9%)	2298	+147 (+7%)	3.40	215	+10 (+5%)
Average	--	297	--	2151	--	3.60	205	--
Duct Tape (2 layers)								
DT1 (June 30, 2014)	34.95	329	-1 (0%)	2208	-132 (-6%)	3.5	209	-8 (-4%)
DT2 (July 1, 2014)	34.86	334	+4 (1%)	2240	-100 (-4%)	3.4	213	-4 (-2%)
DT3 (July 1, 2014)	35.09	327	-3 (-1%)	2572	+232(+10%)	3.2	230	+13 (+6%)
Average	--	330	--	2340	--	3.37	217	--
Mover's Tape (10 layers)								
MT1 (July 1, 2014)	34.76	325	+38 (13%)	2179	+147 (+7%)	3.3	213	+12 (+6%)
MT2 (July 25, 2014)	34.94	261	-26 (-9%)	1964	-68 (-3%)	3.7	195	-6 (-3%)
MT3 (July 25, 2014)	35.03	275	-12 (-4%)	1952	-80 (-4%)	3.7	194	-7 (-3%)
Average	--	287	--	2032	-	3.6	201	--

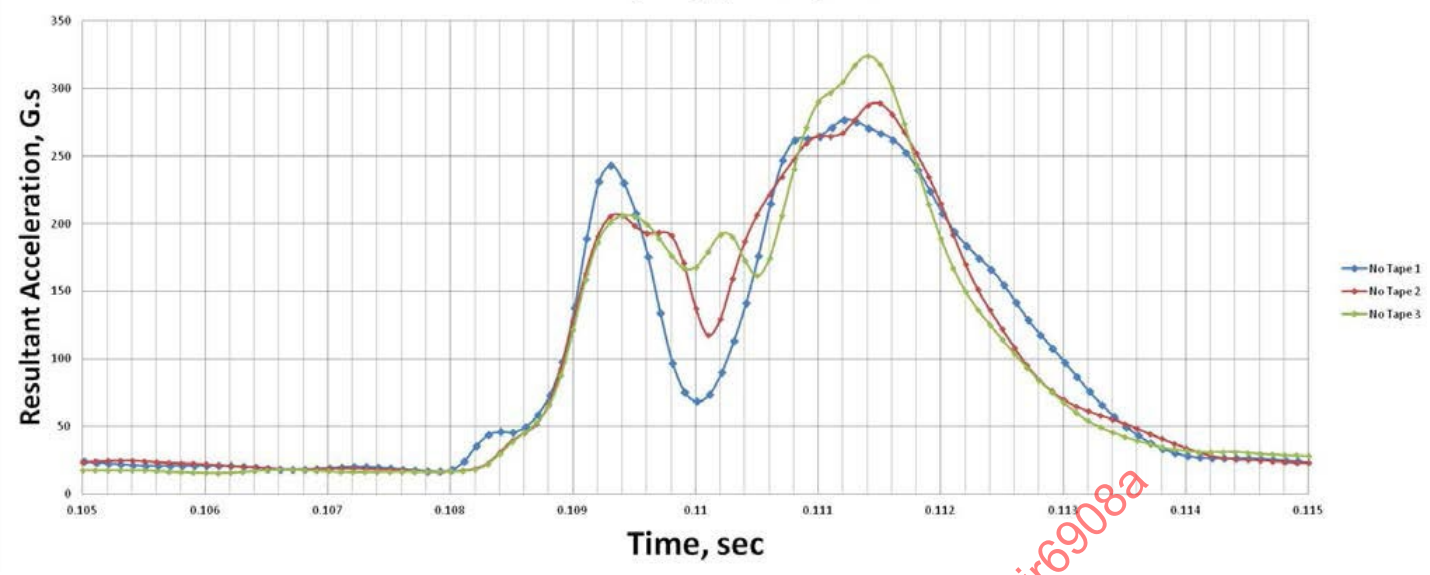

Figure I1 - Head acceleration over time, baseline monitor, impact location #1

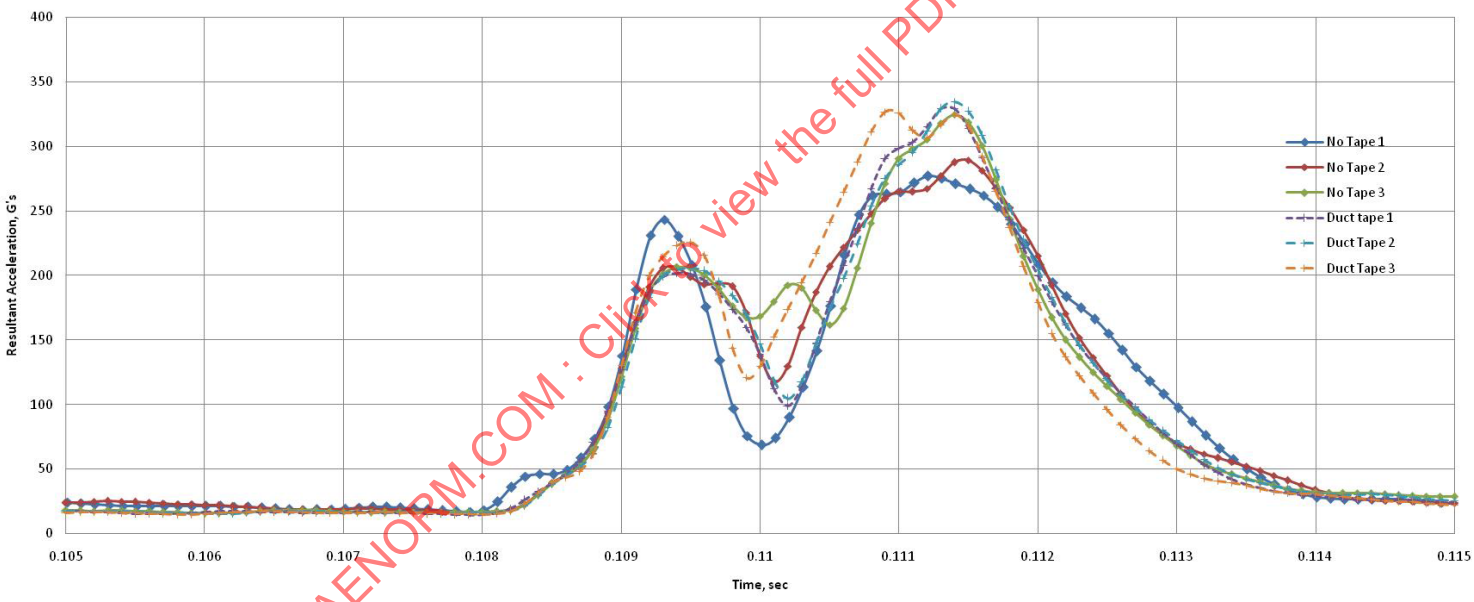

Figure I2 - Head acceleration over time, baseline versus duct tape monitor configuration, impact location #1

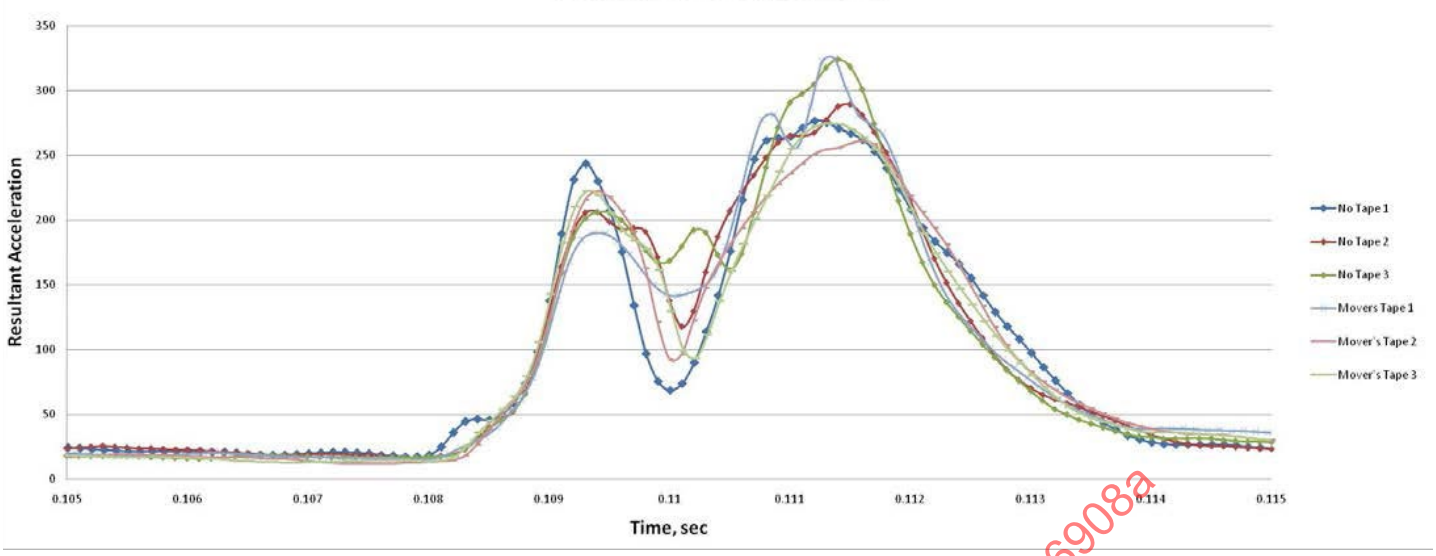

Figure I3 - Head acceleration over time, baseline versus mover's tape monitor configuration, impact location #1

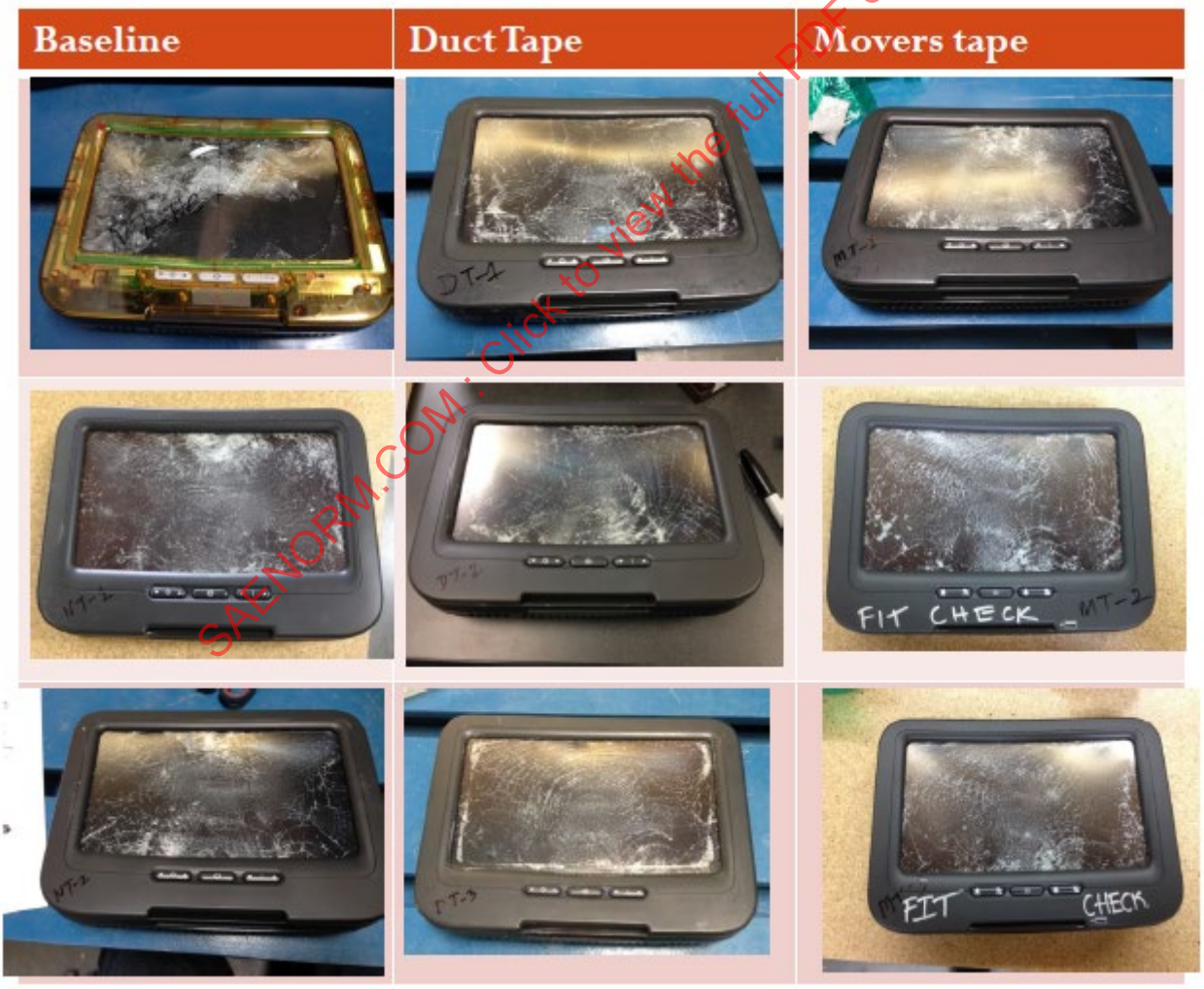

Figure I4 - Photos of monitors post-test

I.2 IMPACT LOCATION #2

Head component test data is located in Table I2. Head acceleration plots for the three monitor configurations tested (baseline, duct tape added, mover's wrap added) are provided in Figures I5, I6, and I7.

Table I2 - Impact location #2 test data

Test Number and Date	Head Velocity (ft/s)	Peak g (Resultant)	Δ From Average	HIC	Δ From Average	Delta T, ms	Average Acceleration (Resultant)	%Δ From Average
No Tape (baseline)								
EBT1 (July 14, 2014)	34.84	227	+11 (-7%)	1384	-21 (-1%)	4.0	164	-1 (-1%)
EBT2 (July 14, 2014)	34.77	205	-11 (-7%)	1425	+20 (+1%)	4.0	166	+1 (+1%)
Average	--	216	--	1405	--	4.0	165	--
Duct Tape (2 layers)								
EDT1 (July 14, 2014)	34.91	214	+1 (+0%)	1236	-51 (-4%)	4.5	150	-6 (-4%)
EDT2 (July 15, 2014)	34.46	211	-2 (-1%)	1338	+51 (+4%)	4	162	+6 (+4%)
Average	--	213	--	1287	--	4.25	156	--
Mover's Tape (10 layers)								
EMT1 (July 15, 2014)	34.69	230	+1 (+0%)	1385	+51 (+4%)	4.2	161	+4 (+3%)
EMT2 (July 16, 2014)	34.76	227	-2 (-1%)	1282	-52 (-4%)	4.4	153	-4 (-3%)
Average	--	229	--	1334	--	4.3	157	--

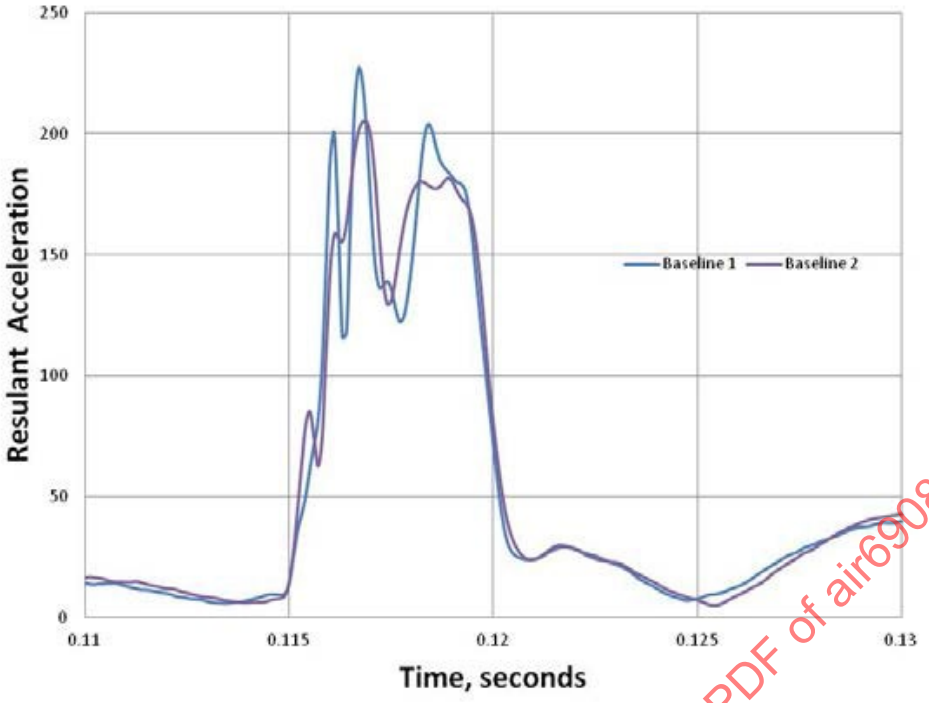

Figure I5 - Head acceleration over time, baseline monitor, impact location #2

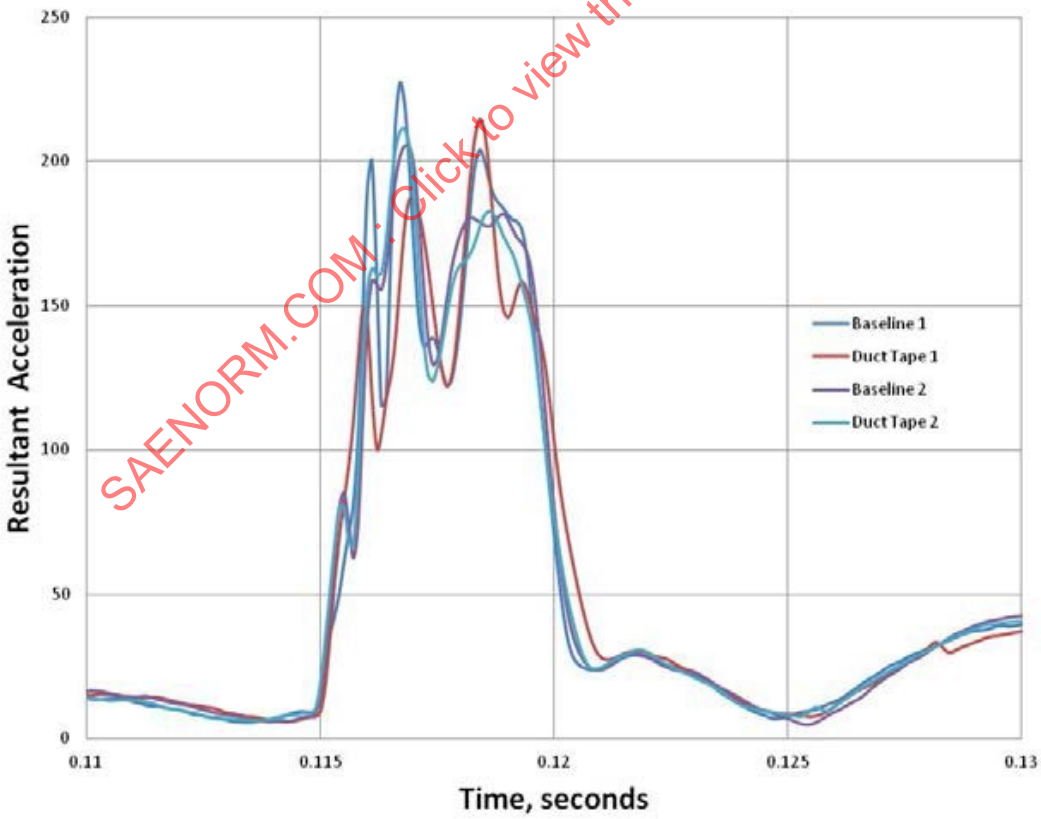

Figure I6 - Head acceleration over time, baseline versus duct tape monitor configuration, impact location #2

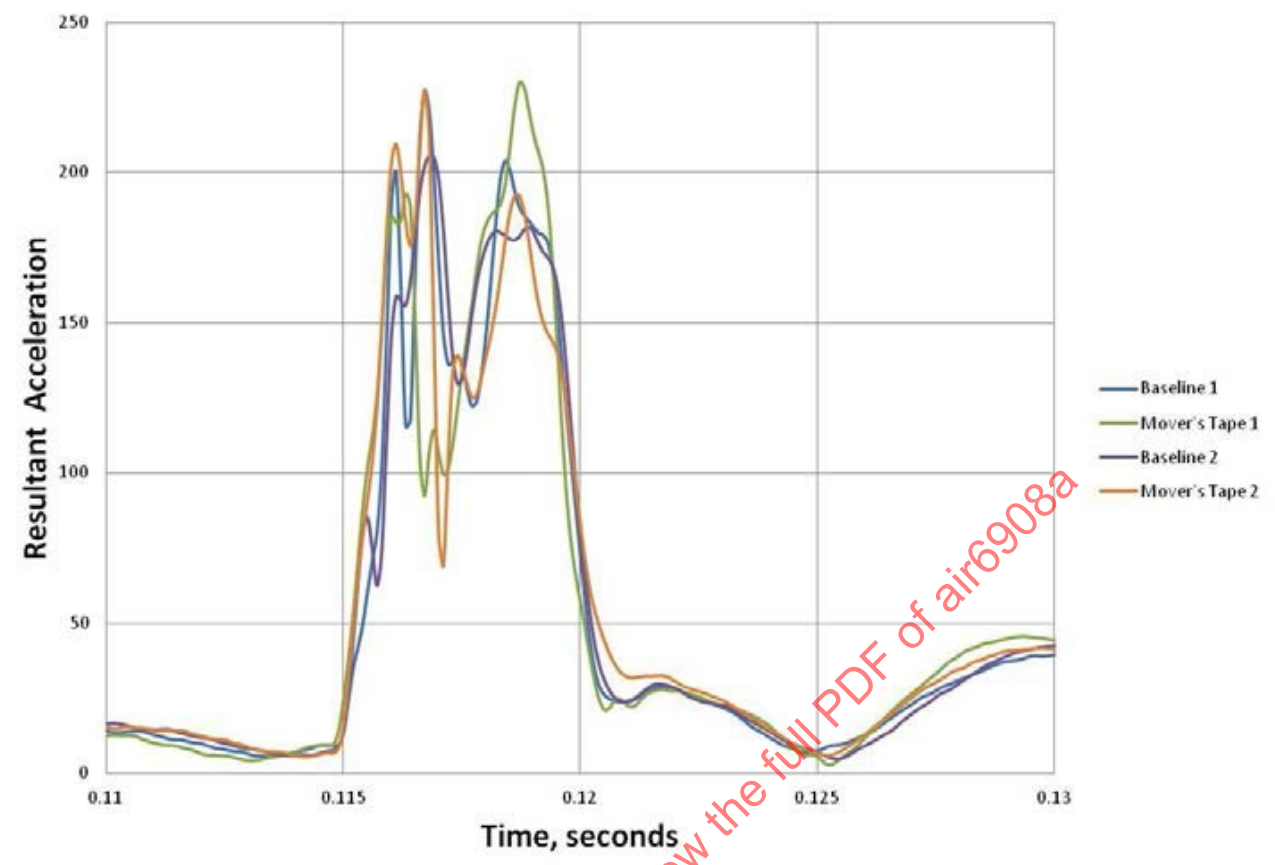

Figure I7 - Head acceleration over time, baseline versus mover's tape monitor configuration, impact location #2

APPENDIX J - IMPACTOR SIMULATION RESULTS

Simulation results using various impactors and aluminum sheet thicknesses with an impact velocity of 34 ft/s (10.4 m/s) are provided in this appendix. The Hybrid II-like impactor is the same pendulum tester as the Hybrid IIII neck, but with the rubber plates in the neck fused together such that they act as one column, roughly approximating a Hybrid II neck. Monitor is the baseline Panasonic 10.6-inch seat back monitor design.

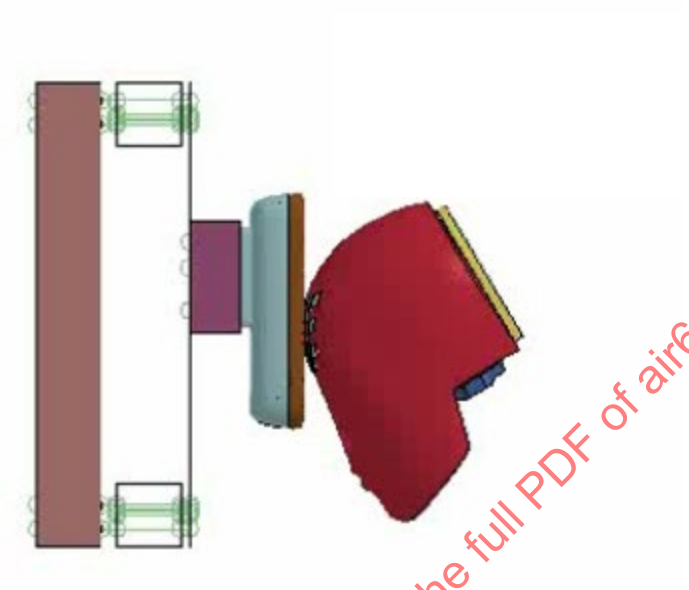

Figure J1 - Free motion headform simulation

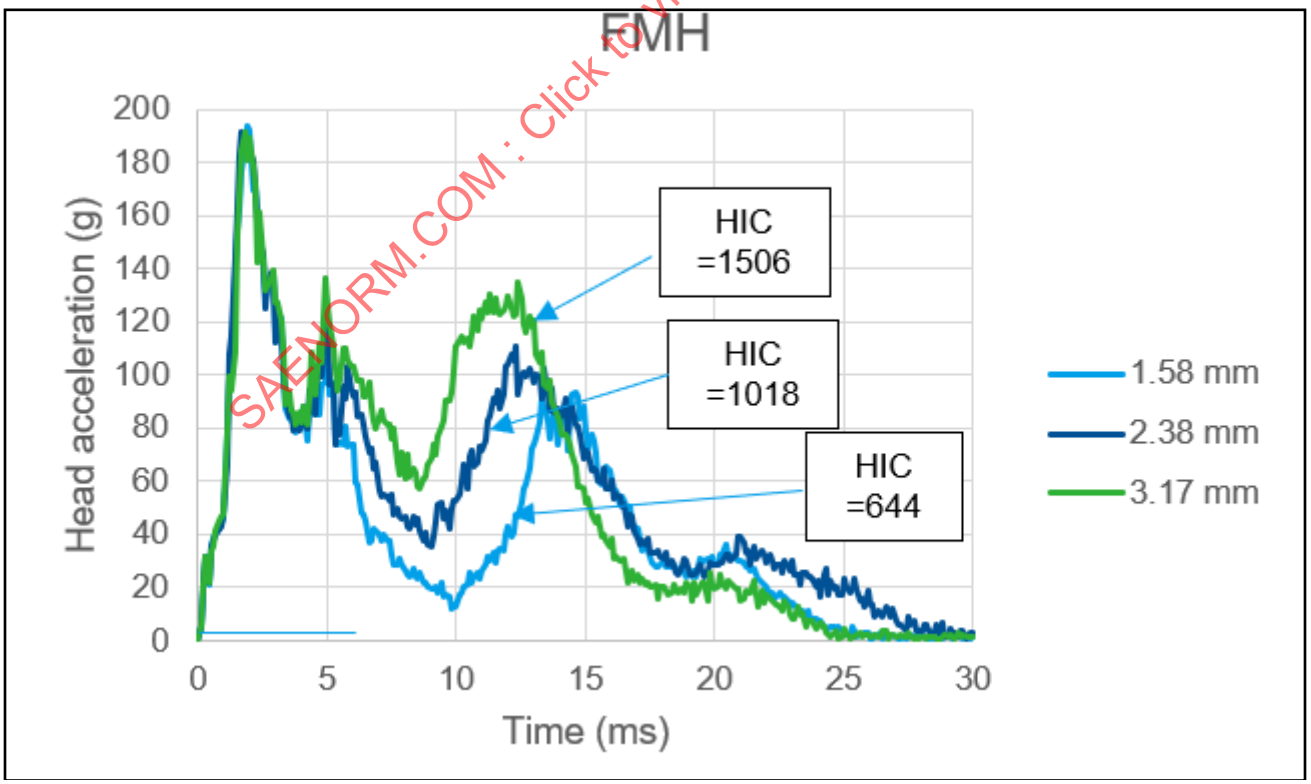

Figure J2 - Free motion headform simulation results

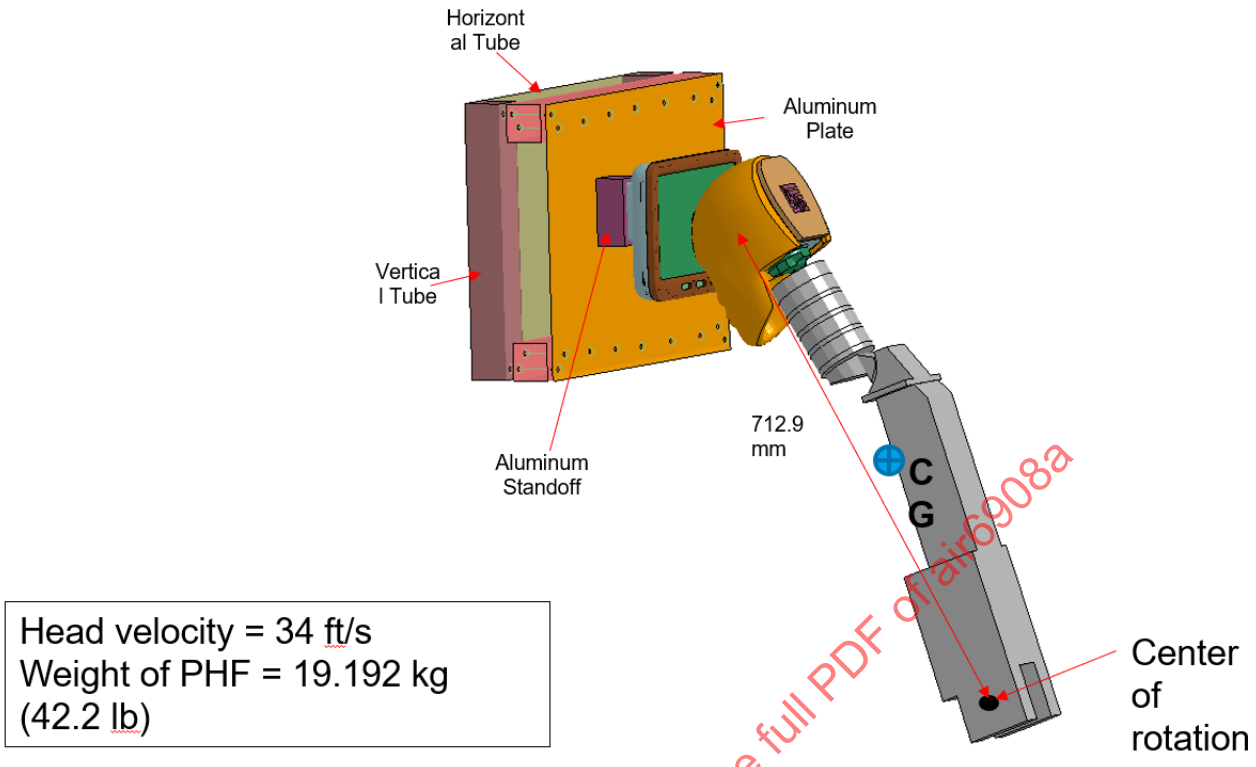

Figure J3 - Pendulum tester simulation

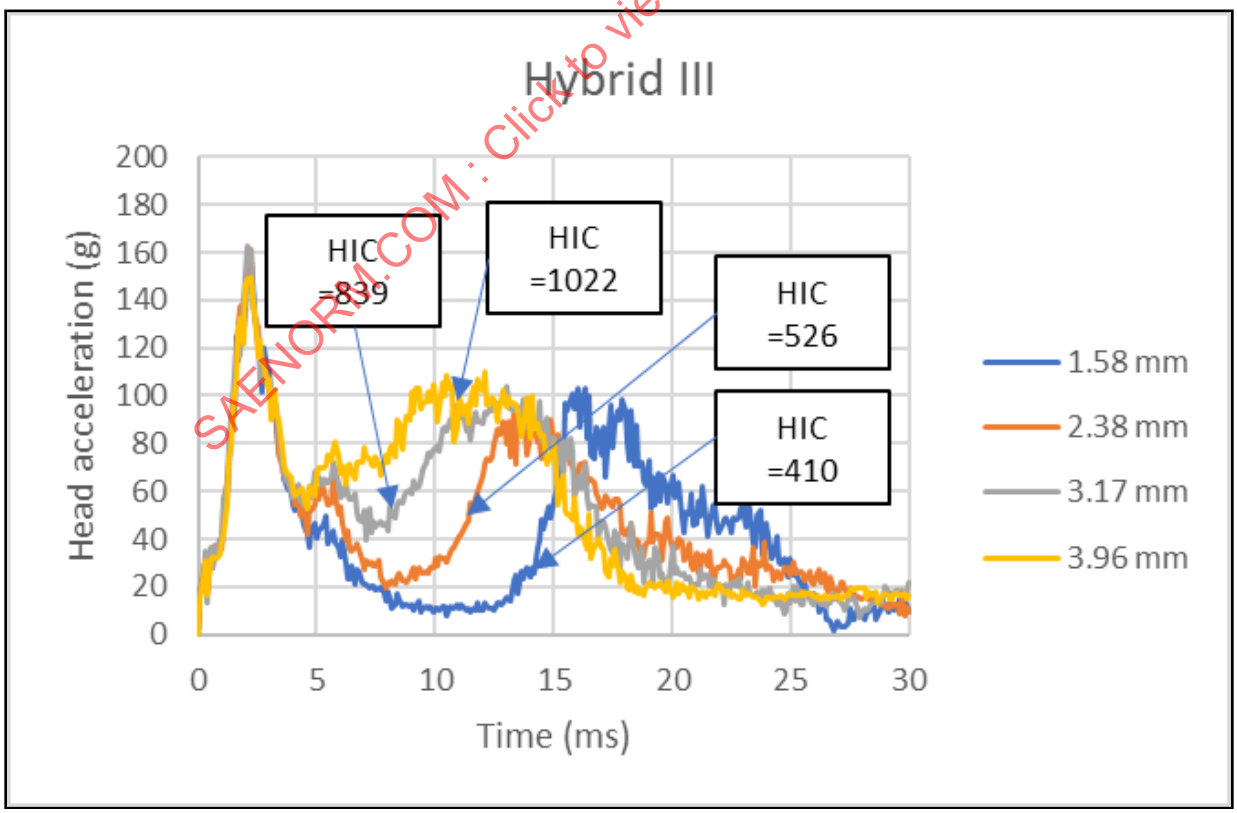

Figure J4 - Pendulum tester simulation results

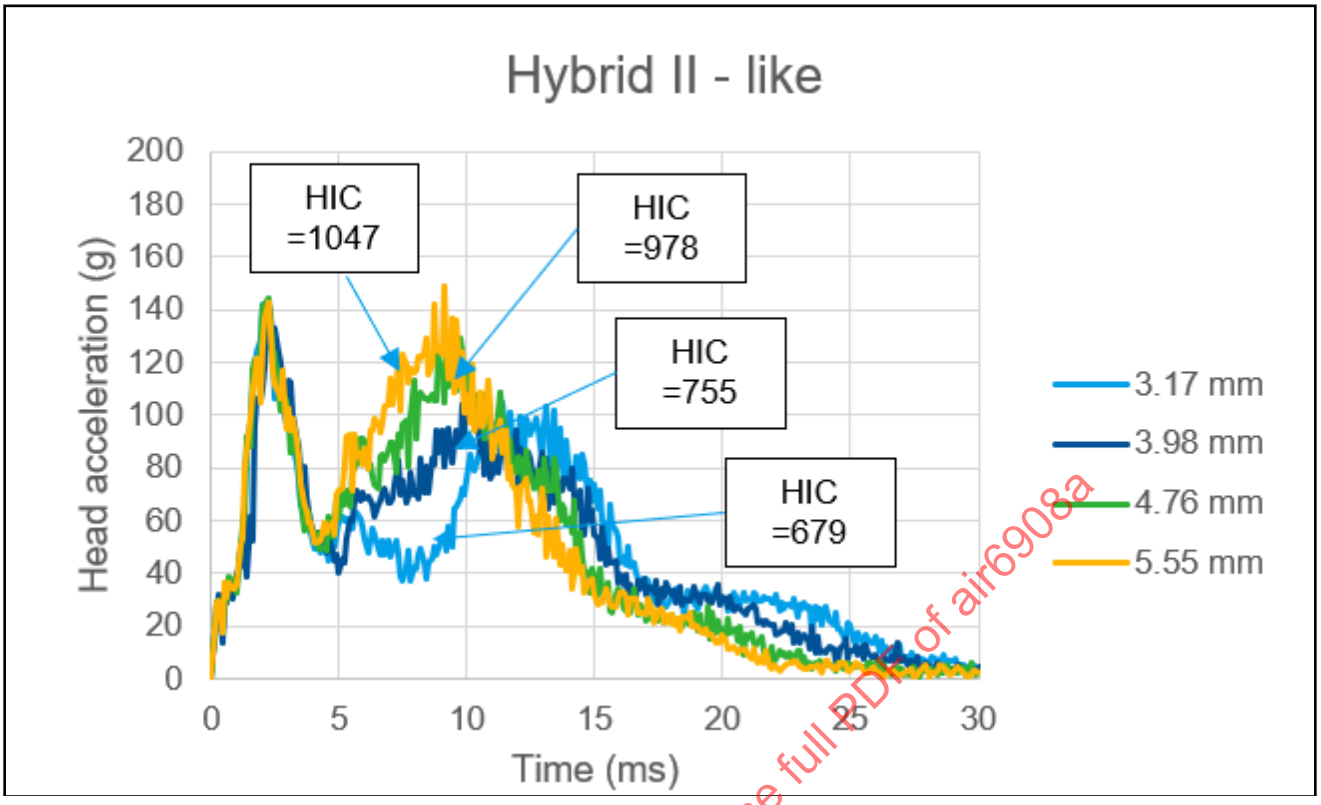

Figure J5 - Pendulum tester with Hybrid II type neck - simulation results

Impactor acceleration plots showing the variations due to the impactor type are provided below.

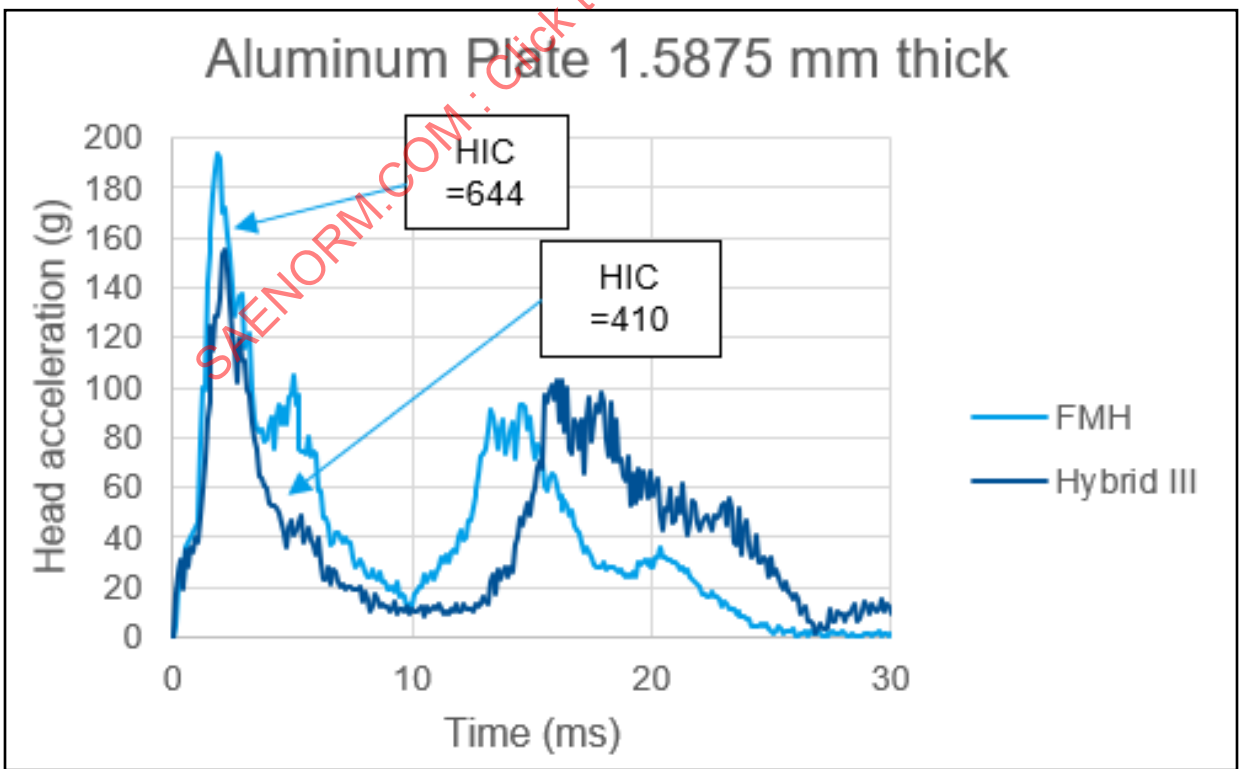

Figure J6 - Acceleration comparison between impactors - 1.58-mm aluminum thickness

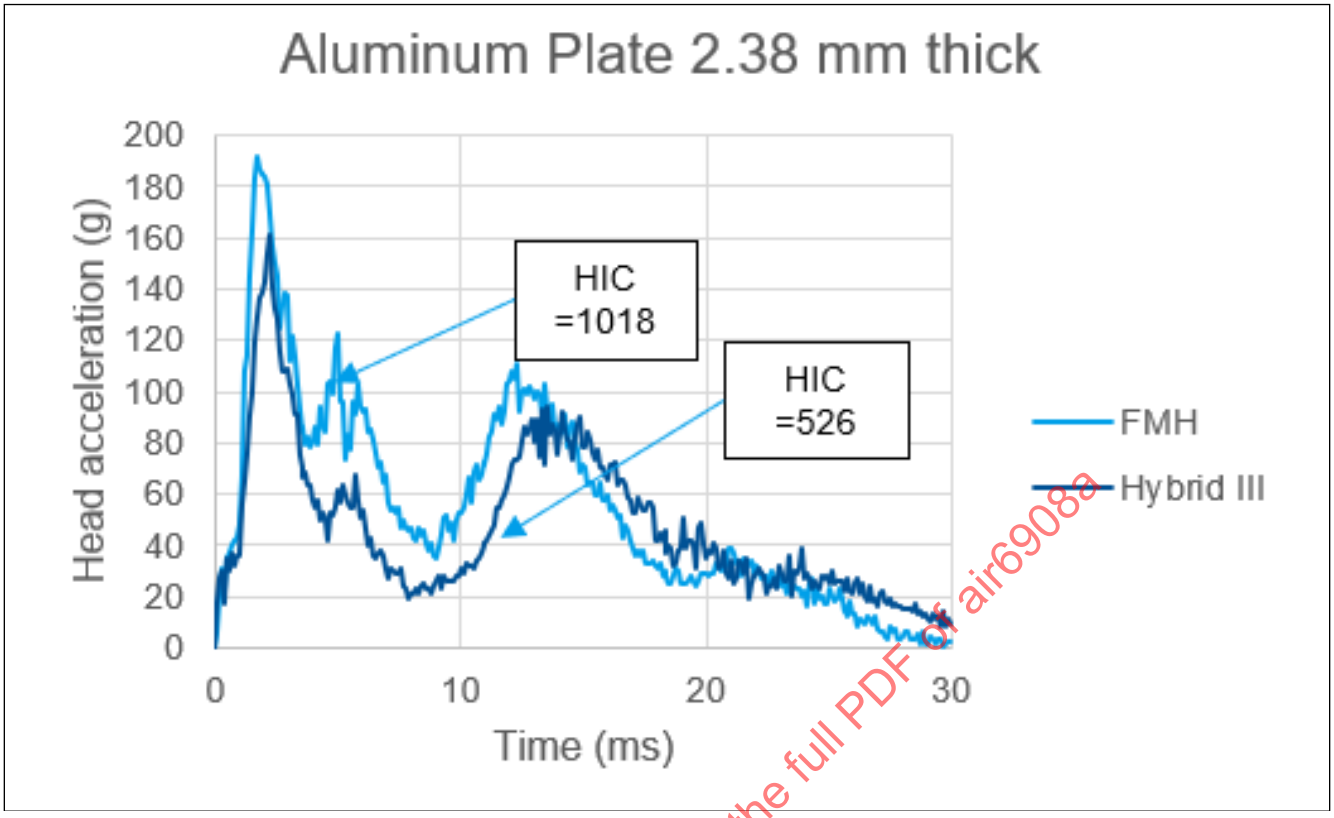

Figure J7 - Acceleration comparison between impactors - 2.38-mm aluminum thickness

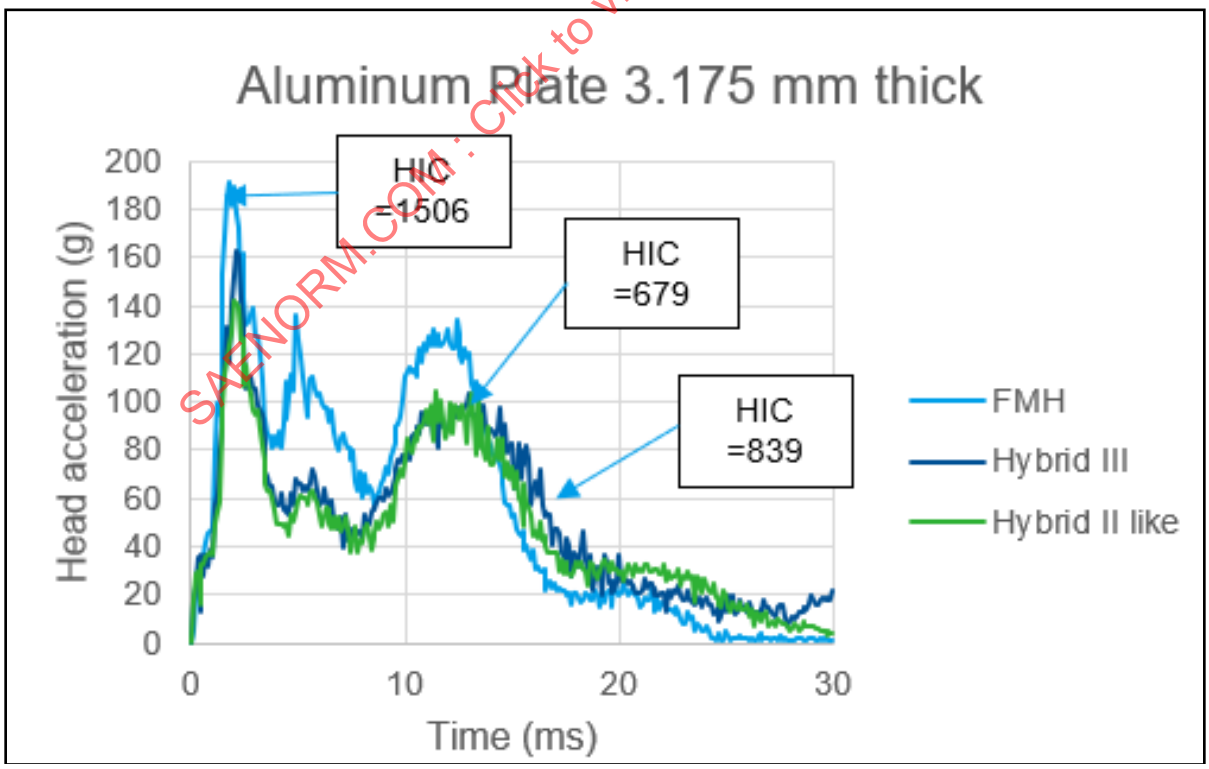

Figure J8 - Acceleration comparison between impactors - 3.175-mm aluminum thickness